The cAMP receptor protein controls *Vibrio cholerae* gene expression in response to host colonisation

by

Jainaba Roussel

A thesis submitted to the University of Birmingham for the degree of

DOCTOR OF PHILOSOPHY

School of Biosciences

College of Life and Environmental Sciences

University of Birmingham

January, 2018

Abstract

The bacterium *Vibrio cholerae* is the causative agent of the acute diarrhoeal disease cholera. *V. cholerae* is naturally found in aquatic environments, where it attaches to chitinous surfaces for survival, but can switch lifestyles to cause disease in humans. The switch in lifestyle requires modulation of genetic systems and much of the regulation occurs at the level of gene expression and is controlled by transcription factors. In this work, I show that the global transcription regulator, cAMP receptor protein (CRP), plays an integral role in the regulatory network that controls lifestyle switching. I have identified two sites for CRP in the intergenic region between *rtxHCA* and *rtxBDE*, a locus which encodes the multifunctional-autoprocessing repeats-in-toxin (MARTX) toxin and toxin transport system respectively. Using a combination of genetics, biochemistry and *in vivo* animal studies, I have determined a CRP dependent regulation of gene expression for toxin transport in response to infection of the host. This work shows that *rtxHCA* is constitutively expressed and not subject to regulation by CRP whist CRP acts as a repressor of *rtxBDE* transcription. Examination of further CRP targeted genes reveals a similar behaviour upon host colonisation. These findings suggest that toxin export occurs in nutritionally rich environments such as the intestines, where the MARTX toxin can exert cytopathic and cytotoxic effects on host cells.

Acknowledgements

I would like to thank my sponsor, the IDB, for making this journey possible. I would also like to say a huge thank you to my supervisor David Grainger. It has been an interesting and, at times, challenging few years, but you've always had faith in me. Thank you for the constant words of encouragement and providing an amazing environment to work in. I would like to thank my friends and colleagues in the G-team (both past and present); Shivani, Laura, Lisa, James, Gemma, Prateek, Rachel, Emily, Tom, Alistair and Andres. Thank you for the laughs and the hugs, when cultures simply refuse to grow, and for being my sounding boards. Thanks to my extended "lab family" (downstairs in the Busby Lab) for being so generous and accomodating with your time, reagents and plasmids. Thank you to Nico (HAPI Lab) for helping with all of the work involving the zebrafish and to Joao (HAPI Lab) for the training on the microscope. I would like to thank Andy Camilli for a fun packed and very informative few weeks in Boston whilst I learnt the MuGENT technique, and, again, Dave, for making the trip happen. Thank you to my wonderful family, Yaya, Papa, Fatou, Saul and the kids for the love and support throughout these past years. Thank you for listening to my never ending theories about my sometimes wacky results and allowing me to think solutions out loud without thinking I'd gone mad. A big 'merci' to Marie-Christine and Pascal for your words of support and encourgement. To my brilliant husband, Jimmy, father of my beautiful boys Emile and Alexander, for believing in me, for loving me and for keeping me company all those weekends in the lab. Thank you for being so supportive, understanding and nudging me to keep going.

It has truly been an awesome few years and a big thank you to all the people who played a part in making it so.

Table of Contents

List of Figures

List of Tables

List of Abbreviations

A	Adenine
Amp	Ampere
Amp^{R}	Ampicillin resistance
APS	Ammonium persulphate
AR1	Activating region 1
AR2	Activating region 2
AR3	Activating region 3
bp	Base pair
BSA	Bovine serum albumin
C	Cytidine
cAMP	Cyclic AMP
CAP	Calf alkaline phosphatase
c-di-GMP	Cyclic di-GMP
ChIP	Chromatin immunoprecipitation
ChIP-seq	ChIP combined with sequencing
Ci	Curie
CRP	cAMP receptor protein
CTD	C-terminal domain
CTX	Cholera toxin
ddH2O	Double distilled water
DEPC	Diethylpyrocarbonate
DNA	Deoxyribonucleic acid
DNAse	Deoxyribonuclease

dNTP	2'-deoxyribonucleoside 5'-triphosphate
dsDNA	Double stranded DNA
DTT	Dithiothreitol
E	Glutamic acid
E. coli	*Escherichia coli*
E3	E3 media
EDTA	Diaminoethanetetra-acetic acid
G	Guanine
HEPES	4-(2-hydroxyethyl)-1- piperazineethanesulfphonic acid
H-NS	Histone-like nucleoid structuring protein
K	Lysine
Kan^R	Kanamycin resistance
kb	Kilobase
LB	Luria-Bertani broth (Lennox or Miller)
MARTX	Multiple autoprocessing repeat in toxins
$MARTX_{Vc}$	Multiple autoprocessing repeat in toxins of *Vibrio cholerae*
Mg	Magnesium
MM	Minimal media
mRNA	Messenger RNA
MuGENT	Multiplex genome editing by natural transformation
nt	Nucleotide
NTD	N-terminal domain
NTP	Nucleoside triphosphate
ºC	Degree Celsius

OD	Optical density
Oligo	Oligonucleotide
ONPG	Ortho-nitrophenyl-β-galactosidase
PAGE	Polyacrylamide gel electrophoresis
PCR	Polymerase chain reaction
psi	Pounds per square inch
R	Arginine
RNA	Ribonucleic acid
RNA-seq	RNA sequencing
RNAP	RNA polymerase holoenzyme
RNAse	Ribonuclease
RPC	Closed promoter complex
RPO	Open promoter complex
RTX	Repeat in toxins
SDS	Sodium dodecyl sulphate
Sm^R	Streptomycin resistance
SOE	Splicing by overlap PCR
$Spec^R$	Spectinomycin resistance
T	Threonine
T	Thymine
T4 PNK	T4 polynucleotide kinase
TCP	Toxin coregulated pilus
TEMED	Tetramethylethylenediamine
Tet^R	Tetracycline resistance
TF	Transcription factor

Tris	Tris (hydroxymethyl) aminoethane
U	Uracil
UP element	Promoter upstream element
V	Valine
V	Volts
V. cholerae	*Vibrio cholerae*
W	Watts
WT	Wild-type
ZF	Zebrafish larvae
σ^{70}	Sigma 70
Ω	Ohm

Introduction

Chapter 1

1.1 Bacterial gene expression and regulation

Bacterial cells use intricate molecular processes to regulate the activity of genes and proteins (Watson, 2014). These processes allow bacteria to respond to their varied environments (Watson, 2014). Hence, transcriptional control determines which messenger RNA (mRNA) is transcribed from the DNA template and translational control which mRNA molecules are translated to make polypeptides (Figure 1.1)

1.2 Transcription by RNA polymerase

RNA polymerase (RNAP) catalyses the synthesis of RNA using the DNA as a template in a process called transcription. This is the first step of gene expression and is carefully regulated. The RNAP core enzyme is approximately 400 kDa and is made up of multiple subunits (Browning and Busby, 2016). Hence, there are two copies of the α subunit and one each of β, β' and ω subunits, arranged in a 'crab-claw' structure (Browning and Busby, 2016). Alone, the RNAP core enzyme is capable of catalysing transcription of RNA non-specifically (Yang and Lewis, 2010). A high resolution structure of the RNAP, and a simplified schematic, is shown in Figure 1.2. For specific transcription of genes to occur, RNAP must recognise defined sites on the DNA strand (Feklistov, 2013; Lee *et al.*, 2012). To do this, the core enzyme associates with a specialised DNA binding protein called a sigma (σ) factor (Figure 1.2).

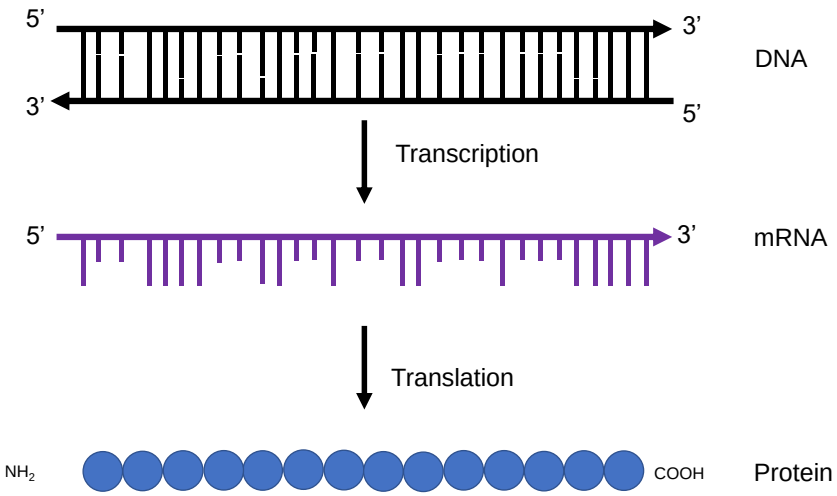

Figure 1.1. Bacterial gene expression

Schematic diagram of bacterial gene expression. The DNA helix is shown in black. The rungs represent nucleotide base pairs and the rails represent the sugar phosphate backbone. The 5’ and 3’ notations represent carbons attached to the phosphate and hydroxyl groups of the backbone respectively. DNA serves as the template from which mRNA is synthesised (transcription). The resulting mRNA molecules, shown in purple, provide the template from which polypeptides are synthesised (translation). The protein chain and the amino acids that make up the polypeptide chain are shown as blue circles. NH_2 and COOH represent the amino and the carboxyl terminals of the protein respectively.

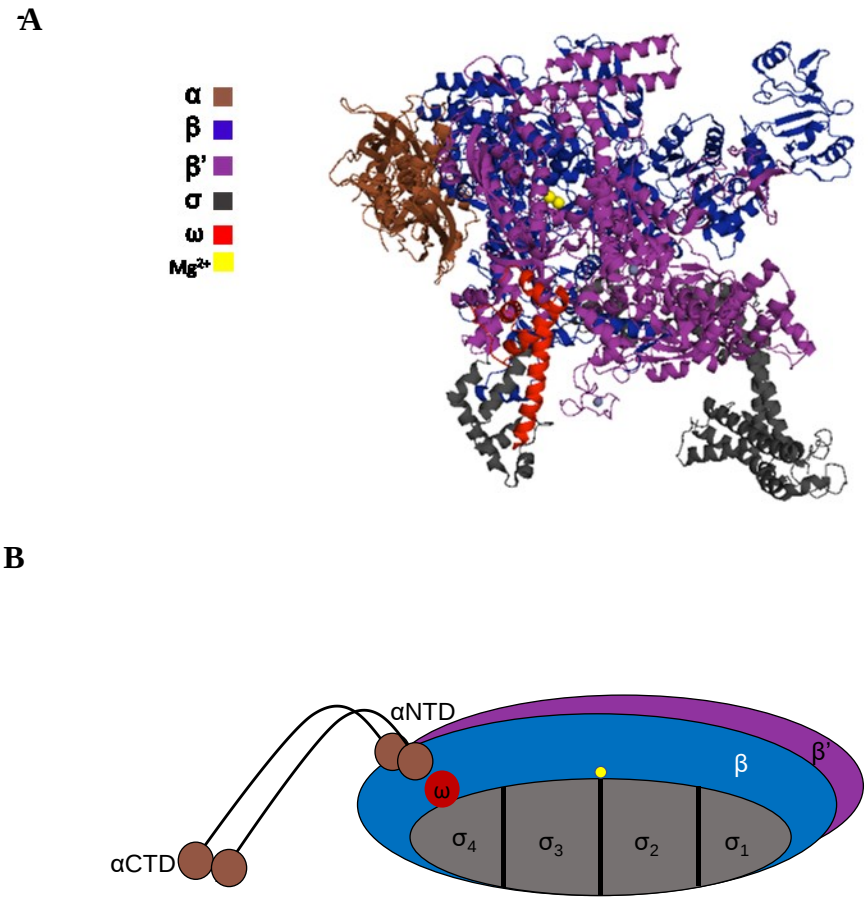

Figure 1.2. RNA Polymerase holoenzyme

A) Crystal structure of *E. coli* RNAP holoenzyme. The subunits are colour coded and the Mg^{2+} is shown in yellow. Image is based on Murakami (2013), and was generated using PyMOL (The PyMOL Molecular Graphics System, Version 2.0 Schrödinger, LLC.) Protein data bank accession number 4YG2(Murakami, 2013).

B) Schematic diagram of the RNA polymerase holoenzyme. The β and β' subunits are shown in blue and purple respectively. The αCTD and αNTD domains are shown in brown and the sigma factor (σ) is shown in grey. The ω subunit is shown in red and the catalytic Mg^{2+} is shown in yellow (Browning and Busby, 2004; Feklistov, 2013).

This form of RNAP (the holoenzyme) is able to recognise specific DNA sequences called promoters, thereby transcription initiates at defined sites (Feklistov, 2013). Many regulatory steps occur at the transcription initiation stage and determine whether a gene will be transcribed or not (Browning and Busby, 2016).

1.3 Promoters

Promoters are regions of DNA that stimulate transcription and are found upstream of genes (Bae *et al.*, 2015). Housekeeping promoters typically contain two conserved regions of six nucleotides. These are called the -10 and -35 elements and are separated by 16-19 nucleotides (Estrem *et al.*, 1999; Yang and Lewis, 2010; Shimada *et al.*, 2014; Ruff *et al.*, 2015). The -10 element (TATAAT) and the -35 element (TTGACA) together comprise the core promoter (Feklistov, 2013). Most bacteria have one major housekeeping σ factor. In *Escherichia coli* this is referred to as σ^{70} and is responsible for initiating transcription from thousands of promoters during exponential growth (Shimada *et al.*, 2014). The sequence of promoters usually differs from the consensus and correlates with basal promoter activity (Shimada *et al.*, 2014). Hence, promoters can either be weak (poor sequence similarity to consensus) or strong (high sequence similarity to consensus) drivers of transcription. Promoter strength is also defined by the presence of additional DNA elements that enhance the binding of RNAP (Browning and Busby, 2004). Such elements include the extended -10 element (a TGn motif upstream of a standard -10) and UP element (Figure 1.3). These provide additional contacts for RNAP (Ross *et al.*, 1993; Burr *et al.*, 2000).

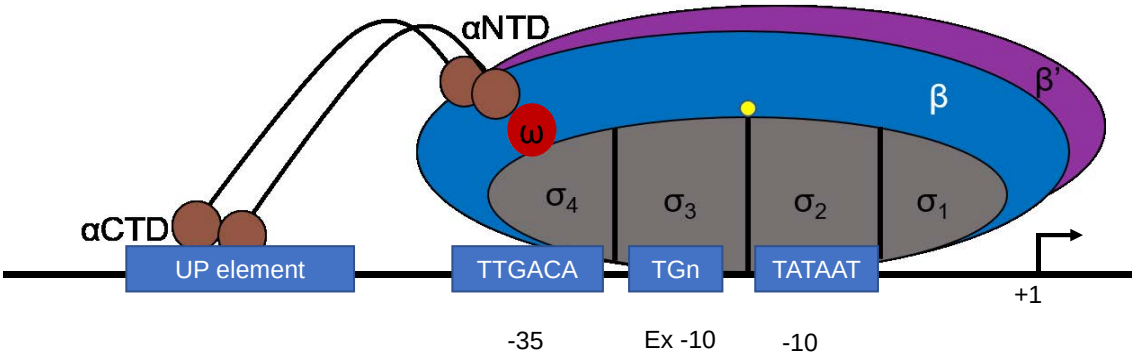

Figure 1.3. Bacterial Promoter

Schematic diagram of a bacterial promoter. The black arrow labelled +1 denotes the transcription start site. The -10, extended -10 and -35 motifs are recognised by σ (grey), and the UP element is recognised by αCTD (brown circles) subunit of RNAP. The omega subunit is shown as a red circle and the Mg^{2+} catalytic site is represented by a yellow circle (Feklístov *et al.*, 2014).

The process of transcription can be divided into several stages; initiation, elongation and termination (Yang and Lewis, 2010). The first step in initiation is the binding of RNAP holoenzyme to the promoter DNA as illustrated in Figure 1.4 (Browning and Busby, 2016; Murakami and Darst, 2003). Two models exist to describe this step. The first school of thought is that RNAP recognises the -10 element in double stranded form as a closed complex (Zuo and Steitz, 2015). Subsequently, it is suggested that both RNAP and the promoter DNA undergo conformational changes (isomerisation) that result in the separation of the two DNA strands, to form an open complex (Zuo and Steitz, 2015). Conversely, Feklistov and colleagues offer an alternative to the formation of a closed complex (Feklistov and Darst, 2011). Instead, they propose that recognition of the -10 element is coupled with DNA strand separation and comes into play only in the open complex. Hence, x-ray crystal structures show that specific bases of the promoter are captured by σ^{70} pockets, only in the context of the open promoter complex (Feklistov and Darst, 2011; Bae *et al.*, 2015). In both models, the open complex contains DNA denatured between positions -11 upstream and +3 downstream of the transcription start site (Yang and Lewis, 2010; Bae *et al.*, 2015; Browning and Busby, 2004; Tsujikawa *et al.*, 2002). In this conformation an uptake channel, made of regions from the RNAP β and β' subunits, is formed (Zuo and Steitz, 2015). The channel allows ribonucleotides to enter the enzyme and assemble in the active site to create a new mRNA chain (Goldman *et al.*, 2009; Feklístov *et al.*, 2014).

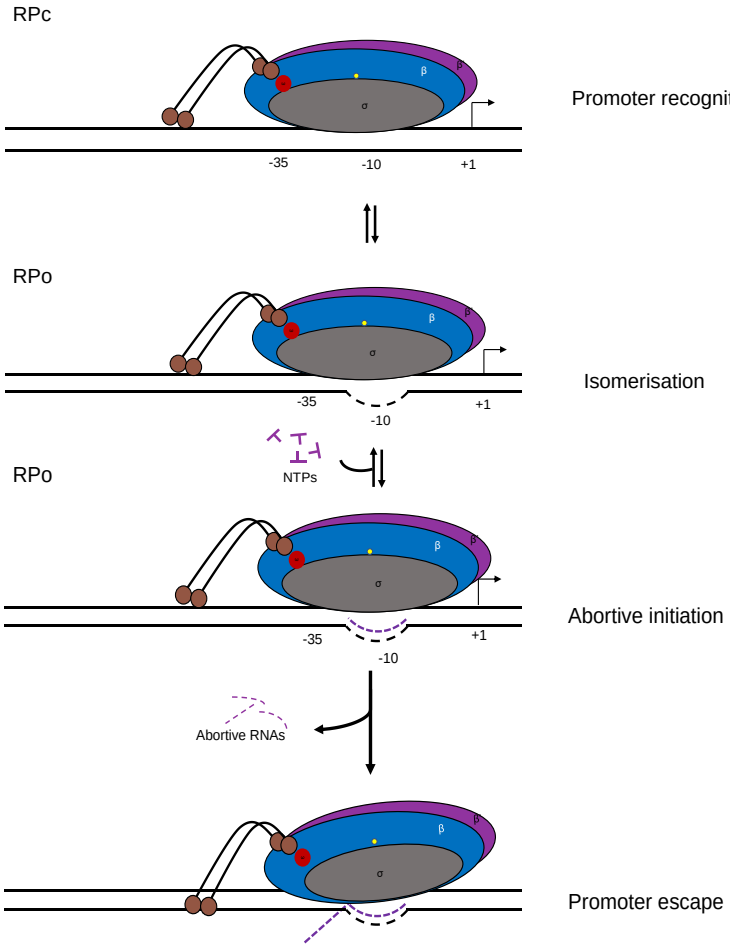

Figure 1.4. Transcription Initiation

Schematic of transcription initiation at promoter DNA. Transcription initiation occurs when RNAP binds to promoter DNA (promoter recognition) to form the closed complex (RPc). Approximately 12 bp of promoter DNA is unwound (isomerisation) to form a transcription bubble to generate an open complex (RPo). A channel is formed which enables the uptake of NTPs into the active site of RNAP to assemble mRNA. During several attempts to escape the promoter, abortive transcripts are generated (abortive RNAs). However, once more than 10 bps are transcribed, RNAP unbinds the promoter (promoter escape) and transverses along the DNA until transcription is terminated

(Marchetti *et al.,* 2017; Zhang *et al.,* 2012). The omega subunit is shown as a red circle and the Mg^{2+}, a yellow circle, represents catalytic site.

The assembly of the new mRNA chain begins with "scrunching", whereby RNAP remains fixed on the promoter DNA and pulls the downstream DNA towards itself (Kapanidis *et al.*, 2006). This typically leads to synthesis and release of short transcripts of mRNA (Kapanidis *et al.*, 2006). Once the nascent mRNA chain reaches ten ribonucleotides long, the enzyme undergoes promoter escape and moves into the elongation phase of transcription (Marchetti *et al.*, 2017). Elongation continues until RNAP reaches a pause, or terminator (Marchetti *et al.*, 2017). Termination allows accurate expression of genes by preventing the inappropriate transcription of adjacent genes. The process also ensures that RNAP is removed from the end of transcripts and recycled for use elsewhere on the chromosome (Peters *et al.*, 2011; Ray-Soni *et al.*, 2016). Bacteria utilise two main mechanisms for transcript termination; intrinsic termination and Rho-dependent termination (Ray-Soni *et al.*, 2016).

Intrinsic termination, also called Rho-independent termination, occurs when RNAP encounters a terminator sequence (Peters *et al.*, 2011). Terminator sequences are often found at the end of genes and are characterised by GC rich repeats followed by a stretch of Ts (Peters *et al.*, 2011). When transcribed, terminators create stem-loop structures, called terminator hairpins, RNA in molecules. These structures disrupt the elongation complex and the nascent RNA chain dissociates from RNAP (Peters *et al.*, 2011; Ray-Soni *et al.*, 2016).

In Rho-dependent termination, an auxiliary protein called Rho, an RNA-dependent ATPase, is required for termination (Banerjee *et al.*, 2006). Rho binds to the nascent RNA and translocates along the mRNA chain until it encounters the elongation complex and

causes the dissociation of RNAP from the DNA (Banerjee *et al.*, 2006; Grylak-Mielnicka *et al.*, 2016). In contrast to intrinsic terminators, natural Rho utilisation (*rut*) sites are less-specific and contain few common features apart from high C content sequences (Peters *et al.*, 2011).

1.4 Transcriptional Regulation

In bacteria, control of gene expression often responds to extracellular signals (Browning and Busby, 2004; Marchetti *et al.*, 2017). These signals lead to the regulation of target genes by regulatory proteins such as transcription factors (TF) (Browning and Busby, 2004; Lee *et al.*, 2012). These proteins can positively regulate gene transcription (activators) or negatively regulate transcription (repressors) (Browning and Busby, 2004). Since RNAP binds weakly at many promoters (Lee *et al.*, 2012) transcription initiation can be enhanced by the direct or indirect effect of activators on RNAP (Browning and Busby, 2004). Hence, activators often bind in the proximity of promoters to enhance transcription (Browning and Busby, 2004; Martínez-Antonio and Collado-Vides, 2003). One such transcription factor is a global regulator called cyclic AMP receptor protein (CRP). *E. coli* encodes seven global regulatory proteins that directly and indirectly modulate 50% of all genes in *E. coli* (Martínez-Antonio and Collado-Vides, 2003). The widely accepted role of CRP is as the main regulator of catabolism in enteric bacteria (Shimada *et al.*, 2011). In *E. coli*, CRP controls carbon metabolism by regulating the

transcription of genes that facilitate the use of alternate carbon sources in a regulatory process called catabolite repression (Botsford and Harman, 1992).

In addition to its role in catabolite repression, CRP also regulates the expression of genes involved in pathogenicity and processes not related to metabolism (Botsford and Harman, 1992; Skorupski and Taylor, 1997a; Chattopadhyay and Parrack, 2006; Zahid *et al.*, 2015). Usually, CRP activates transcription by binding upstream of, or adjacent to, the -35 promoter element. Depending on the position of the CRP site, promoters are called Class I, II or III (Browning and Busby, 2004).

1.5 Transcription regulation by CRP

The *E. coli* CRP binds as a 45 kDa dimer and is composed of two identical 209 amino acid subunits (Kolb *et al.*, 1993). The protein shares structural properties with CRP from other enteric bacteria, suggesting a similar role in different species (Chattopadhyay and Parrack, 2006). Each CRP subunit consists of a DNA binding domain and a dimerization domain that interacts with the effector molecule cAMP (Figure 1.5) (de Crombrugghe *et al.*, 1984). The C-terminal domain (CTD) of CRP binds DNA upstream of promoters at a 22 base pair (bp) sequence 5'AAA**TGTGA**TCTAGA**TCACA**TTT 3' containing an inverted repeat motif (in bold) (Shimada *et al.*, 2011). In the absence of cAMP, CRP can be found in free solution or weakly bound to DNA (Chattopadhyay and Parrack, 2006; Kolb *et al.*, 1993). When bound to its allosteric effector molecule, cAMP, CRP undergoes conformational changes that increase sequence-specific binding to DNA (de Crombrugghe *et al.*, 1984; Botsford and Harman, 1992). In *E. coli*, CRP directly regulates transcription from more than 100 promoters by either interacting with RNAP directly (activation), or by blocking promoter access (repression) (Busby and Ebright, 1999; Müller-Hill, 1998; Kolb *et al.*, 1993). Transcription activation at CRP-dependent promoters often involves a direct contact between RNAP and surface exposed regions on CRP called activating regions (Williams *et al.*, 1996). These regions are involved in direct protein-protein interactions with RNAP but are not required for DNA binding (Zhou *et al.*, 1993).

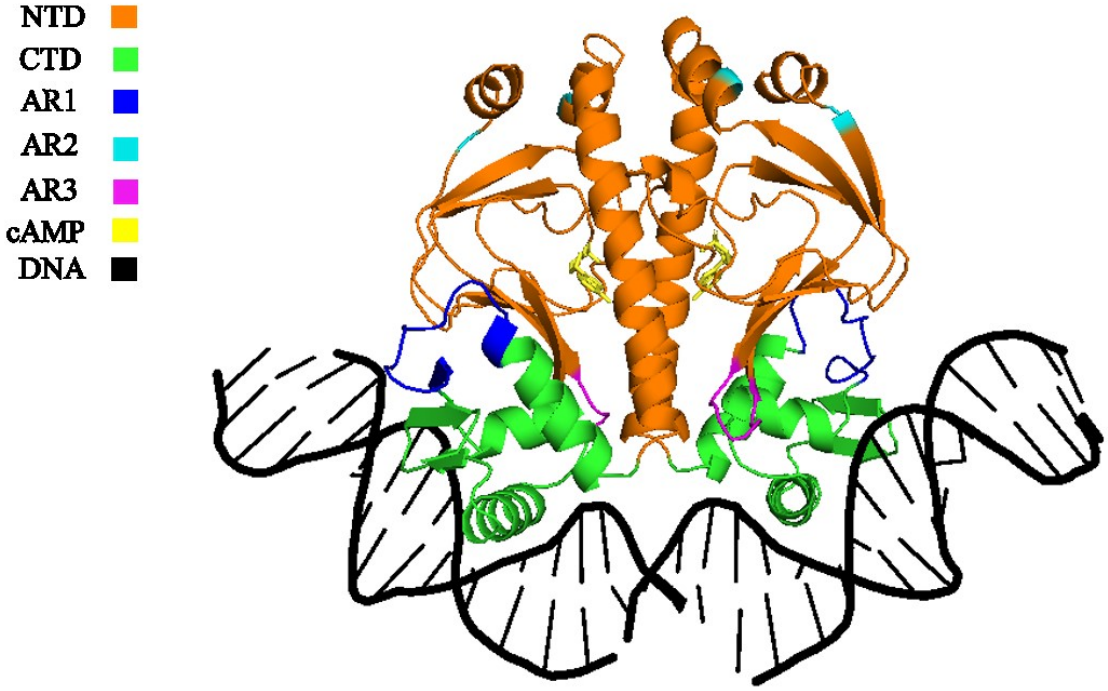

Figure 1.5. Crystal structure of CRP cAMP and DNA complex

Crystal structure of CRP subunits bound to DNA. CRP subunits shown in orange, contain cAMP molecules (yellow) bound within the dimerization N-terminal domain. Activating regions 1 (blue), 2 (cyan) and 3 (magenta) make direct contact with RNAP to activate transcription at certain promoters. DNA (shown in black) is bound by the residues (shown in green) within the C-terminal domain. Image was generated using PyMOL (Liu *et al.*, 2017). Protein data bank accession number 1J59.

1.6 CRP activated Promoters

1.6.1 Class I promoters

At class I promoters, CRP binds to DNA sites upstream of the -35 promoter element (Browning and Busby, 2016; Lawson *et al.*, 2004). CRP recruits RNAP using a single interaction requiring residues 156-164 of activating region 1(AR1) and the 287 determinant of the RNAP αCTD (Figure 1.6) (Browning and Busby, 2004; Browning and Busby, 2016; Savery *et al.*, 1998; Liu *et al.*, 2017; Savery *et al.*, 2002). Due to its ability to bend DNA, CRP binding sites can be found at various distances upstream of the transcription start site centred close to positions -61, -71, -82 or -93 (Lawson *et al.*, 2004; Zhou *et al.*, 2014). Hence, in order to activate transcription, CRP and RNAP must be bound on the same face of the DNA helix (Ebright, 1993; Zhou *et al.*, 2014). The best known example of class I activation is the *E. coli lac* promoter (Figure 1.6a), where CRP binds at position -61.5 (Ebright, 1993; Estrem *et al.*, 1999; Lawson *et al.*, 2004).

1.6.2 Class II promoters

At class II promoters, CRP binds near to position -41, overlapping the -35 promoter element (Busby and Ebright, 1997). As a result, CRP makes three interactions with RNAP to activate transcription; AR1 contacts the αCTD, AR2 the αNTD and AR3 contacts region 4 of the σ subunit (Browning and Busby, 2004; Savery *et al.*, 1998; Savery *et al.*, 1996; Rhodius and Busby, 2000). Seven residues (R265, K271, T285, E286, V287, E288 and R317) identified within the RNAP αCTD were important for the activation of transcription by CRP (Savery *et al.*, 1998). Residues T285, E286, V287, E288 and R317

were determined to be required to form interactions between CRP and RNAP αCTD but not required for RNAP αCTD- DNA interactions (Savery *et al.*, 1998). Examples of class II promoters are the *E. coli galP1* and *melR* promoters (Figure 1.6b) that have a CRP site at position -41.5 (Busby and Ebright, 1999; Lawson *et al.*, 2004).

1.6.3 Class III promoters

Class III promoters have a more complex architecture (Browning and Busby, 2004). Unlike class I and class II promoters, which contain only one CRP site, class III promoters often contain multiple CRP sites at varying distances between each other and the RNAP binding site (Ebright, 1993). Class III promoters usually require multiple RNAP contacts (Figure 1.6c), that activate transcription through a combination of class I and class II mechanisms (Busby and Ebright, 1999). At some class III promoters, CRP interacts with other activators to synergistically enhance transcription (Busby and Ebright, 1999). These interactions can either be independent, whereby CRP and the second activator each make seperate contacts with different surfaces of RNAP; or direct, in which CRP forms protein-protein interactions with another activator to allow interaction of RNAP with the -35 and -10 elements (Kolb *et al.*, 1993; Busby and Ebright, 1999).

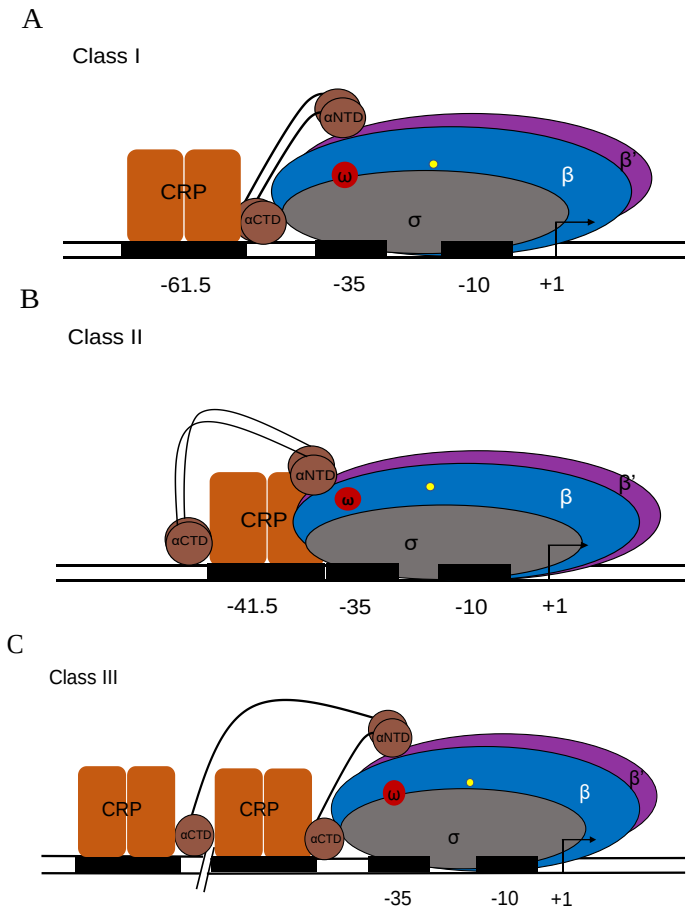

Figure 1.6. Transcription activation at different CRP promoters

Schematic of transcription activation at class I, II and III promoters.

A) At class I promoters, CRP (orange) binds as a dimer upstream of the promoter -35 element and interacts with the αCTD of RNAP to activate transcription.

B) At class II promoters the CRP binding site is adjacent to or overlaps the promoter -35 element. This leads to multiple interactions between CRP and RNAP. One copy of the αNTD interacts with activating region (AR) 2 of CRP and another interaction is made between αCTD and AR1 of CRP.

C) Class III promoters, multiple dimers of CRP act in synergy to activate transcription. Multiple interactions are made with RNAP in a combination of both class I and class II mechanisms. (Browning and Busby, 2004; Busby and Ebright, 1999).

1.7 Repression by transcription factors and nucleoid associated proteins

Repressor proteins also control transcription by binding to promoters. However, repressor binding seems to reduce or prevent RNAP binding or other steps in transcription initiation (Browning and Busby, 2004). Repression can result from interference with RNAP directly or via an activator (Browning and Busby, 2016). As reviewed by Browning and Busby (2004), there are three general mechanisms of repression; steric hindrance, repression by looping and repression by modulation of the activator (Figure 1.7).

1.7.1 Repression by steric hindrance

In repression by steric hindrance, the repressor binds close to, or overlapping, the core promoter elements (Figure 1.7a). Binding of the repressor protein may interfere with the recruitment of RNAP. This is exemplified by binding of the LexA repressor at the *uvrA* promoter and the Lac repressor to the *lac* operator region of the *lac* promoter (Browning and Busby, 2004; Rojo, 1999).

1.7.2 Repression by looping

This type of repression is caused by the interaction of distal DNA sites through the binding of multiple repressors (Figure 1.7b). An example of this type of repression is seen at the *gal* promoter that is repressed by GalR (Choy and Adhya, 1992). Interactions between repressors bound at distal promoter sites may lead to the looping of the DNA around the core promoter elements. This either prevents the recruitment of RNAP or traps RNAP at the promoter (Browning and Busby, 2004).

1.7.3 Repression by modulation of an activator

Here, the repressor interacts with the activator protein and hinders its interaction with RNAP. A classic example of such repression is the interaction between CytR and CRP at certain CRP controlled promoters (Figure 1.7c). The CytR repressor binds between two CRP dimers and shields the activating region of the activator from RNAP (Müller-Hill, 1998; Valentin-Hansen *et al.*, 1996; Browning and Busby, 2004).

1.7.4 Repression by multiple CRP sites

This type of repression is found at some promoters carrying tandem DNA sites for CRP (Lee and Busby, 2012). At these sites, the distance between the promoter and the CRP binding site determines whether promoter activity was upregulated or downregulated (Tebbutt *et al.*, 2002). Repression at these promoters was determined by the upstream CRP dimer which, when bound at position -122.5, interacts with the αCTD of RNAP preventing promoter escape (Lee and Busby, 2012).

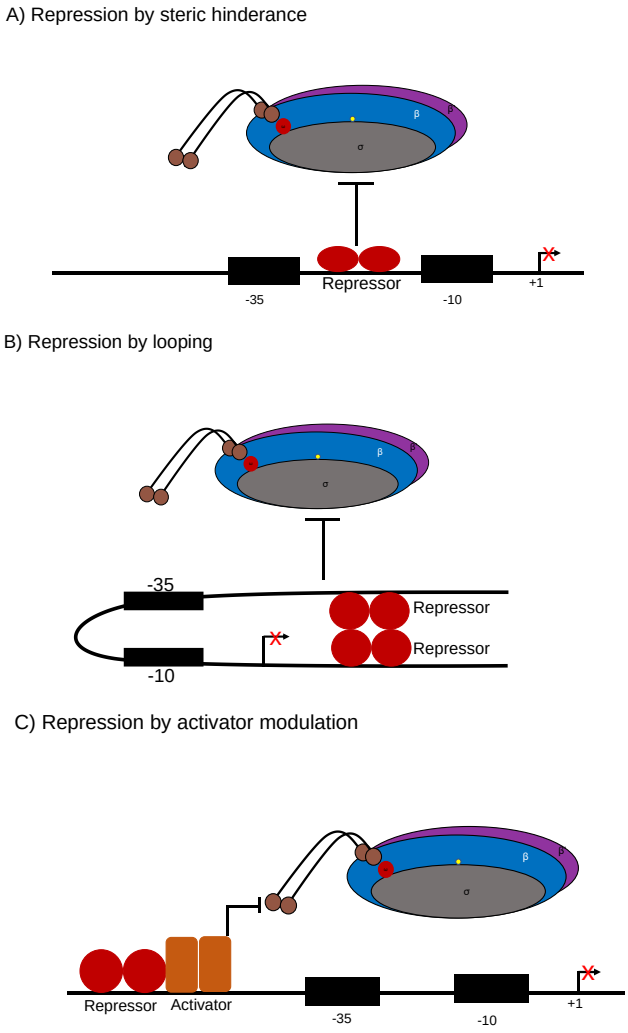

Figure 1.7. Repression mechanisms at promoters

Schematic diagram showing repression at bacterial promoters by transcription factors.

A) In repression by steric hindrance the repressor binds within the promoter elements, therefore competing with and excluding RNAP from its binding site.

B) Repression by looping occurs when repressors bind to different sites along the DNA and interact with each other. The interaction leads to the looping of DNA thus repressing the adjacent promoter.

C) Repression by modulation of activator occurs when the repressor interacts to stop transcription activators functioning. In this case CRP (orange), is prevented from interacting with RNAP (Browning and Busby, 2004; Busby and Ebright, 1999).

1.8 Transcriptional regulation by the histone-like nucleoid structuring protein

The histone-like nucleoid structuring protein (H-NS) is a nucleoid associated protein and repressor of transcription (Wang *et al.*, 2015). H-NS is an abundant nucleic acid binding protein with high affinity for AT-rich, curved DNA (Ayala *et al.*, 2017). The H-NS protein modulates gene expression by binding to, and silencing, horizontally acquired genes (Atlung and Ingmer, 1997; van der Valk *et al.*, 2017; Dorman, 2013). H-NS is a 15.4 kDa protein consisting of 137 amino acids. The protein has two domains, a C-terminal DNA binding domain and an N-terminal self-association domain (Atlung and Ingmer, 1997). H-NS binds DNA in two distinct ways, by stiffening of DNA and by bridging of the double helix as shown in Figure 1.8 (Ayala *et al.*, 2017; van der Valk *et al.*, 2017). Transcription repression by H-NS requires cooperative binding to AT-rich DNA (Ayala *et al.*, 2017). The formation of H-NS filaments across target promoter regions can exclude RNAP or trap the enzyme at promoters (Lucht *et al.*, 1994; Fang and Rimsky, 2008). Formation of filaments is through determinants in the N-terminal dimerization domain. These regions of interaction give rise to sequential head-to-head and tail-to-tail interactions that enable H-NS to self-associate and bind across stretches of DNA in a sequence independent manner (Grainger, 2016; Ayala *et al.*, 2017).

Like many regulatory proteins, H-NS controls the expression of genes through environmental signals such as pH, osmolarity and temperature (van der Valk *et al.*, 2017). The precise mechanism of how each of these factors modulate H-NS activity is unclear (van der Valk *et al.*, 2017). However, H-NS activity is subject to temperature control, with a higher affinity for DNA at 23ºC- 25ºC (Ono *et al.*, 2005; Amit *et al.*, 2003). As a result, it is believed that repression by H-NS can be relieved when bacteria encounter different temperatures and diverse environments (such as osmolarity and pH change), which act as cues for the expression of other activators that antagonise H-NS binding (Wang *et al.*, 2015).

A) Stiffening of DNA

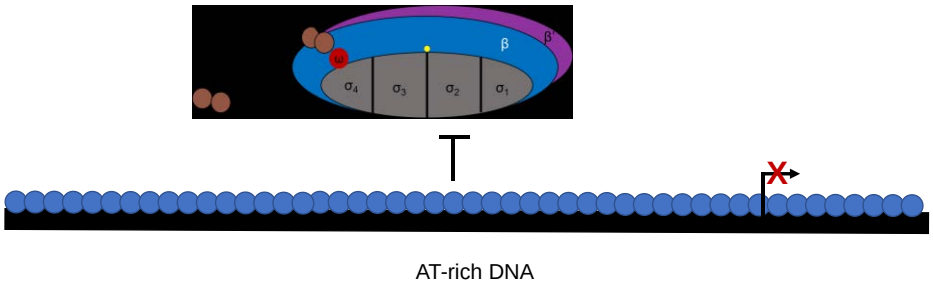

B) Bridging of DNA

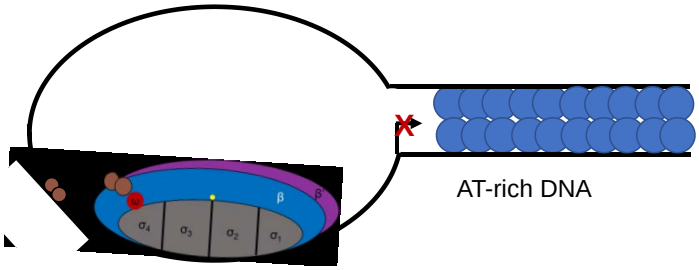

Figure 1.8. H-NS binding to DNA resulting in transcription repression

Schematic of the two main binding activities of H-NS.

A) H-NS protein (blue circles) binds across stretches of AT-rich DNA (black solid line), forming filaments that occlude RNAP from binding to promoter DNA, therefore repressing the transcription of target genes.

B) The H-NS protein can also bridge two segments of AT-rich DNA, forming a repression loop at promoter DNA.

1.9 *Vibrio cholerae*

Regulation of gene expression by environmental signals allows bacteria to compete effectively with other microbes within their host (Hibbing *et al.*, 2010). The human gut is a classic example of a niche where enteric bacteria compete for nutrients and survival (Hibbing *et al.*, 2010; Maynard *et al.*, 2012). Some bacterial species can occupy the intestines as commensals, having evolved to decrease their pathogenicity and benefit from the gut's environment. Other bacteria cause disease (Maynard *et al.*, 2012). *Vibrio cholerae* is a Gram negative bacterium that causes the disease cholera (Kaper *et al.*, 1995). *V. cholerae* is found throughout the world, particularly in coastal areas, where the bacterium is often associated with aquatic fauna (Colwell and Huq, 1994; Ayala *et al.*, 2017). Cholera is caused by the ingestion of food or water contaminated with *V. cholerae* (Kim *et al.*, 2014). Every year, it is estimated that 4.3 million people are infected by *V. cholerae*, resulting in 142, 000 deaths (Ali *et al.*, 2015; WHO, 2017).

Since 1817, when the first recorded cholera pandemic began, more than 200 different serogroups of *V. cholerae* have been isolated from the environment (Beyhan *et al.*, 2006). Of these, only two serogroups, the O139 serogroup and the O1 serogroup, have been the causative agents of epidemic and pandemic cholera (Matson *et al.*, 2007). The most predominant serogroup, O1, exists as two biotypes; classical and El Tor. The El Tor biotype is most persistent in aquatic environments and now dominates (Matson *et al.*, 2007; Dziejman *et al.*, 2002).

Classical and El Tor biotypes of *V. cholerae* O1 are genetically, phenotypically, and pathogenically different. The El Tor strain contains two horizontally transferred elements; *Vibrio* Seventh Pandemic islands one and two (VSP-I and VSP-II), which are absent in classical strains (Dziejman *et al.*, 2002). The presence of an intact six gene repeat-in-toxin (RTX) cluster is also unique to El Tor strains compared to the truncated version found in classical strains (Safa *et al.*, 2010). *V. cholerae* El Tor is better adapted for survival inside the human than the classical strain and has a longer duration of carriage after infection. This decreased virulence and longer carriage time enables the strain to be widely disseminated by the host to become endemic and thus outnumber the classical strain (Chaudhuri and Chatterjee, 2009; Mandal *et al.*, 2011). Hence, the classical biotype has largely been replaced by El Tor biotype (Nair *et al.*, 2006).

1.10 Transition from environmental reservoir to host

The natural reservoir of *V. cholerae* is brackish waterways where the bacterium is often bound to the chitinous exoskeletons of zooplankton (Matson *et al.*, 2007; Colwell and Huq, 1994; Ayala *et al.*, 2017). Chitin, a polymer of N-acetylglucosamine (GlcNAc) is a widespread polysaccharide found in the cell wall of fungi and the exoskeletons of crustaceans (Markov *et al.*, 2015). Furthermore, GlcNAc is a common modification of glycoproteins in the human intestinal epithelium (Meibom *et al.*, 2004; Matson *et al.*, 2007). *V. cholerae* expresses a protein called GbpA which allows the bacterium to effectively bind to GlcNAc (Kirn *et al.*, 2005). This attachment enables *V. cholerae* to survive in nutrient poor environments by utilising GlcNAc as a sole source of carbon and nitrogen (Meibom *et al.*, 2005).

Whilst in these environments, some *V. cholerae* enter into a viable but non culturable (VBNC) state or transition into the rugose phenotype often associated with biofilms (Morris, 2011). VBNC cells are metabolically dormant, but still capable of effective intestinal colonisation (Teschler *et al.*, 2015; Almagro-Moreno *et al.*, 2015). The formation of biofilms containing VBNC, and high doses of infective *V. cholerae*, are considerable contributors to the disease process (Hobley *et al.*, 2015; Tamayo *et al.*, 2010).

Ingestion of biofilms are one form in which *V. cholerae* infects its host, due to the concentration of cells present within them (Colwell *et al.*, 2003). Once ingested the biofilm protects resident bacteria from stomach acids and enables them to reach the small intestine and establish infection (Zhu and Mekalanos, 2003). The intestinal environment

is associated with changes in pH, osmolarity and temperature. These signals cause changes in the bacterium's transcriptome; expression of genes required for virulence and survival within the host increases (Silva and Benitez, 2016). Elucidating the exact regulators of this switch from environment to host continues to be the subject of intense study.

1.11 The ToxR Regulon

Expression of virulence determinants in *V. cholerae* involves a cascade of regulatory factors. The master regulator of this cascade is the 32 kDa membrane bound transcription factor, ToxR (Faruque *et al.*, 1998). Expression of ToxR is under the control of environmental factors such as change in temperature, the presence of bile and osmolarity (Chaudhuri and Chatterjee, 2009). ToxS, another transmembrane protein, enhances the activity of ToxR and acts as a stabiliser or assembly point for ToxR monomers to form dimers. The major role of ToxR is to induce the expression of *toxT* in concert with a second activator called TcpP (Figure 1.9). Once expressed, ToxT activates the expression of genes encoding the major *V. cholerae* virulence factors and other colonisation genes (Kazi *et al.*, 2016).

As well as activating genes encoding virulence factors via ToxT, ToxR directly regulates *V. cholerae's* major outer membrane porins OmpU and OmpT (Kazi *et al.*, 2016). Expression of these outer membrane porins is crucial for *V. cholerae's* survival in the host; they enable the bacterium to resist antimicrobial peptides, bile and organic acids (Merrell *et al.*, 2001; Mathur and Waldor, 2004). Recently, it has been shown that ToxR shares more than a third of its regulon with H-NS and antagonises H-NS repression to activate gene expression (Kazi *et al.*, 2016; Nye *et al.*, 2000).

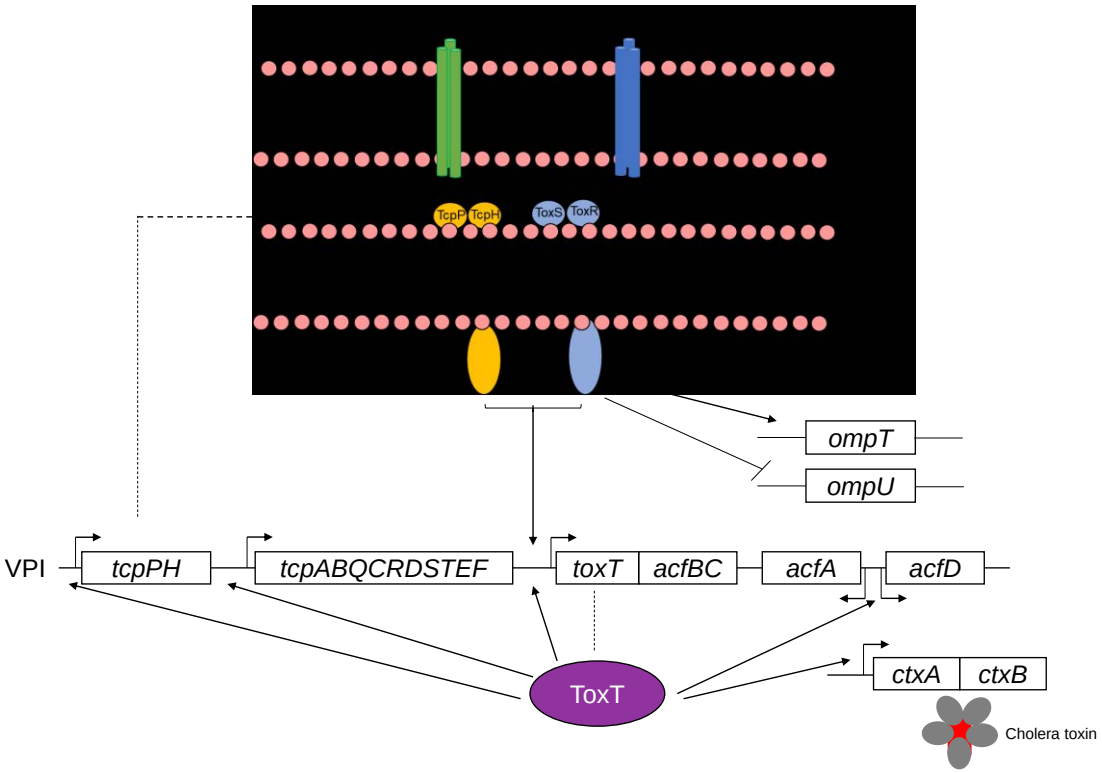

Figure 1.9. ToxR Regulon

Schematic representation of the ToxR regulon. Environmental signals are the primary initiators of virulence factor expression. This leads to the expression of *tcpPH*. TcpPH interacts with ToxRS to activate transcription of *toxT*. ToxT (purple) activates transcription of other virulence factors and accessory toxins. ToxR also regulates the transcription of OmpU and OmpT, enabling the bacteria to tolerate resistance to antimicrobial peptides, bile, and tolerance to organic acids (Childers and Klose, 2007). Broken lines point to the protein encoded by the genes.

1.12 ToxT structure and function

ToxT is directly responsible for the activation of virulence gene expression in *V. cholerae*. The ToxT protein (32 kDa) is a member of the AraC family of transcriptional regulators. Hence, the protein is composed of two domains, an NTD of 164 aa and a 112 aa CTD (Withey and DiRita, 2006). The NTD functions as an environmental sensor and is involved in dimerization while the CTD binds DNA (Lowden *et al.*, 2010). ToxT directly activates the expression of the major virulence genes and autoregulates its own expression from the *tcp* promoter (Figure 1.9) (Li *et al.*, 2016). ToxT binds to DNA promoter regions upstream of target genes to activate transcription.

Unlike regulatory proteins such as CRP, which binds to specific DNA motifs, tracts of four or more consecutive T/A nucleotides are the only common features found upstream of ToxT activated genes (Withey and DiRita, 2006). These sequences can occur singularly and form direct or inverted repeats. The motifs enable ToxT to bind DNA and positively regulate gene expression as a dimer or monomer, depending on the structure of the binding site (Lowden *et al.*, 2010). The ToxT binding sites, or 'toxboxes', are all located upstream of the -35 promoter element (Bellair and Withey, 2008).

This configuration makes all ToxT-dependent promoters class I promoters, suggesting an interaction with αCTD of RNAP (Weber *et al.*, 2011). Genetic analysis using a *rpoA* truncation mutation, conducted by Hulbert and colleagues, showed that ToxT-dependent activation at the *tcpA* promoter involved interaction with αCTD of RNAP (Hulbert and Taylor, 2002).

1.13 Overview of virulence factors

V. cholerae produces an array of virulence and colonisation factors that exert toxic effects on the host and provide a growth and survival advantage to the pathogen. The *V. cholerae* genome consists of two circular chromosomes of 2.9 million and 1.07 million bps in length respectively (Heidelberg *et al.*, 2000). Most of the genes required for growth, viability and virulence are found on chromosome I. In comparison, Chromosome II contains a larger number of hypothetical genes and genes of unknown function (Heidelberg *et al.*, 2000).

1.14 Cholera Toxin

The cholera toxin (CT) is the best understood virulence factor produced by *V. cholerae* and is the cause of many clinical manifestations of cholera (Chaudhuri and Chatterjee, 2009). The operon encoding the CT toxin, *ctxAB*, is found on chromosome I within the lysogenic bacteriophage CTXϕ (Chaudhuri and Chatterjee, 2009; Waldor and Mekalanos, 1996). Horizontal acquisition of *ctxAB* distinguishes nontoxigenic and toxigenic strains of *V. cholerae* (Chaudhuri and Chatterjee, 2009). The CT holotoxin is made up of one A and five B subunits (Figure 1.10). The B subunit is 11.6 kDa, made up of 103 aa, and directs the holotoxin to the ganglioside GM_1 receptors on the intestinal mucosa membrane. Translocation of the 27.2 kDa A subunit into the epithelial cell follows (Kaper *et al.*, 1995). Upon translocation, the A subunit undergoes proteolytic cleavage into A_1 (195 aa) and A_2 (45 aa) (Field, 1979). The target for the internalised CT toxin is adenylate cyclase. This enzyme mediates the conversion of ATP to cAMP and is one of the most important regulatory systems of eukaryotic cells (McDonough and Rodriguez, 2012). Regulation of adenylate cyclase is mediated by heterodimeric G proteins, which links surface receptors to effector proteins (Kaper *et al.*, 1995). CT ADP-ribosylates G proteins, rendering adenylyl cyclase constitutively active (McDonough and Rodriguez, 2012). Increased intracellular levels of cAMP leads to alterations in cellular ion transport. This causes an increase in secretion of Cl^- and decreased absorption of NaCl (Figure 1.10). The osmotic difference causes water to be drawn up from intravascular and extracellular spaces and this is rapidly lost as the characteristic 'rice-water' secretory diarrhoea (Chaudhuri and Chatterjee, 2009).

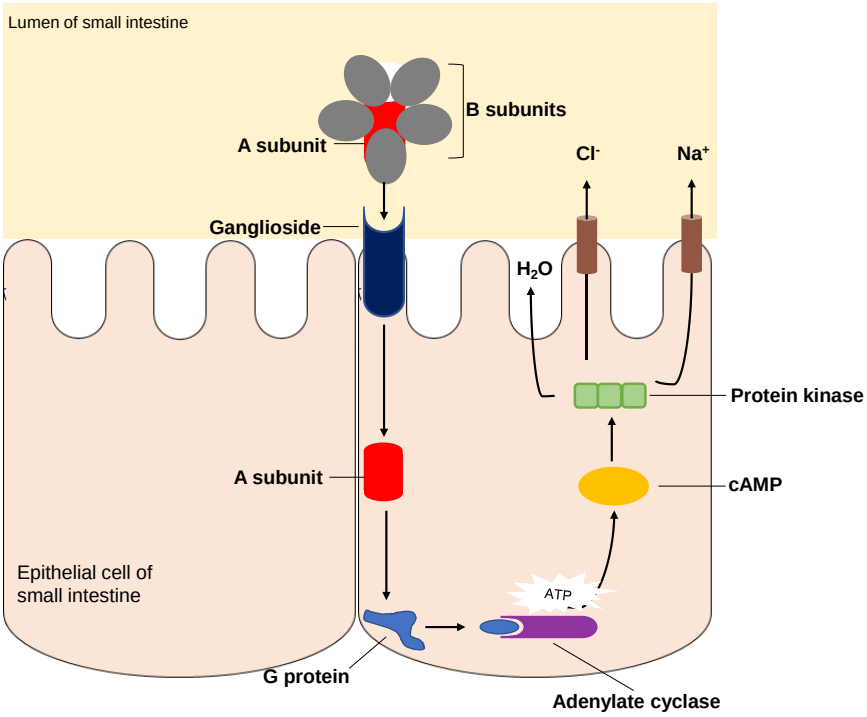

Figure 1.10. Pathway of Cholera Toxin

Schematic of *V. cholerae* cholera toxin (CT) action. The CT holotoxin is composed of five B subunits (grey circles) and one A subunit. The ganglioside receptor (blue) is bound by the B subunit of the toxin, which enables the translocation of the A subunit into the cell. Once inside the cell, the A subunit undergoes proteolytic cleavage, that leads to a cascade of reactions such as the ribosylation of G proteins which ultimately leads to the constitutive expression of adenylate cyclase. Adenylate cyclase catalyses the production of cAMP which leads to alterations in the cellular transport membrane. This results in loss of nutrients and water as diarrhoea (Thiagarajah and Verkman, 2005).

1.15 Toxin co-regulated pilus

The genes encoding the toxin co-regulated pilus (TCP) proteins are located in the horizontally acquired *tcp* operon (Figure 1.9). This operon locates to the vibrio pathogenicity island (VPI) on chromosome I (Waldor and Mekalanos, 1996; Chang *et al.*, 2017). The TCP is the receptor of the CTXϕ bacteriophage that encodes CT. Thus, the presence of TCP is a vital prerequisite that enables benign non-toxigenic strains of *V. cholerae* to become pathogenic (Chang *et al.*, 2017). TCP is co-ordinately expressed with CT and is an essential virulence factor for *V. cholerae*. In 1988, Herrington *et al.* (1988) showed that TCP was one of the main colonisation factors that contributed to human disease (Herrington *et al.*, 1988; Kaper *et al.*, 1995). In *V. cholerae*, TCP are self-aggregating type IV pili made up of TcpA subunit polymers (Chang *et al.*, 2017). The pili enable motility, and the formation of microcolonies and biofilms (Taylor *et al.*, 1987; Kirn *et al.*, 2000). Formation of microcolonies protects the bacterium from the host's immune response and locally concentrates the secreted CT toxin (Taylor *et al.*, 1987). ToxT activates expression of the *tcp* genes as shown in Figure 1.9.

1.16 Multifunctional-autoprocessing repeats-in-toxin toxin

The *V. cholerae* multifunctional-autoprocessing repeats-in-toxin (MARTX or $MARTX_{Vc}$) toxin is one of the accessory toxins of *V. cholerae*. The toxin and toxin export machinery are encoded by divergently transcribed *rtxHCA* and *rtxBDE* genes respectively. The $MARTX_{Vc}$ toxin belongs to a superfamily of RTX (repeats-in-toxin) toxins that contain repeated GD-rich Ca^{2+} binding motifs (Lin *et al.*, 1999; Kudryashova *et al.*, 2014). *V. cholerae* exports $MARTX_{Vc}$ via an atypical type one secretion system made up of transport ATPases (*rtxB, rtxE*), a linker protein (*rtxD*) and TolC (Boardman and Fullner Satchell, 2004). The toxin, encoded by *rtxA*, functions by promoting intestinal colonisation and evasion of host immune response (Olivier *et al.*, 2007; Queen and Satchell, 2013). $MARTX_{Vc}$ is a large 4545 aa toxin that causes the cross-linking of actin molecules and works with the pore-forming haemolysin and CT to avoid neutrophil clearance (Ma *et al.*, 2009; Queen and Satchell, 2013; Sheahan *et al.*, 2004). The toxin carries three main effector domains; actin cross-linking domain (ACD), the Rho inactivation domain (RID) and cysteine protease domain (CPD) and an alpha/beta hydrolase effector all linked by four unstructured regions (J.F, 2011). The N and C terminal domains of the toxin contain glycine rich repeats that are proposed to function as transmembrane pores for the translocation of the toxin (J.F, 2011). Once in the cytosol, the translocated CPD is activated by the small molecule inositol hexakisphosphate ($InsP_6$). $InsP_6$, is present in the eukaryotic cytosol at high concentrations but is absent from bacteria (Satchell, 2015). Once activated, the CPD can autoprocess the rest of the holotoxin at the unstructured regions between the effector domains. These effector

domains are then released into the cytosol where they proceed to induce cytotoxic and cytopathic effects (Satchell, 2015).

A) MARTX$_{Vc}$

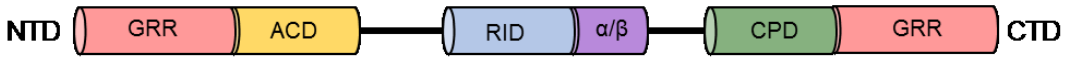

B) Activation of toxin

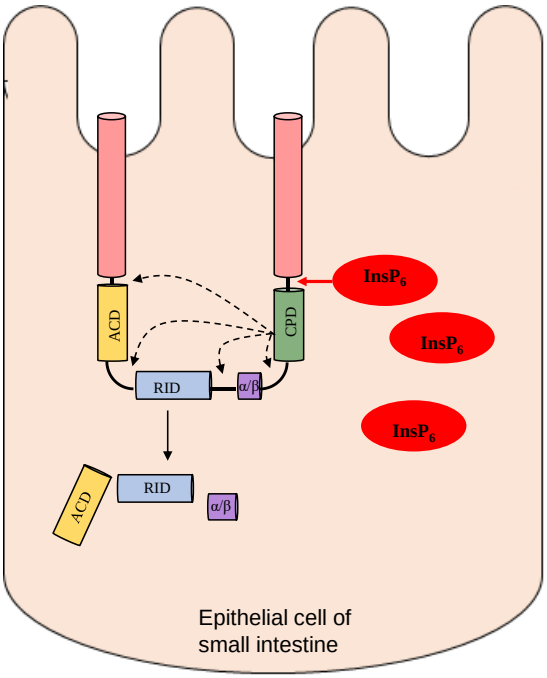

Figure 1.11. MARTX$_{Vc}$ toxin pathway

Schematic of MARTX$_{Vc}$ toxin pathway. A) MARTX$_{Vc}$ is made up of glycine rich repeats (GRR) (pink) which form the translocation domain, and the three main effector domains; actin crosslinking domain (yellow), rho-inactivating domain (blue), alpha beta hydrolase (purple) and cysteine protease domain (green). B) Once in the cytosol, the CPD is activated by InsP6 (red). CPD proteolytically activates the rest of the effector domains enabling them to carry out cytotoxic and cytopathic effects on the cell (Satchell, 2015).

1.17 Animal models for Cholera disease and colonisation

Since the discovery of *V. cholerae*, there have been numerus attempts to generate the 'perfect infection model' to study the disease. These models have ranged from the use of white mice by Roux in 1883, dogs by Nicati and Rietsch in 1884 and again by Carpenter and colleagues in 1966 and guinea pigs by Pfeiffer in 1894 (Carpenter *et al.*, 1968; Pullitzer, 1959). However, the results generated by such models are erratic and seldom display the same disease characteristics as those seen in humans (Aziz *et al.*, 1968). One reason for lack of reproducible results is that normal adult mammals, except humans, are not colonised by the bacterium (Klose, 2000). As a result, animals must be surgically altered to allow colonisation of their intestines. This is invasive and requires extensive surgical manipulation (Klose, 2000).

An alternative model is the adult rabbit ileal loop, developed in 1953 by De and Chatterje (De and Chatterje, 1953). However, this again requires surgical intervention. More recently, work has shown that, *V. cholerae* can efficiently colonise the intestines of the suckling rabbit and mouse due to their naïve host defences (Richardson, 1994). These models do yield consistent results and are, to date, the most widely used models to study *V. cholerae* (Ritchie *et al.*, 2010).

However, despite their extensive use, no pathogenesis is evident in the infant mouse and the pathogenesis seen in the rabbit model does not strongly resemble that seen in humans (Runft *et al.*, 2014). Due to limitations of mammalian models, the use of non-mammalian models has increased. These models include *Drosophila melanogaster* and the zebrafish, *Danio rerio* (Blow *et al.*, 2005; Engeszer *et al.*, 2007; Perez-Soto *et al.*, 2017). Fish are

suggested to be a suitable model due to widespread intestinal colonisation of various species with *V. cholerae* (Senderovich *et al.*, 2010). Specifically, the zebrafish's natural habitat overlaps areas where cholera is endemic, suggesting a natural association between *V. cholerae* and zebrafish in the wild (Engeszer *et al.*, 2007).

1.18 *Vibrio cholerae* CRP

The *V. cholerae* CRP (VcCRP) protein shares 95% sequence identity with *E. coli* CRP (Figure 1.12) (Skorupski and Taylor, 1997b). Like *E. coli* CRP, VcCRP is dimeric and, when bound by its effector molecule cAMP, can regulate gene transcription from target promoters (Chattopadhyay and Parrack, 2006). VcCRP plays an important role in the regulation of *V. cholerae* virulence and pathogenesis (Chattopadhyay and Parrack, 2006). For example, CRP can reduce virulence through the activation the master quorum sensing regulator HapR and decreasing expression of CT and TCP (Skorupski and Taylor, 1997a).

1.19 Deciphering transcription regulons in bacteria

In recent years, interest has grown in mapping all binding sites of transcription factors and characterising the effects of binding to sites at target promoters (Li *et al.*, 2016; Carey *et al.*, 2012; Bellair and Withey, 2008). Experimental strategies include chromatin immunoprecipitation (ChIP) and the use of bioinformatics (Carey *et al.*, 2012). The ChIP technique can be coupled with deep sequencing (ChIP-seq) to identify the genome wide binding profiles of transcriptional regulators and other DNA binding proteins. In 2015, Haycocks *et al.* (2015) used this technique to identify CRP and H-NS as the triggers of enterotoxin gene expression in enterotoxigenic *E. coli* (ETEC). A similar experiment was conducted, by James Haycocks, to identify binding sites of CRP and σ^{70} across both chromosomes of *V. cholerae* (Figure 1.13) (unpublished data).

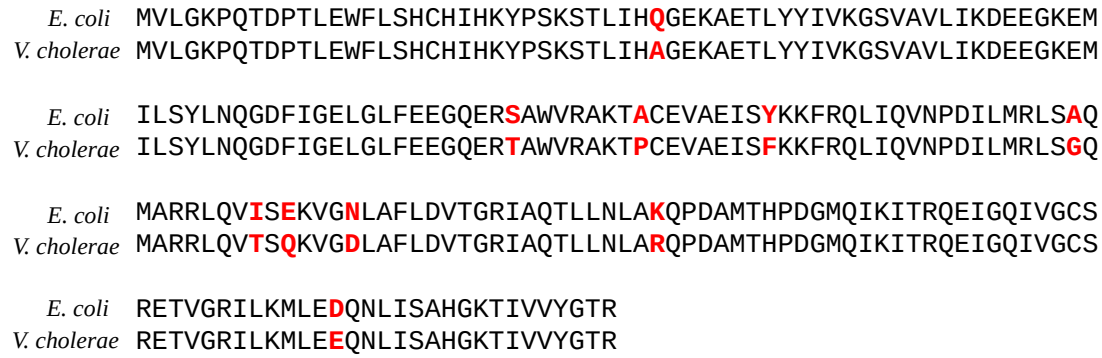

Figure 1.12. Amino acid sequence alignment of *E. coli* and *V. cholerae* CRP

Sequence alignment of *E. coli* and *V. cholerae* CRP. The black letters show regions of identity and the red letters shows regions of disparity between the two sequences. Each letter represents an amino acid.

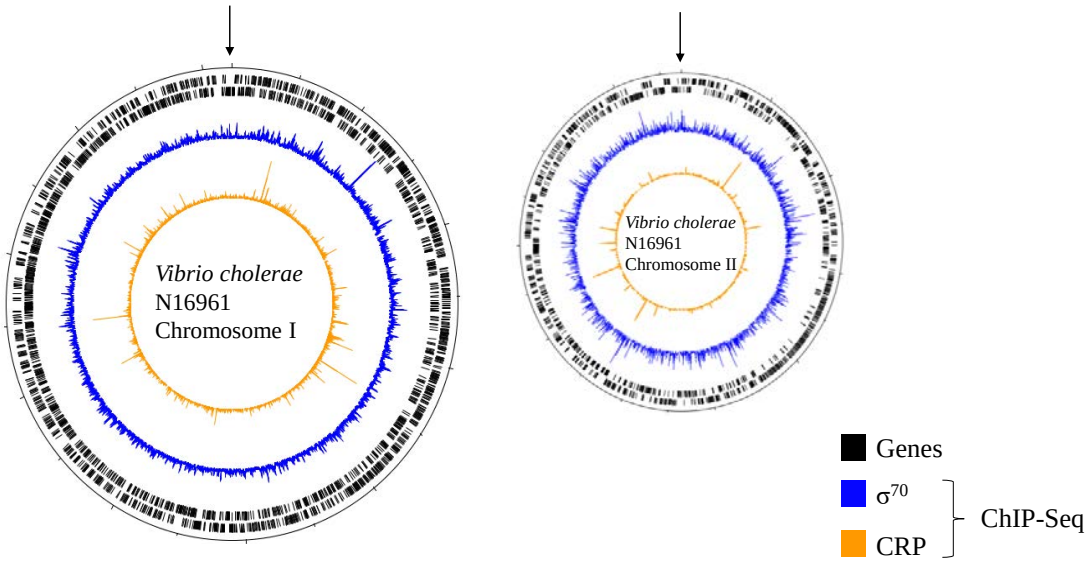

Figure 1.13. CRP and RNAP σ^{70} binding across *V. cholerae* genome

Plots show the genome wide binding of CRP and RNAP σ^{70} for the two N16961 chromosomes. The experiment was conducted on *V. cholerae* N16961 grown to mid-log phase at 200 rpm in LB broth. In each plot, the black arrow points to the tick mark at the 12 o'clock position representing the first base pair (bp) of the chromosome. In each plot, tracks 1 and 2 (black lines) show the position of genes, track 3 (blue) is the σ^{70} binding profile and track 4 (orange) is the CRP binding profile.

1.20 Brief overview of ChIP-seq

In a ChIP-seq experiment, the protein of interest is cross-linked to DNA by treating the cells with formaldehyde. Sonication shears the DNA, and an antibody specific to the target protein is used to immunoprecipitate protein-DNA complexes. The crosslinks formed between the DNA and target protein are reversed and the released DNA is sequenced to identify sequences bound by the protein (Park, 2009; Grainger and Busby, 2008).

1.21 Overview and aims of this work

As stated above, CRP is a global transcription factor and plays a major role in *V. cholerae*. For example, VcCRP regulates both CT and TCP gene transcription. VcCRP also mediates the resistance of some *V. cholerae* strains to multiple environmental bacteriophages (Zahid *et al.*, 2015). However, excluding the unpublished ChIP-Seq analysis from our laboratory, only 7 VcCRP sites have been experimentally confirmed. Hence, it is likely that VcCRP regulates many key genes in *V. cholerae* but the regulation has not been identified.

Given the two distinct habitats of *V. cholerae*, and the use of GlcNAc for survival in the aquatic environment and the host, I hypothesised that VcCRP may be important for regulation of *V. cholerae* genes during lifestyle transitions (Kirn et al., 2005). To investigate this, I used the unpublished binding profile of VcCRP and σ^{70} across the genome of *V. cholerae* El Tor N16961 (unpublished data). This provided a catalogue of VcCRP and σ^{70} binding sites. The aim of my work was to investigate one such site at the shared regulatory region of the $MARTX_{Vc}$ toxin and transport system. I seek to determine and characterise by primer extension assays and DNAse I footprinting i) the VcCRP binding and transcription start site across the *rtxBDE* and *rtxHCA* regulatory region and ii) in using zebrafish assays, investigate the role played by VcCRP in the transition of *V. cholerae* from the environment to the host.

Chapters 3 details the optimisation of the tools used to monitor gene expression in *V. cholerae* and chapters 4 and 5 contain results of the effect of VcCRP on the *rtxBDE* and *rtxHCA* regulatory region and zebrafish assays respectively.

Materials and Methods

Chapter 2

2.1 Generic reagents and buffers

All reagents were obtained from Bioline, Thermo Fisher Scientific, Sigma-Aldrich or VWR, unless otherwise stated. Solutions used in this work were made by dissolving or diluting components in deionised distilled water (ddH_2O) and autoclaving at 121^oC at 5 psi for 20 minutes. All radioactive nucleotides were obtained from MP Biochemicals. A list of solutions and buffers used is provided below.

Phenol/chloroform extraction:

- Phenol/ chloroform/ isoamyl alcohol pH 8 (25:24:1)

Ethanol precipitation:

- 100% (*v/v*) ethanol
- 70% (*v/v*) ethanol
- 3 M sodium acetate pH.5.2
- 20 mg/ml glycogen

Preparation of competent cells:

- 100 mM calcium chloride ($CaCl_2$)
- 50 % (*v/v*) glycerol

Conjugation of bacterial cells:

- 0.9% (*w/v*) sodium chloride (NaCl)
- 20 g/L (*w/v*) Luria Bertani (LB) broth, Miller

Preparation of naturally competent cells (*V. cholerae*):

- 25 mg shrimp chitin in 2 ml microcentrifuge tubes (autoclaved)
- 0.7% (*w/v*) Instant Ocean (obtained from SwellUK aquarium systems)
- 20 g/L (*w/v*) LB Broth, Miller

Denaturing sequencing gel and Polyacrylamide gel electrophoresis (PAGE) reagents:

- 5x TBE (0.445 M Tris borate pH 8.3, 10 mM EDTA) diluted to 1X with ddH_2O prior to use
- Ammonium persulphate
- TEMED (N,N,N′,N′-Tetramethylethylenediamine)
- 30% (*w/v*) Acrylamide: 0.8% (*w/v*) bisacrylamide mix (Purchased from Geneflow)
- Sequagel ureagel system (Purchased from Geneflow)

Agarose gel electrophoresis:

- 6X Loading dye (10 mM Tris pH 7.5, 1 mM EDTA, 20% (*v/v*) glycerol, 0.025% (*v/v*) bromophenol blue, 0.025% (*v/v*) xylene cyanol FF)
- 5X TBE (0.445 M Tris borate pH 8.3, 10 mM Na_2EDTA) diluted to 1X with ddH_2O prior to use
- Agarose

β-galactosidase assays:

- 1% (*w/v*) Sodium deoxycholate
- 100% (*v/v*) Toluene
- 1 M sodium carbonate
- Z-buffer (8.53 g Na_2HPO_4, 4.87 g $NaH_2PO_4.2H_2O$ 0.75 g KCl, 0.25 g $MgSO_4$ per L of ddH_2O)
- 13 mM (8 mg/ml) 2-Nitrophenyl β-D-galactopyranoside (ONPG) made up to 100 ml in Z-buffer
- β-mercaptoethanol, 271 μl per 100 ml of Z-buffer before use

In vitro transcription:

- 10X Transcription (TNSC) buffer (400 mM Tris acetate pH 7.9, 10 mM, $MgCl_2$, 1 M KCl, 10 mM DTT)
- STOP solution (97.5% (*v/v*) deionised formamide, 10 mM EDTA, 0.3% (*v/v*))
- Bromophenol Blue/ Xylene Cyanol FF
- α-^{32}P-UTP

Radiolabelling of DNA fragments:

- Tris-EDTA (TE) buffer: 10 mM Tris-HCl, 1 mM EDTA (pH 8.0)
- G-50 sephadex beads resuspended in 12% (*v/v*) TE
- T4 polynucleotide kinase
- T4 polynucleotide kinase 10x buffer
- γ-^{32}P-ATP

M13 sequencing reactions:

- 2 M Sodium hydroxide (NaOH)
- Annealing buffer 10x (1 M Tris-HCl pH 7.5, 100 mM $MgCl_2$, 160 mM DTT)
- 'A' mix short (840 µM each of dCTP, dGTP, and dTTP, 14 µM ddATP, 93.5µM dATP, 40 mM Tris-HCl pH7.5, 50 mM NaCl)
- Label mix 'A': 1.375 mM of dCTP, dGTP, and dTTP each, 333.5 mM NaCl
- T7 polymerase (purchased from Promega)
- T7 polymerase dilution buffer (25 mM Tris-HCl pH 7.5, 5 mM DTT, 100 µg/ml BSA, 5% (*v/v*) glycerol)
- STOP solution (0.025% (*v/v*) bromophenol blue, 0.025% (*v/v*) xylene cyanol FF, 10 mM EDTA pH 7.5, 97.5% (*v/v*) formamide)
- α-^{32}P-dATP

Primer extension:

- 1X Hybridisation buffer (20 mM HEPES, 0.4 M NaCl, 80% (*v/v*) formamide) DEPC treated
- 100% (*v/v*) ethanol
- 70% (*v/v*) ethanol (diluted with DEPC-treated ddH_2O)
- 3 M Sodium acetate pH 5.2
- 3 M Sodium acetate pH 7

G+A ladder generation:

- DNAse I blue (5 M urea, 20 mM NaOH, 1 mM EDTA, 0.025% (*v/v*) bromophenol blue, 0.025% (*v/v*) xylene cyanol FF)
- 10 M Piperidine, diluted to 1 M with ddH2O before use
- 100% (*v/v*) Formic acid

DNAse I footprinting:

- Recombinant DNAse I. Supplied by Roche.
- DNAse I blue: 5 M urea, 20 mM NaOH, 1 mM EDTA, 0.025% (*v/v*) bromophenol blue, 0.025% (*v/v*) xylene cyanol FF.
- 10X Transcription buffer (TNSC buffer): 400 mM Tris acetate pH 7.9, 10 mM
- $MgCl_2$, 1 M KCl, 10 mM DTT.
- DNAse I STOP solution: 0.3 M sodium acetate, 10 mM EDTA.

Zebrafish Assays

- E3 media 50X 1 L: 14.6 g NaCl, 0.65 g KCl, 2.20 g $CaCl_2$, 4.05 g MgSO4 and 23.85 g HEPES adjusted to pH 7. Working concentration used was 1X diluted in ddH_2O.
- 1-phenyl 2-thiourea (PTU): 1 mg/ml dissolved in ddH_2O, filter sterilised and stored at -20^oC. The working concentration used was 0.02 mg/ml.
- Tricaine: 40 mg/ml dissolved in ddH_2O, filter sterilised and stored at -20^oC. Concentration used for anaesthetisation was 4 mg/ml; and 40 mg/ml for euthinisation.
- Methylene blue: 0.1% (*v/v*) in ddH_2O, filter sterilised and stored at room temperature. Working concentration used was 0.03% (*v/v*) in E3 media.
- X-Gal (5-bromo-4-chloro-3-indolyl-β-D-galactopyranoside): Dissolved in dimethylformamide to obtain a stock of 40 mg/ml. The working concentration used was 40 $\mu g/ml$.
- Low melting point agarose

2.2 Media Preparation

2.2.1 Solid Media:

All solid media was made up to 1 L in ddH_2O and sterilised by autoclaving or bringing to a boil.

- Luria-Bertani (LB) Agar, Lennox (15 g/L Agar, 10 g/L Tryptone, 5 g/L Yeast Extract, 5 g/L NaCl): 35 g in 1 L of ddH_2O and autoclaved
- Luria-Bertani (LB) Agar, Miller (15 g/L Agar, 10 g/L Tryptone, 5 g/L Yeast Extract, 10 g/L NaCl): 35 g in 1 L of ddH_2O and autoclaved
- MacConkey Agar: 52 g in 1 L of ddH_2O and autoclaved
- Thiosulfate citrate bile salts sucrose (TCBS): 88 g in 1 L of ddH_2O brought to a boil.

2.2.2 Liquid Media:

All liquid media was made up to 1 L in ddH_2O and sterilised by autoclaving unless otherwise stated.

- Luria-Bertani (LB) Broth, Lennox (10 g/L Tryptone, 5 g/L Yeast Extract, 5 g/L NaCl): 20 g in 1 L of ddH_2O
- Luria-Bertani (LB) Broth, Miller (10 g/L Tryptone, 5 g/L Yeast Extract, 10 g/L NaCl): 20 g in 1 L of ddH_2O
- M9 Minimal Salts 10X: 70 g Na_2HPO_4, 30 g KH_2PO_4, 5 g NaCl and 10 g NH_4Cl in 1 L of ddH_2O and adjusted to pH 7.4

- Minimal Media (MM) 100ml: 10 ml of 10X M9 minimal salts, 200 µl 1 M $MgSO_4$ (pre-autoclaved), 100 µl of 0.1 M $CaCl_2$, 1.5 ml 20% (*w/v*) fructose and 500 µl 20% (*w/v*) casamino acids. This solution was made up to 100 ml with autoclaved ddH_2O.

2.3 Antibiotics

Stock solutions of antibiotics were prepared, filter sterilised and stored at -20ºC.

- Ampicillin: Dissolved in ddH_2O to obtain a stock solution of 100 mg/ml. The working concentration used was 100 µg/ml.
- Tetracycline: Dissolved in methanol to give a stock solution of 35 mg/ml. Working concentration used was either 5 µg/ml or 35 µg/ml.
- Kanamycin: Made up in ddH_2O to a stock solution of 50 mg/ml and the working concentration used was 50 µg/ml.
- Streptomycin: Stock solution of 100 mg/ml in ddH_2O. Working solution used was 100 µg/ml.
- Spectinomycin: Made up to a stock solution of 50 mg/ml in ddH_2O to give a working solution of 50 µg/ml.

All antibiotics were added to agar that has cooled to approximately 55ºC after autoclaving.

2.4 Preparation of competent *E. coli* cells

One millilitre of an overnight *E. coli* cell culture was used to inoculate 50 ml of LB broth. This was incubated at 37°C at 200 rpm until the culture reached an OD_{650} of 0.5-0.6 (measured using a Jenway 6300 spectrophotometer). The cell culture was transferred into a 50 ml sterile Falcon tube and chilled on ice for 10 minutes. Cells were pelleted by centrifugation at 1,600 x g for 5 minutes at 4°C and then re-suspended in 25 ml ice cold sterile 100 mM $CaCl_2$. Cells were incubated on ice for 20 minutes then pelleted by centrifugation at 1,600 x g for 5 minutes at 4°C. The cells were then re-suspended in 3.3 ml ice cold 100 mM $CaCl_2$. The suspension was left overnight on ice at 4°C to maximise competency before being aliquoted into microfuge tubes containing 333 µl of ice cold 50% glycerol to every ml of cells for storage at -80°C. Cells were thawed on ice before use.

2.5 Transformation of bacterial cells

One to five µl of plasmid DNA (or entire ligation reaction) was incubated on ice with 100 µl of competent cells for 1 hour. Cells were then heat shocked at 42°C for 2 minutes before briefly returned on ice. Five hundred µl of LB broth was added to the cells and then incubated at 37°C for 45 minutes at 200 rpm to recover. Cells were then pelleted by centrifugation at 2,400 x g for 2 minutes. Cells were re-suspended in 100 µl of LB broth and plated out on appropriate selective media.

2.6 Standard PCR reactions

PCR reactions were done in 50 µl volumes. Each reaction contained 1x reaction buffer, 0.5 mM of each dNTP (ATP/GTP/CTP/TTP), 1 µl of template DNA and 2 µM each of forward and reverse oligonucleotide primers. Velocity DNA polymerase (Bioline) was used to catalyse the reaction. A typical PCR cycle was:

98°C for 1 minute (initial denaturation step)

98°C for 30 seconds (denaturation step)

55°C for 30 seconds (primer annealing) } Repeated for 35 cycles

72°C for 35 seconds (elongation)

72°C for 10 minutes (final elongation step)

The primer annealing temperature varied according to the oligonucleotide length and sequence. Typically, the annealing temperature used was the Tm of the lower primer plus 1°C. The elongation duration was calculated at 30 seconds per 1000 bp. PCR products were separated on 1% agarose gels pre-stained with ethidium bromide using a DNA ladder as a marker.

2.7 Agarose gel electrophoresis

Agarose gels (0.8% or 1% *w/v*) were prepared by dissolving 0.8 g or 1 g of agarose in 100 ml of 1X TBE respectively. The suspension was microwaved on a high setting to dissolve the agarose. One percent (*v/v*) ethidium bromide was added to the cooled suspension prior to pouring the gel. Electrophoresis was done at 100 V in 1X TBE buffer to the required migration distance.

2.8 Ligation of standard PCR products into plasmid vectors

PCR products were purified using Qiagen PCR purification kit according to the manufacturer's instructions. After clean up, PCR products were digested with appropriate restriction enzymes, purified, and then used for ligation reactions. Plasmid vectors used in the ligation reactions were first digested with appropriate restriction enzymes. Vectors were then treated with alkaline phosphatase to remove 5' phosphate groups. All vectors were purified by gel extraction except for pRW50 and derivatives that were purified by phenol-chloroform extraction. Ligation reactions were done in 20 µl volumes containing approximately 50 ng plasmid vector, 150-200 ng of cleaned and restricted PCR product, 4 µl of 10X ligase buffer and 2 µl of T4 DNA ligase for a minimum of 2 hrs.

2.9 DNA and RNA extraction using Qiagen maxiprep, miniprep, or RNeasy extraction kits

DNA and RNA were extracted according to the manufacturer's protocol (Qiagen). In the procedure, DNA is adsorbed to the silica column at high pH in high salt solution, impurities are removed through a series of washes and the nucleic acid is eluted with water. Large scale DNA extraction, such as that used for *in vitro* transcription and DNAse I footprinting template preparation, was done using the Qiagen maxiprep kit. The Qiagen miniprep kit was used for smaller scale extractions such as the isolation of plasmids and cloning vectors. The RNeasy kit was used to extract RNA for use in primer extension assays.

2.10 Sequencing of plasmid constructs

Sanger sequencing of plasmids or PCR fragments was done by the Functional Genomics and Proteomics Facility at the University of Birmingham. Sequencing reactions were submitted in a 10 μl total volume, comprising 1 μl 10 μM primer, and 2-3 μg and 200-500 ng of DNA for plasmid constructs and PCR fragments respectively.

2.11 Transfer of plasmid DNA by conjugation

Conjugation, specifically tri-parental mating, was used to transfer genetic material to *V. cholerae* from *E. coli* DH5α. Overnight cultures of the following were used for the conjugation.

- *V. cholerae* grown in LB (Miller) broth with 100 μg/ml streptomycin.
- DH5α (carrying the *tra* donor pRK2013 helper plasmid) grown in LB (Lennox) broth with 50 μg/ml of kanamycin.
- *V. cholerae* or DH5α (carrying the plasmid to be transferred) grown in either LB (Lennox) or LB (Miller) broth with appropriate antibiotic.

One ml of each overnight culture was aliquoted into correspondingly labelled microcentrifuge tubes and centrifuged at 17 000 x g for one minute. The cells were resuspended in 1 ml 0.9% (*w/v*) NaCl to wash out residual antibiotics. This wash step was repeated three times. After the third wash, each pellet was resuspended in 1 ml of LB broth. The contents of all three microcentrifuge tubes were combined in a 15 ml falcon tube and incubated at 37ºC for at least 4 hours. The cells were vortexed to stop the transfer and pelleted by centrifugation at 3 500 x g for 5 minutes. The supernatant was discarded and cells were resuspended in 5 ml 0.9% (*w/v*) NaCl. One hundred μl of the resuspension was plated onto selective antibiotic media and incubated overnight at 37ºC.

2.12 Preparation of naturally competent *V. cholerae* cells

A single colony of *V. cholerae* was cultured in 2 ml of LB (Miller) broth with 100 μg/ml streptomycin. The culture was grown to mid log phase (OD_{650} of 0.8-0.9) and 1 ml was transferred to a microcentrifuge tube. Cells were collected by centrifugation at 10 000 x g for one minute. The supernatant was discarded and the cells were resuspended in 1 ml of 0.7% (*w/v*) instant ocean aquarium salt. The cells were again collected by centrifugation at 10 000 x g for one minute and resuspended in 1 ml of 0.7% (*w/v*) instant ocean. Nine hundred microliters of 0.7% (*w/v*) instant ocean was added to three tubes containing shrimp chitin, labelled A, B and C. One hundred microliters of resuspended *V. cholerae* was added to each tube and incubated at 30°C for 48 hours.

2.13 Multiplexed Genome Editing by Natural Transformation PCR reactions

A schematic for Multiplexed Genome Editing by Natural Transformation (MuGENT) PCR, which generates DNA fragments used for transformation, is shown in Figure 2.1 (Dalia *et al.*, 2014b). The PCR is done in two stages. The first step generates two overlapping "arms" that are joined in the second step. PCR reactions for each "arm" were done in 50 µl volume reactions containing 5 X reaction buffer, 0.05 mM of each dNTP (ATP/GTP/CTP/TTP), 1 µl of template and 1.6 µM each of forward and reverse primer (Figure 2.1 top). Q5 high-fidelity DNA polymerase from New England Biolabs was used to catalyse the reaction. A PCR cycle of 98^{o}C for 15 seconds; 98^{o}C for 10 seconds; 65^{o}C for 20 seconds; 72^{o}C for 1 minute 30 seconds was used and repeated for a total of 30 cycles and a final elongation step of 72^{o}C for 5 minutes. The product was separated on 0.8% agarose gel pre-stained with ethidium bromide, with a DNA ladder as a marker. The gel was purified, to recover each "arm", using the QIAquick gel extraction kit from Qiagen.

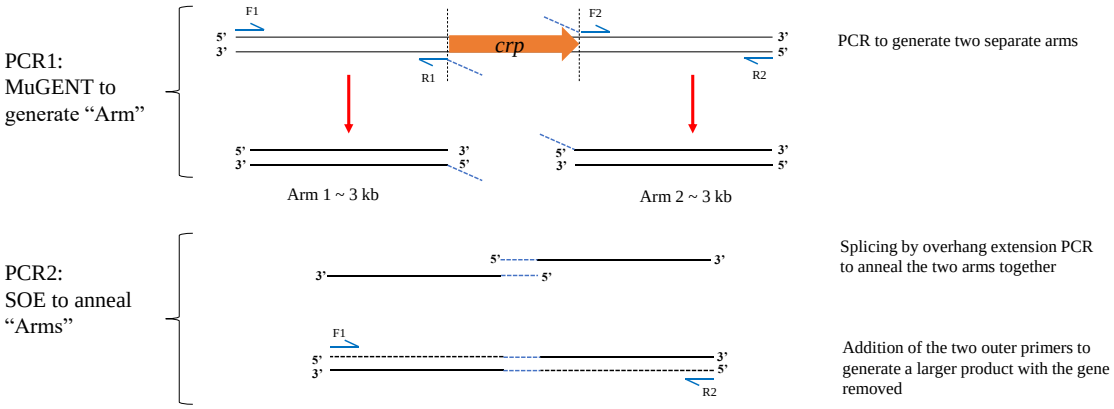

Figure 2.1. MuGENT PCR reaction

Schematic of MuGENT PCR reaction. Two sets of primers (F1 R1; F2 R2) were used to amplify DNA ‘Arms’ upstream and downstream of the *crp* gene. Each “arm” was approximately 3kb long. Primers R1 and F2, listed in table 2.3 each contained inverted repeat sequences of each other to generate complementary ‘sticky overhangs’ in each arm (dashed lines). The overhangs were set to anneal in a splicing by overhang extension (SOE) PCR reaction for 10 cycles before outermost primers F1 and R2 were added to generate 6 kb fragments with the *crp* gene removed.

Prior to the second PCR reaction PCR "Arm" fragments were pooled and excess primers were removed using the Qiagen QIAquick PCR purification kit. Splicing by Overhang Extension (SOE) PCR reactions were done in 50 µl volumes containing 5 X reaction buffer, 0.05 mM of each dNTP (ATP/GTP/CTP/TTP), 2 µl of template (pooled product from MuGENT PCRs) (Figure 2.1). Q5 high-fidelity DNA polymerase from New England Biolabs was used to catalyse the reaction.

SOE PCR cycle

98°C for 10 seconds
65°C for 20 seconds
72°C for 1 minute 30 seconds
} Repeated for 10 cycles

24°C pause — Add 1.6 µM of forward and reverse outer primers

98°C for 10 seconds
68°C for 20 seconds
72°C for 3 minutes
} Repeated for 25 cycles

72°C for 5 minutes (final elongation)

The product was separated on 0.8% agarose gel pre-stained with ethidium bromide, with a DNA ladder as a marker. The correspondingly sized SOE PCR product was excised and purified using the Qiagen Gel extraction kit.

2.14 Transformation of naturally competent *Vibrio cholerae*

After 48 hours incubation on shrimp chitin, the transforming DNA (SOE PCR product) was added to tube B and an equal volume of PCR grade water was added to tube A to serve as a negative control. A selection marker, VC1807::Kan, was also added to tube B. The selection marker was generated by MuGENT and SOE PCR. It was designed to replace the VC1807 gene (encoding a frame-shifted transposase gene) with a kanamycin resistance cassette. The selection marker was also added to tube C to serve as a positive control. The tubes were gently inverted to mix in the DNA, ensuring that the chitin settled at the bottom of each tube. The tubes were incubated at 30ºC for 24 hours (Figure 2.2). After incubation, the tubes were vortexed at maximum speed for one minute to disrupt the biofilms formed on the chitin. One ml of LB broth was added to each tube and the tubes were incubated at 37ºC for a minimum of one hour. Serial dilutions were set up for each tube and 100 µl each of the dilutions 10^{-5}, 10^{-6} and 10^{-7} were plated on LB (Miller) agar with 50 µg/ml kanamycin and 100 µg/ml streptomycin.

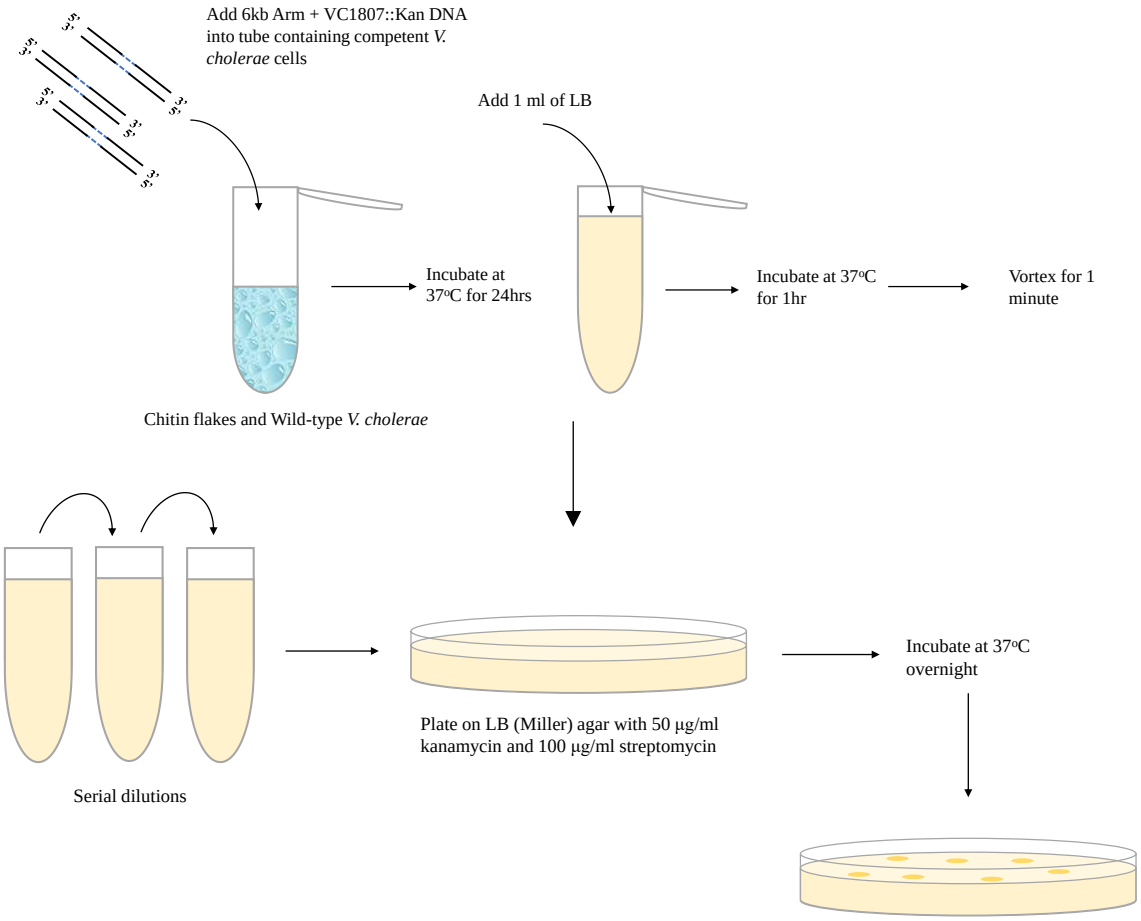

Figure 2.2. Overview of transformation of *V. cholerae* with MuGENT PCR products

Schematic diagram of *V. cholerae* transformation. SOE PCR products, and DNA for the selection marker, were added to microcentrifuge tubes containing chitin flakes and *V. cholerae* cells. The tubes were inverted to mix in the products and incubated for 24 hrs at 37°C. Following incubation, 1 ml of LB broth was added to each microcentrifuge tube, vortexed and incubated at 37°C for 1 hr. The tubes were then vortexed for 1 min and serial dilution of the contents of each tube was made and 100 µl of 10^{-5}, 10^{-6} and 10^{-7} dilutions was plated on LB (Miller) agar plates containing the antibiotics Kan and Sm. The plates were incubated at 37°C overnight.

2.15 Multiplex allele-specific colony (MASC) PCR

Multiplex allele-Specific Colony (MASC) was used to check transformants from MuGENT experiments (Wang and Church, 2011). A schematic of the process is shown in Figure 2.2A. Individual transformants were added directly to PCR tubes. Each PCR reaction tube contained 25 µl containing equal volumes of MyTaq Red mix (Bioline), 0.025µM primers and ddH_2O. PCR cycle of 98^oC for 15 seconds; 98^oC for 10 seconds; 55^oC for 20 seconds; 72^oC for 1 minute 30 seconds were used and repeated for a total of 35 cycles and a final elongation step of 72^oC for 5 minutes. The product was separated on 1% agarose gel pre-stained with ethidium bromide, with a DNA ladder as a marker (Figure 2.3B).

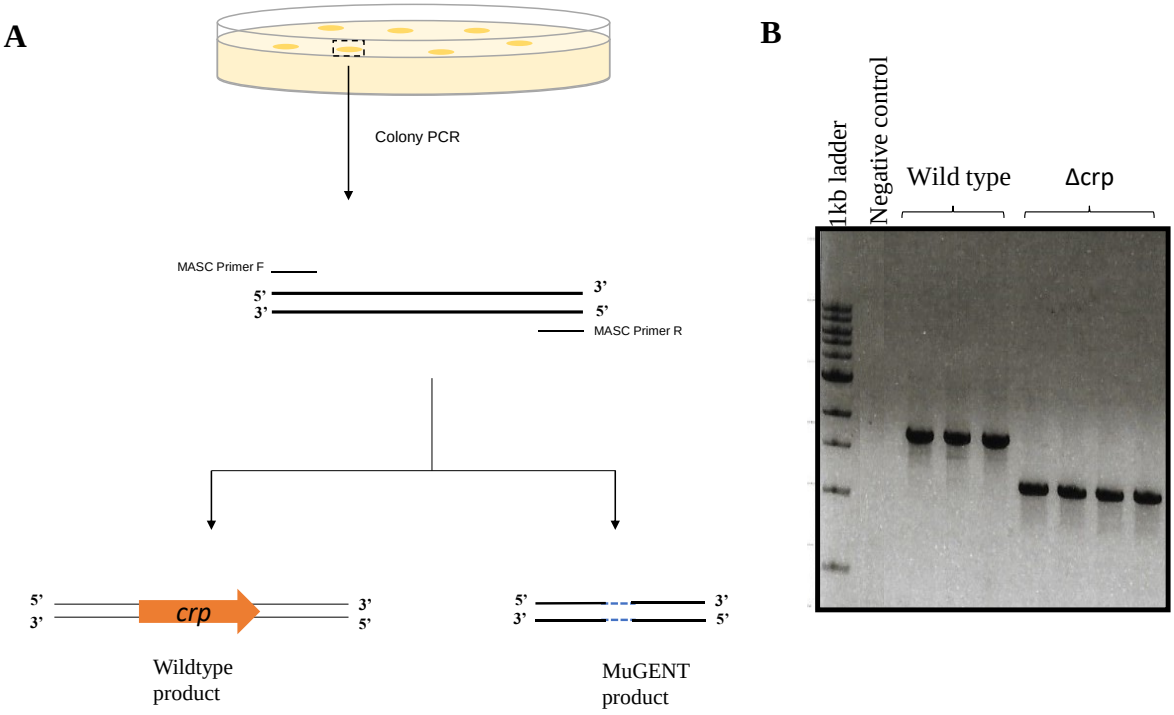

Figure 2.3. MASC PCR

Panel A shows a schematic of MASC PCR. Following transformation with the MuGENT products, the colonies on the transformation plates were each screened for the mutation by colony PCR. MASC primers that anneal approximately 550 bp upstream and downstream of *crp* gene were used to generate PCR products. Panel B shows a 1% agarose gel pre-stained with ethidium bromide alongside a 1 kb DNA ladder. Colonies without the desired mutation generated a 1730 bp PCR product (wild type), whist colonies with the *crp* gene deleted generated a 1100 bp product (Δ*crp*). The negative control contained the PCR master mix and primers only.

2.16 β-Galactosidase assay

β-Galactosidase assays were done as previously described (Miller and Mekalanos, 1988). Overnight cultures were set up from fresh colonies, 100 µl of each overnight culture was used to sub-culture using fresh media in triplicate. Cultures were grown to OD_{650} 0.8-1.0. Cells were lysed with two drops each of 100% toluene and 1% (*w/v*) sodium deoxycholate and then vortexed. Lysates were aerated at 37ºC for 20 minutes. A reaction buffer containing 271 µl of β-mercaptoethanol and 13 mM (8 mg/ml) of 2-Nitrophenyl β-D-galactopyranoside (ONPG) per 100 ml of Z-buffer was prepared. One hundred µl of lysate was transferred to test tubes and the experiment was started by adding 2.5 ml of the reaction buffer to each tube at timed intervals. The reaction was stopped after turning yellow with 1 ml of 1 M sodium carbonate. The OD_{420} of the reaction was measured and the activity in Miller units was calculated using the formula:

$$\text{Activity (Miller units)} = \frac{1000 \times 2.5 \times A \times OD_{420}}{4.5 \times T \times V \times OD_{650}} = \frac{20\,000}{T} \times \frac{OD_{420}}{OD_{650}}$$

T= Time (mins)

A= Final assay volume (3.6 ml)

V= Volume of lysed culture used (0.1 ml).

2.5= Conversion factor to convert OD_{650} into dry protein mass (mg) based on the assumption that OD_{650} of 10 is equivalent to 0.4 mg/ml bacterial dry mass.

1000/4.5= Conversion factor to convert A_{420} into moles of O-nitrophenol, assuming 1mole/ml O-nitrophenol has an absorption of 0.0045 at OD_{420}.

Data shown in the results is the mean activity from three independent replicates.

2.17 *In vitro* transcription assays

Promoter DNA fragments flanked by *Eco*RI and *Hin*dIII restriction sites were cloned into plasmid pSR and used to transform JCB387 cells. The pSR plasmid was purified from transformants using Qiagen Maxiprep kit. Resulting DNA was used as template for *in vitro* transcription as previously described (Kolb *et al.*, 1995). Using plasmid DNA (16 μg ml^{-1}) as template, reactions contained 5 μCi α-^{32}P - UTP, 20 mM Tris pH 7.9, 5 mM $MgCl_2$, 500 μM DTT, 50 mM KCl, 100 μg ml^{-1} BSA, 200 μM each of ATP, GTP, CTP and 10 μM UTP in a volume of 20 μl. RNAP holoenzyme, overexpressed by James Haycocks, from *E. coli* or *V. cholerae* containing σ^{70} was added to the reaction before incubation at 37ºC for 10 minutes. Reactions were stopped with 20 μl of 'STOP' solution containing formamide, 250 mM EDTA, 2.5% (*v/v*) bromophenol blue and 2.5% (*v/v*) xylene cyanol. Four μl of each reaction was analysed by a denaturing PAGE at 60 W for 1 hr. After electrophoresis, the gel was dried and exposed to a Bio-Rad phosphorscreen overnight. The gel image was visualised using the Bio-Rad Molecular Imager FX® system and analysed using Quantity One software.

2.18 Radioactive end-labelling of DNA fragments

DNA fragments used for DNAse I footprinting and generation of G+A ladders were excised from pSR plasmid maxipreps. The plasmid was first digested with *Hin*dIII and treated with calf alkaline phosphatase (CAP) to dephosphorlylate the 5' end of the DNA. The DNA was then purified using phenol chloroform extraction with ethanol precipitation and digested for a second time with *Aat*II. The resulting fragment was purified by gel extraction using the QIAquick Gel Extraction Kit (Qiagen). The fragment was radiolabelled using T4 polynucleotide kinase (PNK). Briefly, each reaction mix contained up to 50 pmol of DNA fragment, 5 µl 10X T4 PNK reaction buffer, 1 µl γ-^{32}P-ATP (10 µCi/ µl) and 2 µl of T4 PNK. The reaction had a final volume of 50 µl and was incubated for 30 minutes at 37^{o}C. The enzyme was inactivated by transferring the reaction to a 65^{o}C heat block for 20 minutes. Unincorporated nucleotides were removed by passing the reaction through two 200 µl G-50 Sephadex columns sequentially.

2.19 M13 sequencing reactions for primer extension assay

The T7 sequencing kit (USB) was used to make sequencing reactions for gel calibration. Ten µg of single-stranded M13mp18 phage DNA (supplied in kit) was diluted to a volume of 32 µl and incubated with 8 µl 2 M NaOH at room temperature for 10 minutes. Seven µl of 3 M sodium acetate (pH 4.8), 4 µl ddH_2O and 120 µl 100% (*v/v*) ethanol was added and incubated at -80^oC for 15 minutes. After incubation, the samples were centrifuged for 15 minutes at 4^oC at 17 000 x g. The supernatant was discarded and the pellet washed with ice-cold 70% (*v/v*) ethanol and centrifuged at 4^oC for 10 minutes at 17 000 x g. The resulting pellet was vacuum dried and resuspended in 10 µl of ddH_2O. Ten ρmol of undiluted stock of the universal primer and 2 µl of annealing buffer was added to the resuspension, thoroughly mixed, and incubated at 65^oC for 5 minutes. The tube was transferred to a 37^oC heat block for 10 minutes, then allowed to cool at room temperature for 5 minutes, before briefly centrifuged. Two point five µl of each of 'A' Mix-short, 'C' Mix-short, 'G' Mix-short, and 'T' Mix-short was transferred into four correspondingly labelled tubes. A dilution of 1: 5 containing 1 µl of T7 polymerase stock (8 units/µl) and 4 µl of dilution buffer was prepared for the labelling step. Fourteen µl of the annealed template/primer mix was mixed with 3 µl labelling mix, 1 µl of α-^{32}P-dATP (10 µCi/µl), and 2 µl of the diluted T7 polymerase mix and then incubated for 5 minutes at room temperature. In the meantime, the four tubes, 'A','G','C', and 'T' were warmed in a 37^oC heat block for 1 minute. Four point five µl of the reaction was transferred into each of the four tubes 'A','G','C', and 'T', mixed by gently pipetting up and down and then incubated at 37^oC for 5 minutes.

The reactions were stopped by mixing in 5 µl of 'STOP' solution and briefly centrifuged. The reaction is stored at -20ºC and a volume of 3 µl is transferred onto a microcentrifuge tube and heated for 2 minutes at 75ºC before use. Sequencing reactions were run on a 6% (*w/v*) denaturing PAGE, alongside primer extension reactions.

2.20 Primer extension assay

RNA was purified from cells carrying plasmid pRW50T derivatives encoding the promoter of interest fused to *lacZ*. The experiment was done over two days.

Day 1

The D49724 primer, which anneals downstream of the *Hin*dIII site on pRW50T, was radiolabelled with γ-^{32}P-ATP and T4 PNK as described above. One µl of the radiolabelled primer (100-400 nM) was mixed with 40 µg of purified RNA, 1/10 volume of 3M sodium acetate and 2.5 volumes of ice-cold 100% (*v/v*) ethanol. The sample was centrifuged at 17 000 x g for 10 minutes at 4^{o}C and the pellet washed with 70% (*v/v*) ethanol. The pellet was vacuum dried and resuspended in 30 µl 1X hybridisation buffer, thoroughly mixed, then incubated at 50^{o}C for 5 minutes. The primer was annealed by incubating the sample at 75^{o}C for 15 minutes immediately followed by 50^{o}C for 3 hours. After incubation, 75 µl of ice-cold (*v/v*) ethanol was added to the sample, mixed with the contents, and then incubated at -80^{o}C overnight.

Day 2

After the incubation, the sample was pelleted and washed in 70% (*v/v*), then vacuum dried. The pellet was resuspended in 31 µl of DEPC treated ddH_2O. Primer extension reactions were carried out in 50 µl reaction volumes containing the resuspended annealed primer 5X reverse transcriptase buffer, 1 mM DTT, 0.2 mM dNTPs, 0.6 µl RNasin (RNAse inhibitor obtained from Promega) and 2.5 µl AMV reverse transcriptase (Promega). Each reaction was incubated at 37^{o}C for 1 hour then stopped by incubation at 72^{o}C for 10 minutes. After a brief centrifugation, residual RNA was degraded by the addition of 1 µl 10 mg/ml RNase A and an incubation at 37^{o}C for 30 minutes. The DNA was precipitated using 6.7 µl 3 M ammonium acetate and 125 µl 100% (*v/v*) ethanol and incubated at -80^{o}C for 30 minutes. The reaction was pelleted, washed, vacuum dried and then resuspended in 4 µl STOP solution. Two µl of this primer extension reaction was run alongside M13 sequencing reactions on a 6% (*w/v*) denaturing gel for at least 2 hours.

2.21 GA ladder

The G+A ladders used to calibrate the DNAse I sequencing gels were generated by Maxam-Gilbert sequencing. Each ladder was derived from the promoter fragment used in the DNAse I footprinting experiment. Reaction tubes contained 12 µl of end-radiolabelled DNA fragment (4 µl of DNA fragment diluted in 8 µl of ddH_2O) mixed with 50 µl formic acid and incubated at room temperature for 2.5 minutes. The reaction was stopped with a solution containing 200 µl 0.3 M sodium acetate, 1 µl (20mg/ml) glycogen and 700 µl ice-cold 100% ethanol (*v/v*). The DNA fragment was precipitated by incubating the reaction tubes at -80^{o}C for 20 minutes. The tubes were then centrifuged at 17 000 x g for 15 minutes at 4^{o}C. Supernatant was discarded and the resulting pellet washed three times with 70% ice-cold ethanol (*v/v*). After the third wash, the pellet was vacuum dried then resuspended in 200 µl 1 M piperidine and incubated for 30 minutes at 90^{o}C. The reaction was stopped with a solution containing 1 µl glycogen, 300 µl ice-cold 100% ethanol (v/v) and 10 µl 3 M sodium acetate and precipitated by incubation at -80^{o}C for 20 minutes. The DNA was pelleted by centrifugation at 17 000 x g for 15 minutes and washed twice with 70% ice-cold ethanol (*v/v*). The DNA pellet was vacuum dried and resuspended in 20 µl DNAse I blue and stored at -20^{o}C.

2.22 DNAse I footprinting

Reactions contained approximately 10-40 µg of radiolabelled DNA with 12.5 µg/ml Herring sperm DNA to act as a nonspecific competitor. Purified *V. cholerae* CRP was diluted in a buffer containing 0.2 mM cAMP before being incubated with the DNA mix, to a total volume of 20 µl, at 37^{o}C for 10 minutes. To each reaction, 3 µl of DNAseI was added for 1 minute before the reactions were terminated with 200 µl 'STOP' solution.

The DNA was extracted from reactions using phenol-chloroform and ethanol precipitation. Purified DNA was resuspended in 4 µl of DNAse I blue. Prior to gel loading, the reactions and G+A ladder were heated to 90^{o}C for 2 minutes. Gels were 6 % denaturing PAGE and electrophoresis was done at 60 W. Footprints were visualised by exposing the dried gel to a Bio-Rad phosphorscreen overnight. The gel image was visualised using the Bio-Rad Molecular Imager FX® system and analysed using Quantity One software.

2.23 Denaturing PAGE gel

Six% (*w/v*) denaturing PAGE was prepared by mixing using 80 ml of Sequagel 6 monomer concentrate and 20 ml Sequagel complete reagents (National Diagnostics) in a beaker. Eight hundred µl freshly prepared 10% (*w/v)* APS (ammonium persulphate) and 40 µl of TEMED (N,N,N′,N′-Tetramethylethylenediamine) was added to the solution to polymerise the reaction. The gel was cast into two glass cassettes and allowed to set for 1-2 hrs. Once set, the gel was mounted in the running apparatus and pre-run at 60 W for 30 minutes before the samples were loaded.

2.24 Bacterial strains and plasmid vectors

The bacterial strains and plasmid vectors used in this work are listed in tables 2.1 and 2.2 respectively. The *E. coli* strain JCB387, a highly competent strain, was used for general DNA manipulation and for cloning new promoter fragments in plasmids pRW50T or pSR. The initial ChIP experiments were done with *V. cholerae* strain N16961 but all other work was done with *V. cholerae* E7946 to facilitate natural transformation. *E. coli* and *V. cholerae* strains were kept in 40% and 30% glycerol solutions respectively for long term storage. To obtain single colonies, the stock was steaked onto selective agar plates and stored overnight at 37^{o}C.

Table 2.1. Strains used in this study

Bacterial Strains	Genotype	Source
M182	*Δ (lacIPOZY), φX74, galK, galU, strA, F-, λ-, strA*	(Casadaban and Cohen, 1980)
M182 Δ *crp*	M182 Δ *crp39*	(Busby *et al.*, 1983)
E. coli DH5α	F– *endA1, glnV44, thi-1, recA1, relA1, gyrA96, deoR, nupG, purB20,* φ80d*lacZ*ΔM15, Δ (*lacZYA-argF*) U169, hsdR17 ($r_K^-m_K^+$), λ–	(Grant *et al.*, 1990)
E. coli DH5α (pRK2013)	DH5α, Kan^R, oriColE1, RK2- Mob+ Tra+	(Taylor *et al.*, 1993)
E. coli JCB387	Δ*nirB* Δ*lac, F-, λ-*	(Typas and Hengge, 2006)
V. cholerae El Tor N16961	Wild-type Inaba El Tor, Sm^R, $HapR^-$	(Heidelberg *et al.*, 2000)
E7946 *Wild type*	SmR derivative of E7946, El Tor Ogawa	(Dalia *et al.*, 2014b)
E7946 *Δcrp*	Derivative of E7946 WT, VC1807::Kan, Δ *crp*	This work
E7946 *Δtcp*	Derivative of E7946 WT, Δ *tcp*	Donated by Andrew Camilli

Table 2.2. Plasmids used in this study

Plasmids	Genotype	Source
pRW50	16.9 kb plasmid featuring *Eco*RI-*Hin*dIII restriction sites upstream of *lacZ,* Tet^R, RK2 origin	(Lodge *et al.*, 1992)
pRW50T	Derivative of pRW50, Tra^+	This work
pRK2013	Kan^R oriColE1 RK2-Mob^+ RK2$^-$$Tra^+$	(Figurski and Helinski, 1979)
pSR	2.6 kb plasmid featuring *Eco*RI-*Hin*dIII restriction sites upstream of a λoop terminator site. A pBR322 derived plasmid encoding Amp^R, ColE1 origin	(Kolb *et al.*, 1995)
pRWXT	Derivative of PRW50T, xylE gene upstream of *Eco*RI restriction site	This work
pMW-GFP	High copy number plasmid with GFP constitutively expressed from lac promoter, $Spec^R$	(Ritchie *et al.*, 2012)

Table 2.3. Primers used in this study

Primer Name (F: Forward, R: Reverse)	Primer Sequence 5'-3'
	Primers used to generate promoter fragments
rtxB F	GGCTGC**GAATTC**ATTCTAATTTAATGGTGCGGTATTCCC
rtxB R	GCCCG**AAGCTT**CACCGCTTGTTAACATGTTCA
rtxH F	GGCTGC**GAATTC**CACCGCTTGTTAACATGTTCAATCC
rtxH R	GCCCG**AAGCTT**CATTCGTACCTCCTTTTATTTTAAGGCG GGATATTACATCGTTAAACCATGGCTATCAACCGACTTA AACAC
tolC F	GGCTGC**GAATTC**TGCCGACTACCAAGTGATGGCT
tolC R	GCCCG**AAGCTT**CATCGGTCCTATTCCTGACGTG
nudF F	GGCTGC**GAATTC**CATCGGTCCTATTCCTGACGTG
nudF R	GCCCG**AAGCTT**CATTCGTACCTCCTATTGATGAAC
acfD F	GGCTGC**GAATTC**ATAACTTGAATAGTTGATTTCA
acfD R	GCCCG**AAGCTT**CATCTTAAGCCTATTAAACAAAAAACA AGAATTAATTATCCTTG
acfA F	GGCTGC**GAATTC**CATCTTAAGCCTATTAAACAAAAAAC AAG

acfA R	GCCCG**AAGCTT**CATTTTTTACTCCTATTTTTACCTGTG
rtxB.1 F	GGCTGC**GAATTC**TTAATTTGTATCAAAATTGAC
rtxB -11-12 F	GGCTGC**GAATTC**TTAATTTGTATCAAAATTGACTACAAA ATAGACTATTTCAACATTGGTCATACAACGCTGACG
rtxB -22-23 F	GGCTGC**GAATTC**TTAATTTGTATCAAAATTGACTACAAA AGGGAC
rtxB CRP3.2.4 R	GCCCG**AAGCTT**CACCGCTTGTTAACATGTTCAATCCTCA ATCACCGTCAGCGTTGTATGACCAATGTTGAAATAGTCC CTTTTGTAGTC

Primers used for Sanger sequencing and amplification of fragments from plasmids

pRW50 F	GTTCTCGCAAGGACGAGAATTTC
pRW50 R	AATCTTCACGCTTGAGATAC
pSR F	GCATTTATCAGGGTTATTGTCTC
pSR R	CATCACCGAAACGCGCGAGG
xylE mid F	TCATAGGTCGCCGGCAATTCG

Primers used to generate new strains and plasmids

Arm 1 delta crp F1	CGCCAAACCAAGATTAACACTG
Arm 1 delta crp R1	GGTTATCGGGGCACTTAGCGAGTGCCCATAATAATCTCACTTCCTCTGC
Arm 2 delta crp F2	GCAGAGGAAGTGAGATTATTATGGGCACTCGCTAAGTGCCCCGATAACC
Arm 2 delta crp R2	GCTGAGATGCGCGGCGTTTCCGATGC
delta crp MASC F	GCACCCACATTAACTTTCAGCGTGTTCC
delta crp MASC R	GCTGAAAGTGGAAGAGTGTTCACC
VC1807::kan F	GTAGAATAAGTGCGGCGTTGAGCC
VC1807::kan R	GCGCCCAATGTTGTCCCTTTGATG
oriT F	ATTCGC**GAATTC**GGTAACCCCCGTTGAGCACCGCCAGGTG
oriT R	ATTCGC**AAGCTT**GCTAGCCTTTTCCGCTGCATAACCCTGC
pRWXT F	GCCTTGAGTCCACGCT**GGATCC**CCGACGACGACATGGC
pRWXT R	GCCCG**GAATTC**GACAACATGAACTATGAAGAGG

Primers used for primer extension

Universal primer for T7 sequencing reactions	GTAAAACGACGGCCAGT
D49724	GGTTGGACGCCCGGCATAGTTTTTCAGCAGGTCGTTG

Text in bold indicates restriction sites. Bold and italicised text describe the application of the primers.

2.25 Zebrafish model

To study host colonisation by *V. cholerae* we used the zebrafish larvae model. The larvae used in this study are of the wild type AB strain.

2.26 Zebrafish embryo maintenance

Adult fish were kept in a recirculating tank system at the [redacted] at a 14/10 hours light/dark cycle at a pH of 7.5 and 26 °C. Zebrafish care, breeding and experiments were performed in accordance with the Animal Scientific Procedures Act 1986, under Home Office Project License 40/3681 (University of Birmingham). Zebrafish embryos were harvested in petri dishes containing water from the fish system. About 50-60 embryos are transferred into individual 90 mm petri dishes containing 25 ml of 1X E3 media, 0.03% of methyl blue and 0.02 mg/ml PTU to inhibit melanisation. The embryos were incubated under a 14h-10h light-dark cycle at 32 °C for 5 days. The larvae were maintained by regularly changing the incubation media to minimise growth of microbes.

2.27 Infection of zebrafish embryos

On day 3, single colonies of *V. cholerae* are used to inoculate universals containing 5 ml of minimal media. These were incubated at 37ºC, shaking at 200 rpm overnight. On day 4, 1 ml of the overnight culture was sub-cultured into new tubes containing 5 ml of minimal media. This culture was incubated at 37ºC, and shaken at 200 rpm, until mid-log phase. The culture was then transferred into 5 ml falcon tubes and pelleted by centrifugation at 4 500 x g for 5 minutes. Cells were resuspended in 5 ml of 1X E3 buffer and washed three times to remove any residual antibiotics. After washing, cells were resuspended in 5 ml of 1X E3 and 10^7 cells/ml were transferred into each well of a 24 well cell culture plate. For each infection strain, triplicate wells were set up and five larvae were transferred into each well. Prior to addition, the larvae stored in the petri dish, were sedated by adding tricaine to a final concentration of 4 mg/ml. The plates were incubated at 32ºC overnight.

2.28 Determination of β-Galactosidase activity in *V. cholerae* colonised zebrafish larvae

After overnight incubation the larvae were euthanised by adding Tricaine to a final concentration of 40 mg/ml. The media was agitated by pipetting up and down to remove any biofilms that may have formed at the bottom of the wells. The media was transferred into sterile bijous and the larvae into 1.5 ml dolphin microcentrifuge tubes. The larvae were homogenised using a hand held motorised homogeniser and 1X E3 was added to each tube to an equivalent volume to that of the transferred media.

Two drops each of 100% toluene and 1% (*w/v*) sodium deoxycholate was added to each bijou and dolphin tube to lyse the cells. The β-galactosidase activity was carried out as described in section 2.16.

2.29 Plating of *Vibrio cholerae* from media and larvae

Following homogenisation and prior to lysing the cells, 0.5 µl of the homogenate and of E3 *V. cholerae* media was transferred into respective microcentrifuge tubes containing 1. 5 ml of 1X E3 media. One hundred µl of this dilution was plated onto LB agar plates containing 5 µg/ml Tetracycline, 100 µg/ml streptomycin, 50 µg/ml spectinomycin and 40 µg/ml of x-gal. These were incubated at 37ºC overnight and the presence of blue colonies were used to confirm *V. cholerae* growth.

2.30 Imaging

Zebrafish embryos colonised with *V. cholerae* were imaged using the Zeiss Axio Observer.Z1 microscope with 10x objective for fluorescent channel and differential interference contrast (DIC) channel. The ImageJ image processing package (NIH) software was used to visualise the images and merge the fields. Visualization of embryos was done by immobilizing them in 0.4% low melting point agarose in E3 supplemented with 4 mg/mL Tricaine. Live Imaging was done at 32°C and humidity maintained at 80% using an OkoLab Stage.

Optimising tools to monitor gene expression in *Vibrio cholerae*

Chapter 3

3.1 Introduction

Vibrio cholerae causes disease in humans and also colonises organisms within aquatic environments. Such organisms include fish, invertebrates and marine mammals (Grimes *et al.*, 2009). Efficient colonisation depends on the bacterium's ability to control gene expression in response to the environment (Reidl and Klose, 2002). This requires transcription factors. Historically, most of the tools used to study bacterial gene regulation have been derived from *E. coli* (DiRita *et al.*, 1991). Hence, many *V. cholerae* studies have used genetic and biochemical materials derived from *E. coli* cells (Dalia *et al.*, 2014a; Duan and March, 2010; Dalia *et al.*, 2015; Wu *et al.*, 2015). For example, Yu and DiRita used *E. coli* to understand the role H-NS plays in control of *V. cholerae* genes regulated by ToxT. Although these approaches have been useful, *V. cholerae* specific regulators like ToxR and ToxT (Yu and DiRita, 2002) are absent from *E. coli*. Furthermore, amino acid sequence differences are apparent when comparing the basal transcriptional apparatus of *E. coli* and *V. cholerae*. As detailed in chapter 1, the RNAP holoenzyme consists of α_2, β, β' and σ^{70} subunits. The amino acid sequence of the subunits in *E. coli* and *V. cholerae* exhibit a 90%, 85%, 82% and 77% identity respectively (Heidelberg *et al.*, 2000; Blattner *et al.*, 1997). It is not known how these differences might impinge on basal activity or interactions with regulators. The aim of this chapter is to assess current tools used to study *V. cholerae* gene regulation. The data presented highlight the need to use endogenous *V. cholerae* enzymes. This chapter also reinforces the importance of integrating host colonisation into studies of *V. cholerae* gene expression.

3.2 Comparing *E. coli* and *V. cholerae in vitro* transcription systems

The first goal was to understand differences in the basal properties of *E. coli* and *V. cholerae* RNA polymerase. Hence, native RNA polymerase core enzyme was purified from each organism, by James Haycocks, and holoenzyme was reconstituted with the cognate σ^{70} purified following overexpression. To compare the enzymes, we used a reconstituted *in vitro* transcription system. The first DNA template used for *in vitro* transcription was the *rtxBDE* regulatory region of *V. cholerae* (fully characterised in chapter 4). This DNA was cloned upstream of *λoop* terminator in pSR plasmid to generate the supercoiled DNA template. A schematic of the DNA template is shown in Figure 3.1A. The *rtxBDE* regulatory region contains two CRP sites and two promoters (P1*rtxB* and P2*rtxB*). The CRP sites are involved in promoter repression (Chapter 4). The RNA products generated by each RNA polymerase from this DNA template were visualised by radiolabelling and electrophoresis (Figure 3.1B, C). Comparison between *E. coli* and *V. cholerae* RNAP revealed that both enzymes synthesised the same transcripts but with different efficiencies. Specifically, the *V. cholerae* RNA polymerase generated more RNA transcript from *rtxBDE* P2 compared to *E. coli* RNAP. Similarly, whilst CRP completely blocked transcription by *V. cholerae* RNAP at this regulatory region, *E. coli* polymerase was only partially hindered. Hence, for *E. coli* RNAP, the P2*rtxB* transcript was detected even in the presence of CRP. In a second experiment we compared the activity of the two RNA polymerases at a class I CRP activated promoter from *E. coli* strain H10407 (Haycocks *et al.*, 2015). The promoter, P*estA*, controls expression of a heat-stable enterotoxin. Organisation of the regulatory region is shown in Figure 3.2A.

Figure 3.2B shows results of the assay with *E. coli* RNA polymerase. As expected, the P*estA* promoter was activated by CRP. Conversely, CRP was unable to activate transcription by *V. cholerae* RNA polymerase (Figure 3.2C).

We conclude that there are subtle differences in the RNA polymerase from *E. coli* and *V. cholerae* which can impact transcription and regulation.

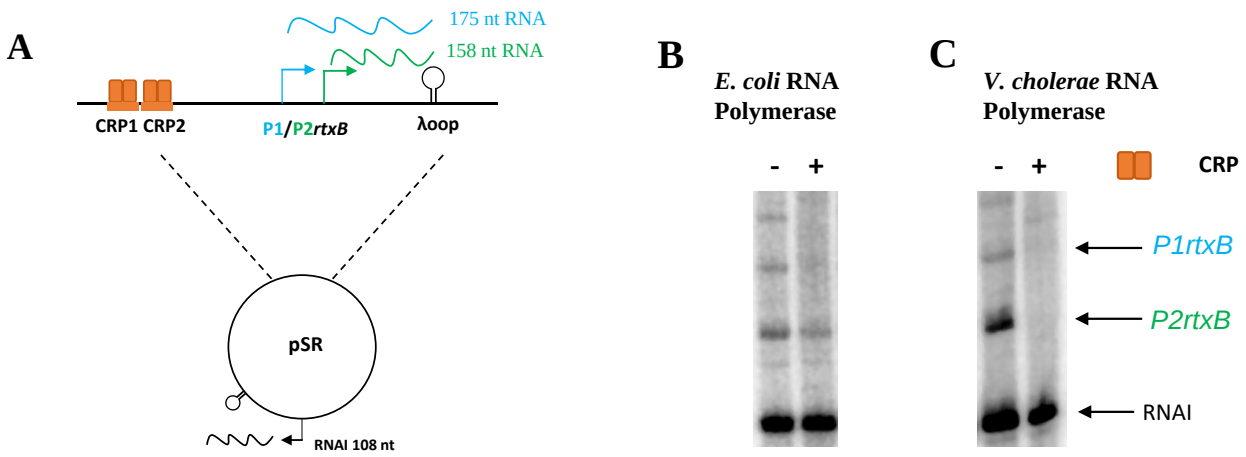

Figure 3.1. *In vitro* multiround transcription comparing *E. coli* and *V. cholerae* RNA polymerase at *rtxB* promoter

Panel A shows a schematic of DNA template cloned upstream of the λoop transcriptional terminator in plasmid pSR showing both CRP sites (orange) and promoters. P1 (blue) and P2 (green) promoters with their transcript sizes are shown. Panels B and C show the transcripts generated for each *rtxB* promoter using *E. coli* RNA polymerase or *V. cholerae* RNA polymerase. *E. coli* polymerase generated a weaker intensity RNA transcript for P2 (green) compared to *V. cholerae* polymerase. The addition of 1μM CRP (orange) and 10 μM of its allosteric effector molecule, cAMP, completely blocks transcription from both *rtxB* promoters by *V. cholerae* RNA polymerase. Bacteria were grown in LB broth overnight at 200 rpm.

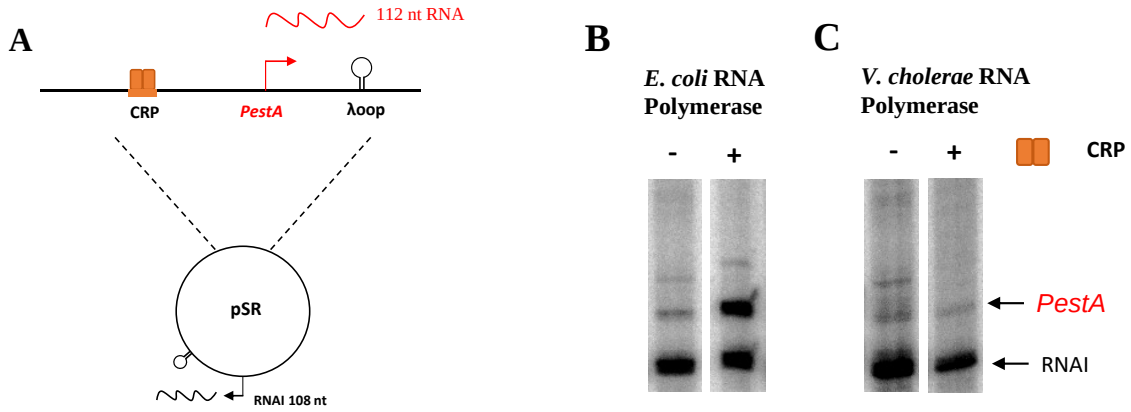

Figure 3.2. *In vitro* transcription comparing *E. coli* and *V. cholerae* RNA polymerase at *E. coli estA* promoter

Panel A shows a schematic of DNA template cloned upstream of the λoop transcriptional terminator in plasmid pSR showing CRP sites (orange) and *estA* promoter (red). Panels B and C show the transcripts generated for *estA* promoter using *E. coli* RNA polymerase or *V. cholerae* RNA polymerase. The addition of CRP (orange) activates transcription from the *estA* promoter by *E. coli* polymerase as seen in the stronger intensity transcript in panel B. On the other hand, the addition of 1μM CRP (orange) and 10 μM cAMP blocks transcription from the *estA* promoter by *V. cholerae* RNA polymerase. Bacteria were grown in LB broth overnight at 200 rpm.

3.3 Comparing gene expression in *E. coli* and *V. cholerae* cells

3.3.1 Modification of an *E. coli* reporter plasmid for use with *V. cholerae*

In the next set of experiments, we sought to compare transcription from a *V. cholerae* promoter in its cognate cellular environment and in the *E. coli* host. Initial experiments were problematic because the low copy number *lacZ* reporter plasmid pRW50 (Figure 3.3A) was able to transform *E. coli* but not *V. cholerae*. This may be because *V. cholerae* secretes two extracellular nucleases, Dns and Xds (Blokesch and Schoolnik, 2008), that might hinder uptake of the large (16, 993 kb) pRW50 plasmid (Lodge *et al.*, 1992). To avoid this problem, the pRW50 plasmid was modified. Specifically, the 517 bp *cynX* gene, which encodes a factor for cyanate transport not important for plasmid function, was replaced with an origin of transfer (*oriT*). The *oriT* sequence, derived from plasmid RK2, was amplified by PCR with the flanking *traJ* and *traK* regions as a 220 bp DNA fragment. This fragment contained *Bst*EII and *Nhe*I restriction sites to enable ligation with pRW50. The resulting plasmid was named pRW50T (Figure 3.3B). Whilst the starting pRW50 plasmid was unable to transform chemically competent *V. cholerae* (Figure 3.4A) the pRW50T plasmid was successfully mobilised during conjugation and transferred to both *E. coli* and *V. cholerae* with similar efficiency with mean values of 257 and 215 respectively (Figure 3.4B).

We also generated a derivative of pRW50T, called pRWXT, that encodes *xylE* upstream of the promoter cloning site (Figure 3.3C). The *xylE* sequence, derived from plasmid pRWX, was amplified by PCR to generate a 1.3 kb fragment containing *Bam*HI and *Eco*RI restriction sites (El-Robh and Busby, 2002). The fragment was ligated into plasmid pRW50T that had been digested with *Eco*RI and *Bgl*II. The resulting plasmid allowed for the assessment of bidirectional regulatory regions (discussed in chapter 4).

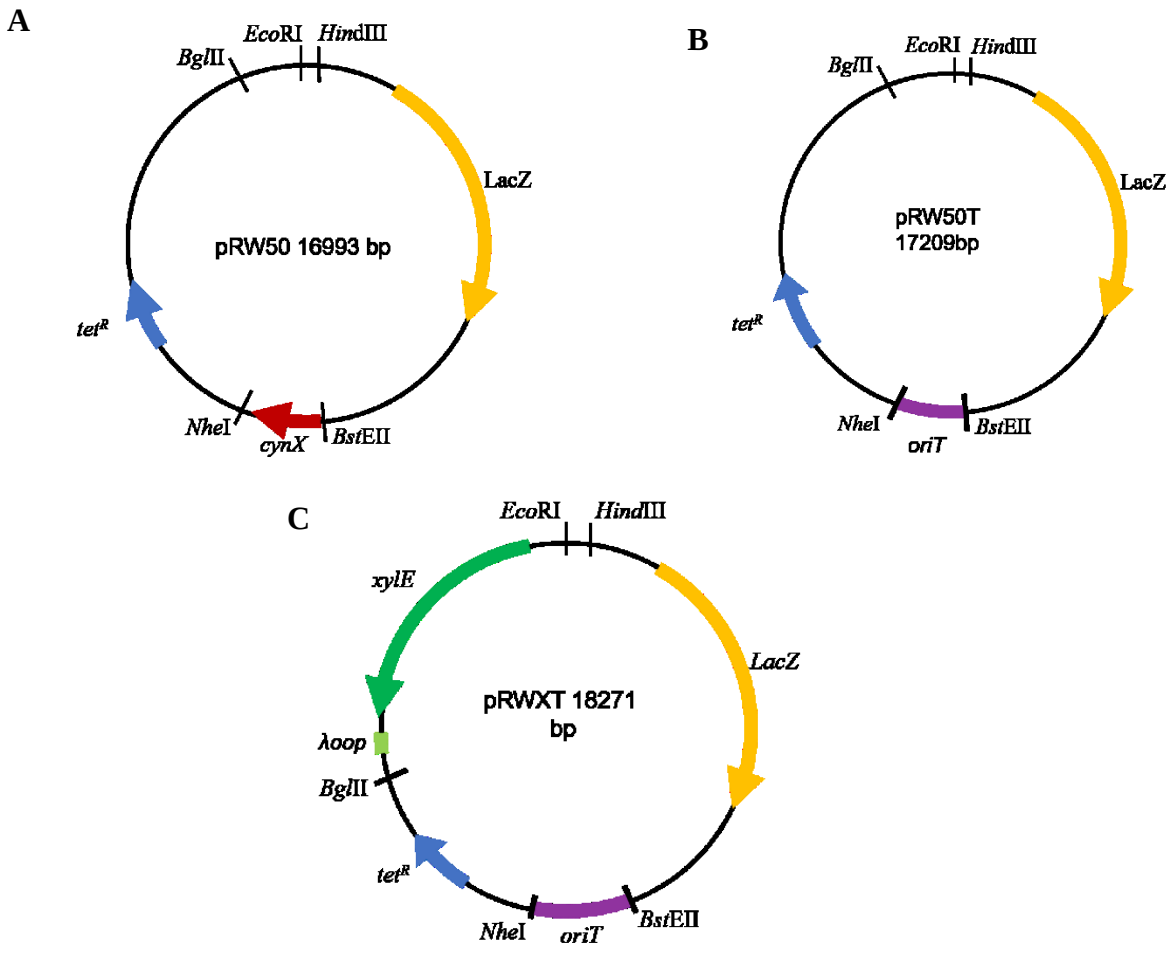

Figure 3.3. Modification of pRW50 plasmid

Schematic representation of pRW50 (A), pRW50T (B) and pRWXT (C) plasmids. To generate pRW50T, the *cynX* gene (panel A) was excised from pRW50 and replaced with *oriT* (purple in panel B). To generate pRWXT plasmid (C), the *xylE* gene (green in panel C) and λoop terminator were cloned upstream of the *Eco*RI and downstream of the *Bgl*II sites to generate a dual reporter plasmid. The tetracycline antibiotic resistance marker is shown in blue, *lacZ* gene is shown in yellow and the black lines represent the sites for the correspondingly labelled restriction enzymes.

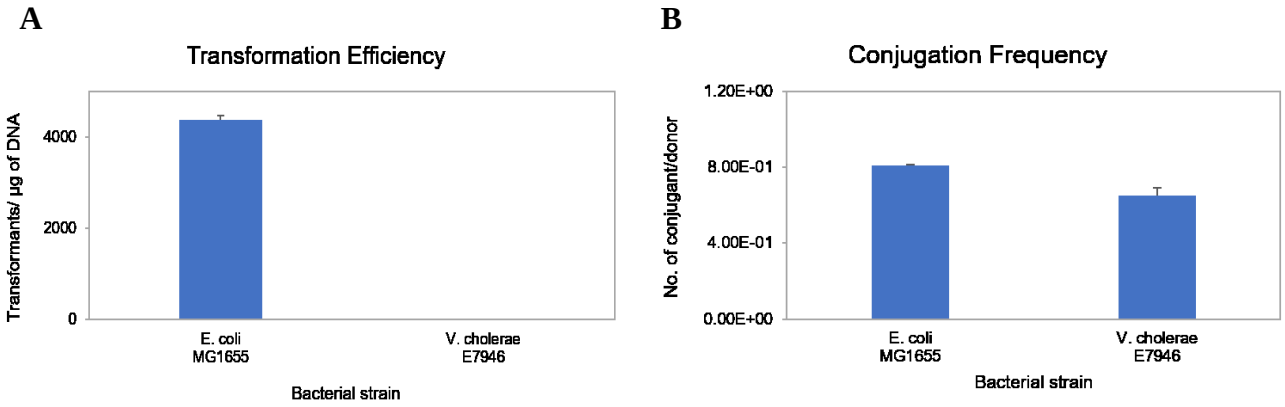

Figure 3.4. Comparing transformation and conjugation in *E. coli* and *V. cholerae*

Panel A shows transformation efficiency of $CaCl_2$ competent *E. coli* and $CaCl_2$ competent *V. cholerae* by plasmid pRW50. Panel B shows conjugation frequencies observed for *E. coli* and *V. cholerae* using pRW50T. Error bars represent the standard deviation obtained from three independent replicates.

3.3.2 Comparison of promoter activity in *V. cholerae* and *E. coli*

To determine if *V. cholerae* promoter activity differed in *E. coli* the regulatory DNA upstream of the *V. cholerae tolC*, *rtxBDE*, *acfA* and *acfD* genes was cloned in pRW50T. The *acfA* and *acfD* genes are accessory colonisation factors arranged in a similar configuration to the *rtxBDE* and *rtxHCA* genes. The derived plasmids were used to transform *E. coli* and *V. cholerae* by conjugation. The two strains were grown in LB broth at 200 rpm, to mid-log phase, and β-galactosidase activity was measured in lysates of the two strains (Figure 3.5). The data show that promoter activities can differ substantially between *E. coli* and *V. cholerae*. Specifically, the *rtxBDE* regulatory DNA stimulated no *lacZ* expression in *V. cholerae* whilst expression was detected in *E. coli*. Activity of the *tolC* regulatory region also differed between the two organisms. Conversely, the *acfA* and *acfD* promoters had similar activities in the two organisms. For the *rtxBDE* regulatory DNA the data are consistent with measurements of transcription *in vitro* shown in Figure 3.2. Hence, CRP was unable to fully supress transcription driven by *E. coli* RNAP but transcription by the *V. cholerae* enzyme was blocked. We conclude that *E. coli* is a poor proxy for investigation of *V. cholerae* gene regulatory regions.

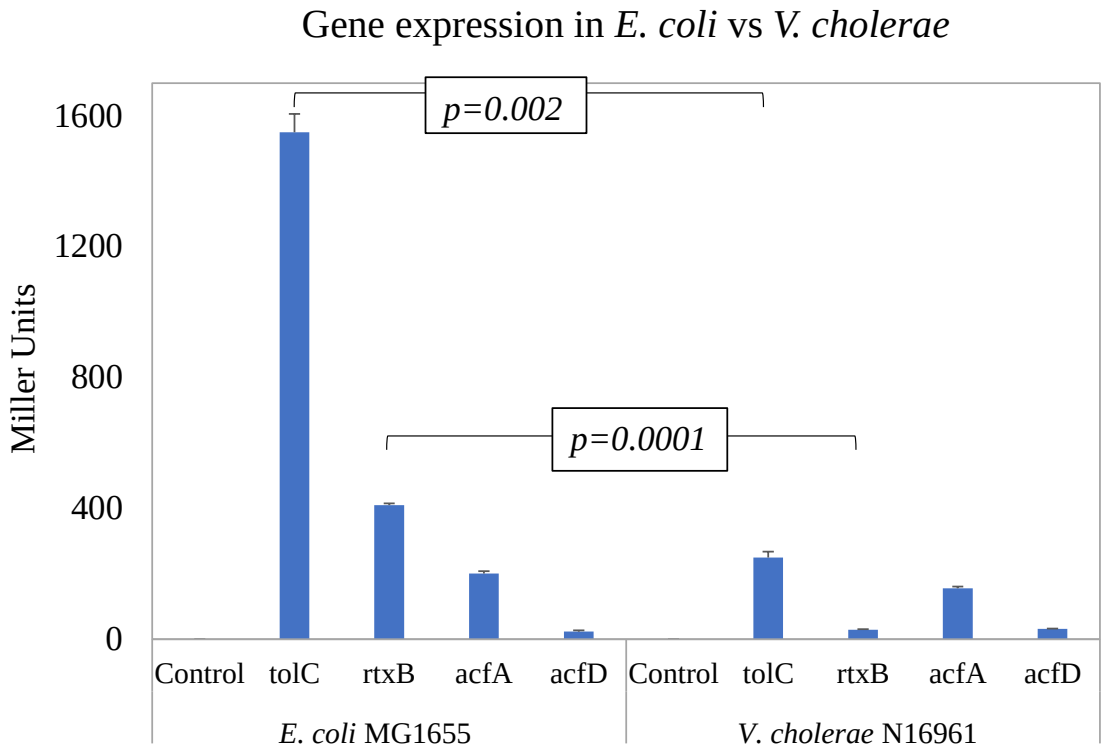

Figure 3.5. Gene expression from regulatory DNA in *E. coli* and *V. cholerae*

β-galactosidase activity measurements of regulatory promoter activity in *E. coli* and *V. cholerae*. The empty plasmid pRW50T was used as a control. Activity is measured in Miller Units. Cells were grown in LB broth at 200 rpm to mid-log phase. The error bars represent standard deviation for three biological replicates.

3.4 Using the zebrafish larvae model to study *V. cholerae* gene expression

3.4.1 Outline of procedure

The zebrafish has, for many years, provided an ideal model to study human infectious diseases (Rowe *et al.*, 2014; Wang *et al.*, 2013). Recently, work by several groups has demonstrated that the intestinal tracts of zebrafish are efficiently colonised by *V. cholerae* (Runft *et al.*, 2014; Saslowsky *et al.*, 2010). The zebrafish model is particularly useful because of the diverse microbiota of the fish. Furthermore, zebrafish share an environmental niche with *V. cholerae* (Runft *et al.*, 2014; Austin, 2010; Senderovich *et al.*, 2010; Gomez *et al.*, 2013). We sought to exploit the pRW50T and pRWXT systems to monitor *V. cholerae* gene expression during colonisation of zebrafish larvae. A schematic representation of the procedure is shown in Figure 3.6. First, bacteria transformed with the appropriate plasmid derivative, encoding promoter::*lacZ* fusions, were used to inoculate E3 media containing zebrafish larvae (Figure 3.6 step 1). After colonisation, free swimming bacteria were recovered from the media. To isolate intestinal bacteria the larvae were washed and homogenised (Figure 3.6 step 2). Cell numbers were determined by plating and gene expression levels determined using *lacZ* assays (Figure 3.6 step 3).

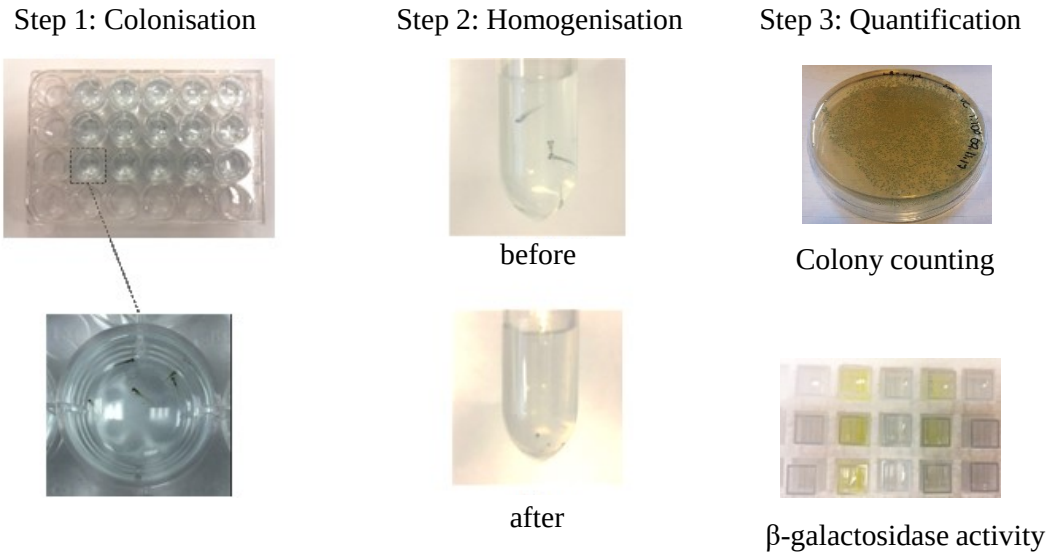

Figure 3.6. Schematic representation of zebrafish infection

In step 1, zebrafish larvae (5 larvae per well) were transferred into 24 well flat bottom cell culture plates and infected with 10^6 cells per ml mid-log phase *V. cholerae* cells. They were incubated overnight at 32^{o}C. Following incubation, the larvae were sedated, then separated from the media which contained the planktonic cells and washed once in sterile 1X E3 media. The larvae were then resuspended in sterile 1X E3 media, euthanised and homogenised as shown in step 2. One hundred µl of a 1:3000 dilution of the homogenate and planktonic cells were each plated onto selective antibiotic plates and incubated at 37^{o}C overnight for colony counting (step 3). Two drops each of toluene and 1% (*w/v*) sodium deoxycholate was added to the rest of the homogenate and planktonic cells to lyse the bacterial cells. The lysate was assayed using the β-galactosidase enzymatic assay to compare promoter activities between the two population. A yellow colour like the one shown in step 3, is indicative of enzyme activity.

3.4.2 Impact of host colonisation on promoter activity

Expression of *lacZ* from the *V. cholerae tolC*, *rtxBDE*, *acfA* and *acfD* promoters was determined using the system described above. Figure 3.7 shows that promoter activities differed between the planktonic and intestinal bacterial populations. Importantly, the changes observed were similar to those previously observed in rabbits and mice (Mandlik *et al.*, 2011). Of particular note is the 15-fold induction of *rtxBDE* promoter activity in the intestinal *V. cholerae* populations.

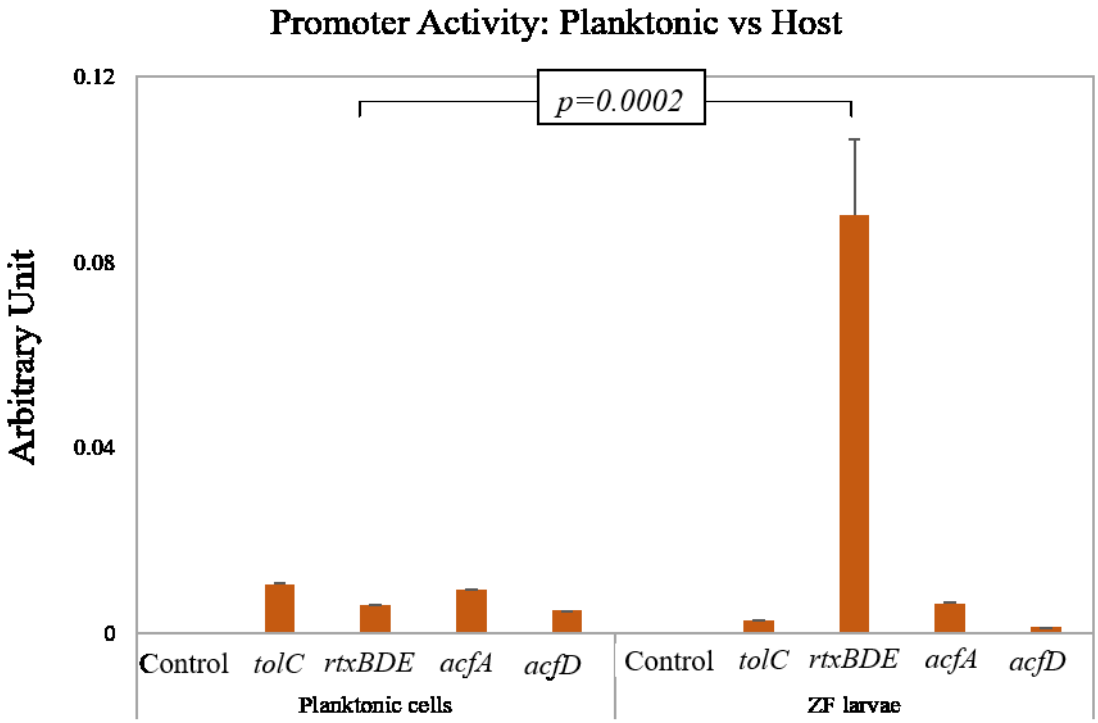

Figure 3.7. Promoter activity of *V. cholerae* regulatory DNA in media vs host

β-galactosidase activity measurements of *V. cholerae* regulatory DNA regions in planktonic cells compared to a host (larvae). Activities for *tolC, acfA* and *acfD* regulatory regions decreased in the host compared to planktonic cells. However, the activity for *rtxBDE* was substantially different in the two environments, with a 15 fold increase in activity from the larvae compared to the planktonic cells. Plasmid pRW50T with no DNA insert was used as a control. Activity is measured as arbitrary units. The error bars represent standard deviation for three biological replicates.

3.5 Zebrafish larvae model to study *V. cholerae* colonisation of the intestinal tract

The plasmid pMW-GFP, with the green fluorescent protein constitutively expressed, was transferred into *V. cholerae* cells via conjugation. The resulting *V. cholerae*-GFP strain was used to inoculate larvae raised in E3 media to allow colonisation of the larval intestinal tract. Figure 3.8 shows a microscopic image of a larva colonised with *V. cholerae*-GFP.

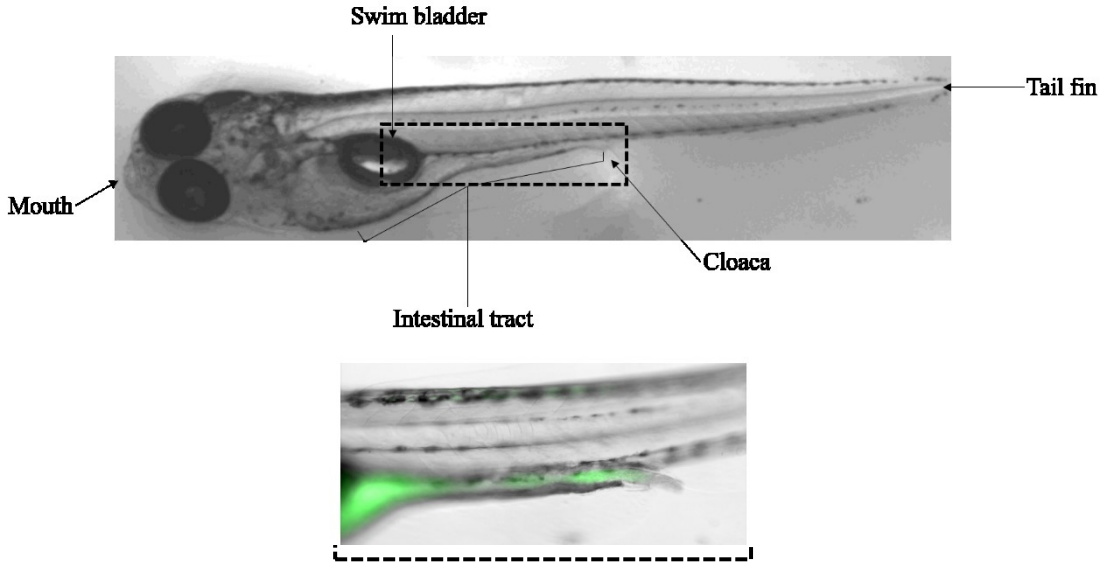

Figure 3.8. Colonisation of the zebrafish larva intestinal tract *by V. cholerae*

The image the anatomy of a 4-day old zebrafish larvae. Five larvae were transferred into a 24 well culture plate with 10^6 cells per ml mid-log phase *V. cholerae*-GFP cells and incubated overnight. The following day, the larvae were separated and washed in sterile 1X E3 media to remove bacterial that may be bound onto the surface of the larvae. Larvae were immobilised by mounting onto 0.4% low melting point agarose dissolved in 1X E3 media and 160 µg/ml tricaine. Epifluorescence in merged bright-field and gfp images shows the colonisation of the intestinal tract with *V. cholerae* cells (magnified in the dashed rectangle).

3.6 Conclusions

In this chapter, we describe simple and optimised protocols for characterising *V. cholerae* gene regulatory regions *in vitro*, *in vivo*, and in the context of a host. We demonstrate that these optimised approaches avoid artefacts associated with reliance on exogenous enzymes and *E. coli* genetic backgrounds. Furthermore, our data demonstrate the importance of considering host-microbe interactions in such studies. We suggest that the zebrafish larvae model for studying effects of host-microbe interactions on gene expression will be particularly useful. This system is better suited to large numbers of replicates than other models and can easily be used to assess many experimental variables.

Characterisation of CRP binding at the *rtxBDE* and *rtxHCA* regulatory region

Chapter 4

4.1 Introduction

Cholera is transmitted to humans through the ingestion of contaminated food or water (Clemens *et al.*, 2017). The bacterium has developed diverse and complex regulatory systems that enable it to modulate gene expression to adapt to the human intestines on exiting the various marine environments it colonises (Clemens *et al.*, 2017; Chaudhuri and Chatterjee, 2009; Peterson, 2002). Upon entering the human host, the bacterium upregulates motility, produces enzymes that degrade mucin and penetrate the mucus layer of the intestinal epithilium (Almagro-Moreno *et al.*, 2015). Once within the mucus layer, *V. cholerae* produces TCP and accessory colonisation factors (ACF) that enable adherence to the epithelial surface of the small intestine. Hence, colonisation is established (Peterson, 2002). Ultimately, disease results from the production of factors including CTX, repeats in toxin (RTX) and haemolysin (HlyA) (Clemens *et al.*, 2017; Chaudhuri and Chatterjee, 2009). Transcription factors including ToxT, ToxR, VpsT, AphA, AphB and VcCRP are involved in regulating genes during host colonisation (Peterson, 2002; Nielsen *et al.*, 2010). As mentioned above, VcCRP binds DNA in response to the intracellular availability of cAMP to control genes involved in metabolism. In *V. cholerae*, VcCRP is also known to influence the ToxR regulon by directly inhibiting *tcpP* expression (Skorupski and Taylor, 1997a; Peterson, 2002). However, gene regulation by VcCRP during colonisation of a host intestinal tract by *V. cholerae* has never been studied (Liang *et al.*, 2007). Previous work by our group, (unpublished data) used ChIP-seq to map the distribution of VcCRP across the *V. cholerae* genome. The data show substantial overlap between VcCRP binding and the ToxR regulon. Furthermore, these data suggest that VcCRP controls additional virulence

factors not regulated by ToxR. This chapter focuses on one such target, the genes encoding RTX and its transport system. Figure 4.1A shows ChIP-Seq data for VcCRP and σ^{70} at this locus. The sequence of the regulatory region is shown in Figure 4.1B. In this chapter, the precise VcCRP binding sites are identified and their role characterised. VcCRP is shown to be essential for specific induction of *rtxBDE* gene expression during intestinal colonisation. Examination of additional VcCRP target genes reveals similar effects at these targets.

4.2 Characterisation of VcCRP binding in the *rtx* locus

The sequence of the *rtxBDE* /*rtxHCA* intergenic region is shown in Figure 4.2B. Analysis of the sequence identified two putative VcCRP sites named CRP1 and CRP2. These are underlined in the figure with each half of the CRP site shown in orange. The centre of the ChIP-seq binding peak for VcCRP is denoted by the asterisk above the sequence and aligns with the CRP2 site. To confirm binding, purified VcCRP was used in DNAse I footprinting assays with a DNA fragment derived from the intergenic region (Figure 4.1). A Maxam/Gilbert GA sequencing ladder was used to calibrate the footprinting gel (Figure 4.2). Lane 1 shows the pattern of cleavage in the absence of VcCRP. Upon addition of VcCRP (lanes 2-7) a distinct change in the cleavage pattern was observed. The results generated from the footprints are consistent with VcCRP binding to both putative sites.

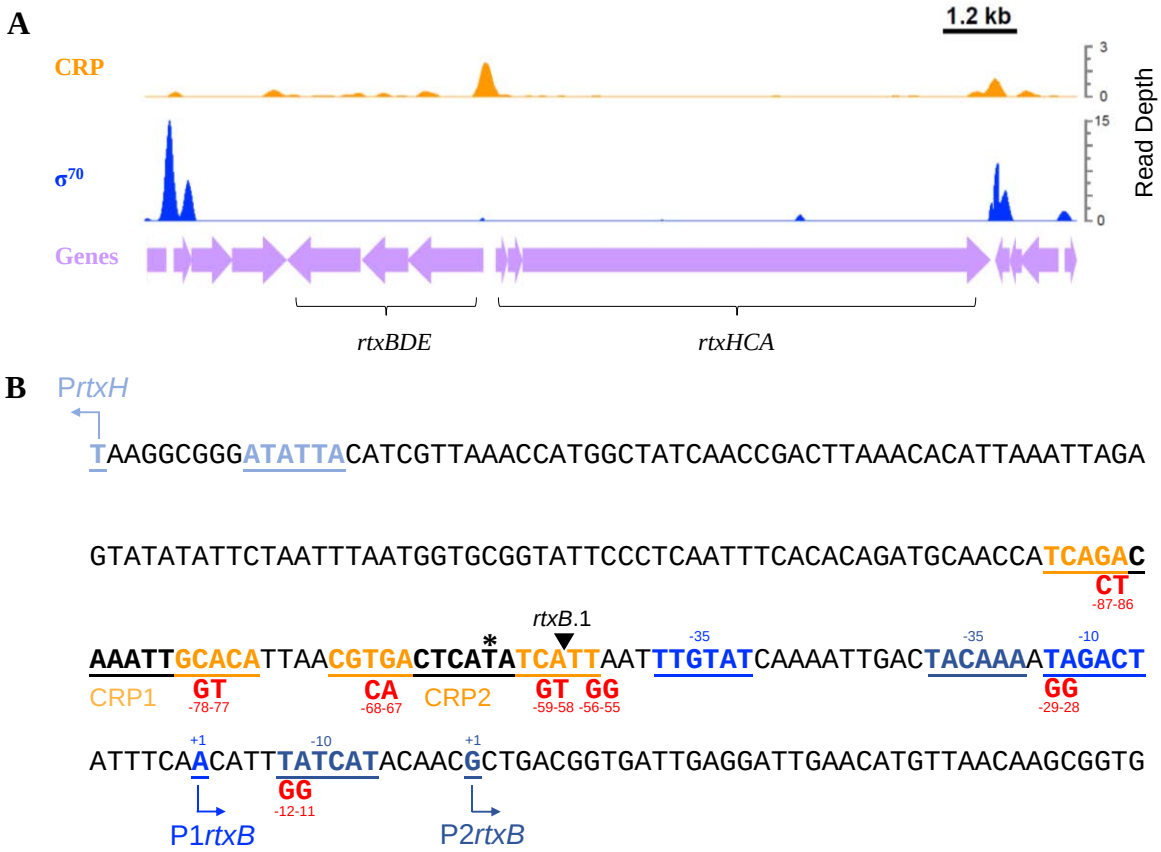

Figure 4.1. CRP and σ^{70} binding in the *rtx* regulatory region

Panel A shows ChIP-seq data for VcCRP (orange) and σ^{70} (blue) binding to the *rtx* locus. Genes are shown in mauve with the divergently transcribed *rtxBDE* and *rtxHCA* genes labelled. Panel B shows the sequence of the gene regulatory region between *rtxBDE* and *rtxHCA*. The centre of the VcCRP binding peak identified by ChIP-seq is indicated by an asterisk. Putative VcCRP sites (orange) are underlined and labelled. The inverted triangle shows the point the fragment was truncated to generate *rtxB.1* fragment. Red letters and their correspondingly numbered positions denote the mutations that were made in the DNA fragment. Putative -10 and -35 elements are underlined and colour coded and transcription start sites with a correspondingly coloured arrow denoting the direction the gene is transcribed.

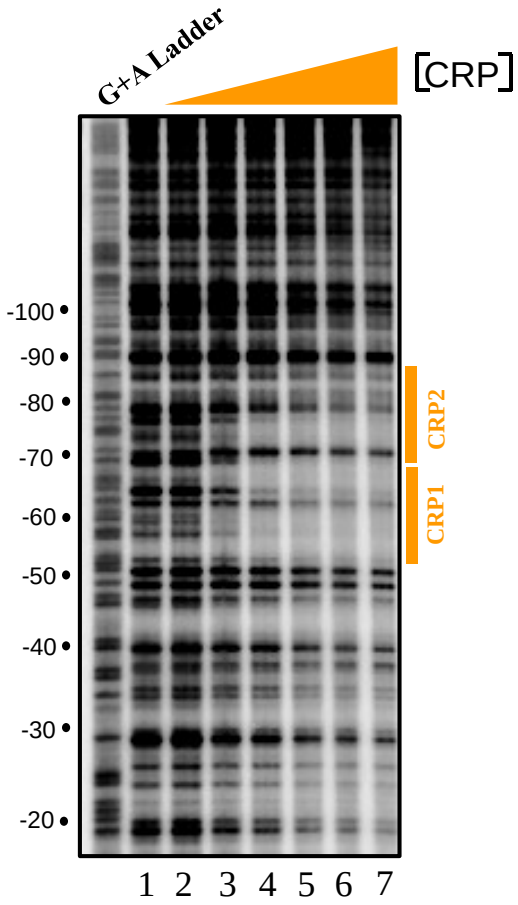

Figure 4.2. DNAse I footprint of CRP binding to *rtxBDE-rtxHCA* regulatory region

The figure shows the results of a DNAseI footprinting experiment using the *rtxBDE* intergenic region and purified *V. cholerae* CRP and cAMP. The experiment was calibrated with a Maxam-Gilbert GA sequencing ladder and positions relative to the P2*rtxB* transcription start site (+1) are labelled. The triangle indicates addition of CRP and lanes 1-7 correspond to concentrations of 0, 0.175, 0.35, 0.7, 1.4, 2.1 and 2.8 µM respectively. Orange boxes show the positions of the predicted CRP binding sites.

4.3 Identification of the *rtxBDE* and *rtxHCA* transcription start sites

To identify promoters in the *rtxBDE-rtxHCA* regulatory region, two approaches were used; mRNA primer extension assays and *in vitro* transcription assays. First, two DNA fragments, corresponding to each orientation, of the regulatory region, were generated. These were cloned upstream of the promoterless *lacZ* gene in pRW50T to create a *lacZ* fusion. The resulting plasmids were then used to transform *E. coli* DH5α strain and transferred to *V. cholerae* El Tor strain N16961 by conjugation. RNA from the conjugants was isolated and primer extension assays were done using an oligonucleotide that bound the *lacZ* mRNA of the plasmid encoded fusion. The results are shown in Figure 4.3. I was unable to derive any extension products for potential *rtxBDE* promoters for the conditions used. However, a single 201 nucleotide extension product was generated from *rtxHCA* transcripts. The corresponding transcription start site (TSS) aligns perfectly with a TSS identified by Papenfort *et al* (2015) and is labelled P*rtxH* in Figure 4.1B (Papenfort *et al.*, 2015). We reasoned that *rtxBDE* may be repressed *in vivo* since this would explain our failure to identify extension products. Hence, the *rtxBDE* intergenic region was cloned upstream of the λ*oop* terminator in pSR plasmid to create a template for *in vitro* transcription. The results of the experiment (Figure 4.4) show the production of three transcripts (Lane 1). The 108 nt control RNAI transcript is derived from the pSR plasmid replication origin.

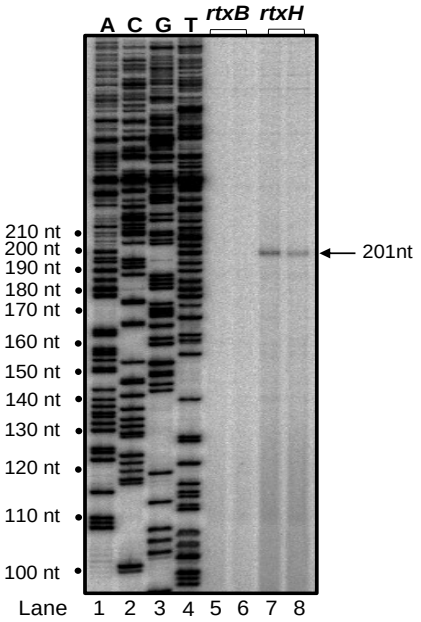

Figure 4.3. Primer extension of *rtxBDE* and *rtxHCA* promoter derived transcripts

The figure shows the primer extension products obtained from the *rtxBDE* and *rtxHCA* promoter fragments. Lanes 1-4 show arbitrary Sanger sequencing reactions for calibration of the gel and primer extension products for *rtxB* (lanes 5 and 6) and *rtxH* (lanes 7 and 8) promoter derived transcripts respectively. The cells were grown to mid-log phase at 200 rpm in LB (lanes 5 and 7) or M9 minimal media (lanes 6 and 8) prior to RNA extraction.

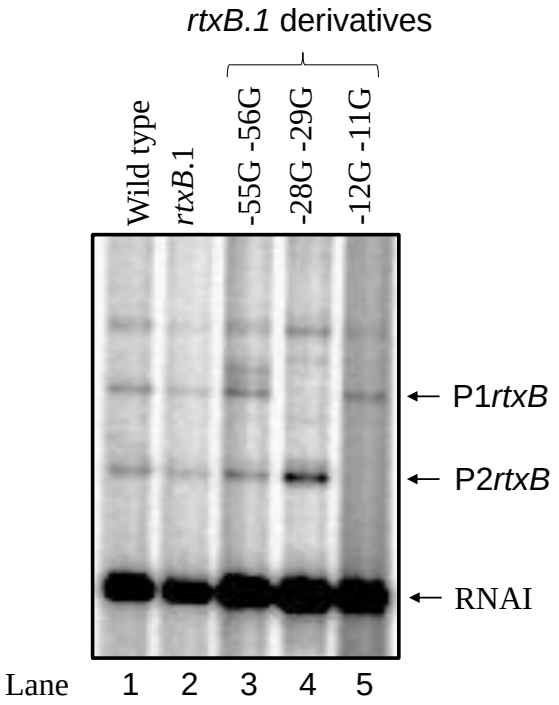

Figure 4.4. Transcripts derived from *rtxBDE* intergenic region *in vitro*

The figure shows transcripts generated by *V. cholerae* RNA polymerase σ^{70} holoenzyme in the absence of CRP using the *rtxBDE* intergenic region, cloned in plasmid pSR, as a DNA template. The RNAI transcript is derived from the plasmid replication origin and serves as an internal control. The *rtxB*.1 derivative contains a truncated version of the *rtxBDE* intergenic region. Point mutations introduced to disrupt potential -10 hexamers with the corresponding nucleotide number are noted above the gel. Cells were grown overnight at 200 rpm in LB broth.

To identify promoters of the *in vitro* transcription products, a series of *rtxBDE* fragment derivatives was generated. These included a truncation of the *rtxBDE* intergenic region that removed upstream sequences (truncation site is shown by an inverted triangle in Figure 4.1B). The truncated fragment was named rtxB.1 and versions of this truncated DNA template, with point mutations in all potential -10 hexamers, were also made (labelled red in Figure 4.B). Results of *in vitro* transcription assays show that truncation of the *rtxBDE* intergenic region did not prevent synthesis of the additional transcripts (Figure 4.4, lane 2). Hence, the transcripts originate downstream of the site marked by the inverted triangle in Figure 4.1B. The -55G-56G mutation (Figure 4.4, lane 3) did not prevent synthesis of additional transcripts. Hence, these mutations do not correspond to the site of an important element. However, the -29G-28G and -12G-11G mutations each prevent the production of a different transcript as seen in Figure 4.4, lanes 4 and 5. We conclude that these transcripts originate from the promoters labelled P1*rtxB* and P2*rtxB* in Figures 4.1 and 4.4.

4.4 Expression of the *rtxBDE* operon is repressed by CRP

The presence of two CRP sites between *rtxBDE* and *rtxHCA* suggests a role in transcription regulation. However, neither CRP site is appropriately positioned to activate P*rtxH*, P1*rtxB* or P2*rtxB*; the sites are positions -126.5 and -148.5, -47.5 and -67.5 and -63.5 -83.5 upstream of each transcription start site respectively. It has previously been shown that promoters with tandem upstream CRP sites can be subject to repression by CRP (Lee and Busby, 2012). To investigate this possibility, derivatives of the full length intergenic region where created in which the CRP sites were inactivated by point mutations shown in Figure 4.1B or altered to match the consensus for CRP binding. The various DNA fragments were cloned in either the *rtxHCA* or *rtxBDE* orientation upstream of *lacZ* in plasmid pRW50T. The constructs are shown schematically in Figures 4.5A and 4.6A. in both cases mutated VcCRP sites are denoted "CRP-dis" and consensus VcCRP sites "CRP-cs". The various constructs were used to transform *V. cholerae* strain N16961 by conjugation. Promoter activity was measured by determining β-galactosidase activity in lysates of the transformants. The data show that P*rtxH* activity is unaltered by any of the mutations (Figure 4.5B). Conversely, expression from the poorly active *rtxBDE* promoters increased when the VcCRP sites were inactivated (Figure 4.6B). These results are consistent with repression by VcCRP seen in previous *in vitro* transcription experiments (Chapter 3) and a further *in vitro* transcription assay testing different concentrations of VcCRP (Figure 4.7). Interestingly, Fong and Yildiz (2008) also made similar observations using transcriptome analysis and reported repression of *rtxBDE* by CRP.

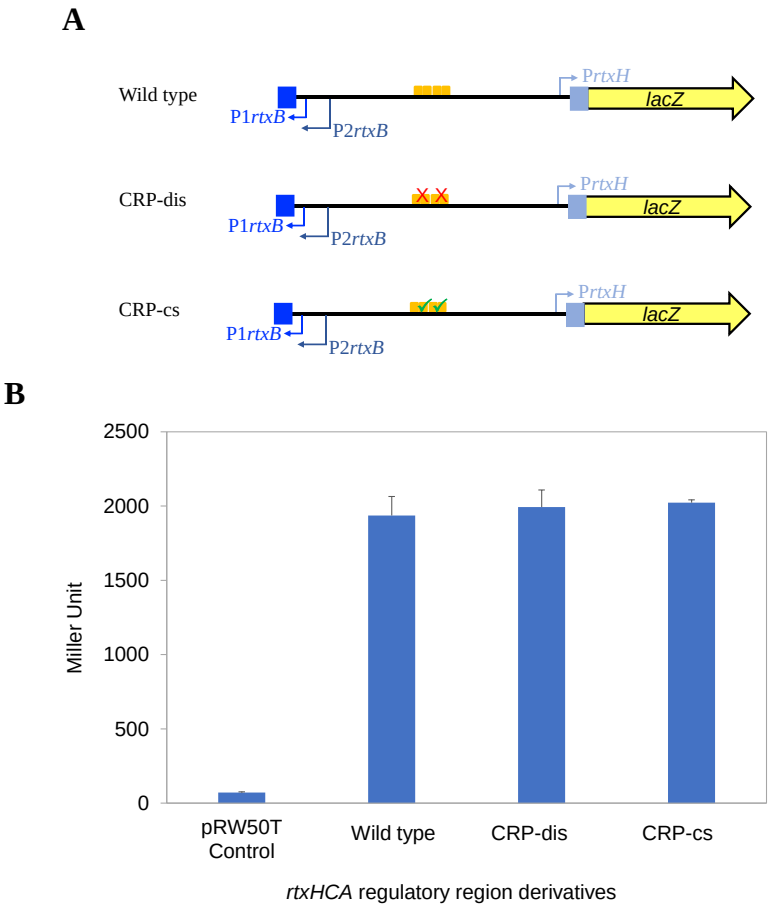

Figure 4.5. Activity of P*rtxH* is not affected by VcCRP

Panel A shows a schematic of each of the constructs whereby the VcCRP sites (orange) are either disrupted (shown with red X) or made consensus (green tick). Yellow arrow represents the *lacZ* gene. Panel B shows results of β-galactosidase assays done using lysates of N16961 cells transformed with derivatives of the *lacZ* reporter plasmid, pRW50T, where *lacZ* expression is controlled by P*rtxH* and its derivatives. Empty pRW50T was used as a control. Assays were done using mid-log phase cultures grown in LB media. Activity is measured in Miller Units. The error bars represent standard deviation for three biological replicates.

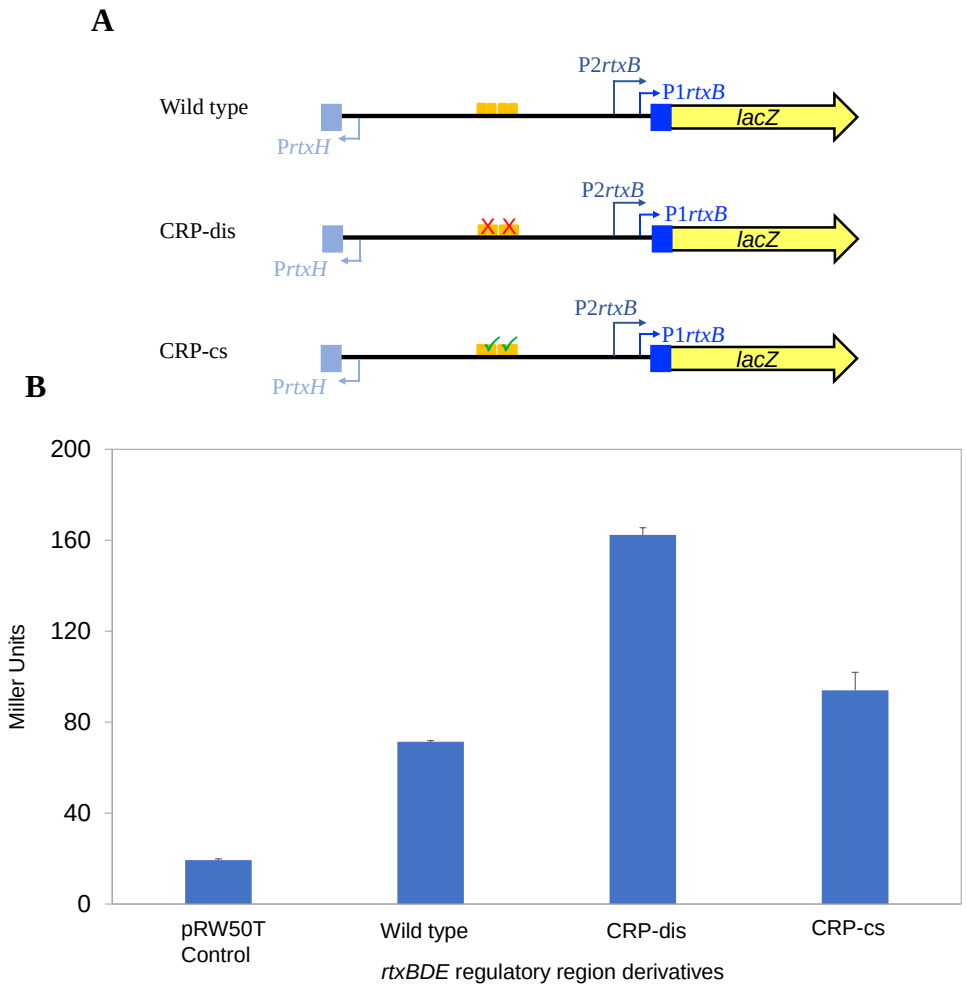

Figure 4.6. Expression of *rtxBDE* is repressed by VcCRP

Panel A shows a schematic of each of the constructs whereby the VcCRP sites (orange) are either disrupted (shown with red X) or made consensus (green tick). Yellow arrow represents the *lacZ* gene. Panel B shows the results of a β-galactosidase assays done using lysates of N16961 cells transformed with derivatives of the *lacZ* reporter plasmid, pRW50T, where *lacZ* expression is controlled by P1*rtxB* and P2*rtxB* and its derivatives. Empty pRW50T was used as a control. Assays were done using mid-log phase cultures grown in LB media. Activity is measured in Miller Units. The error bars represent standard deviation for three biological replicates.

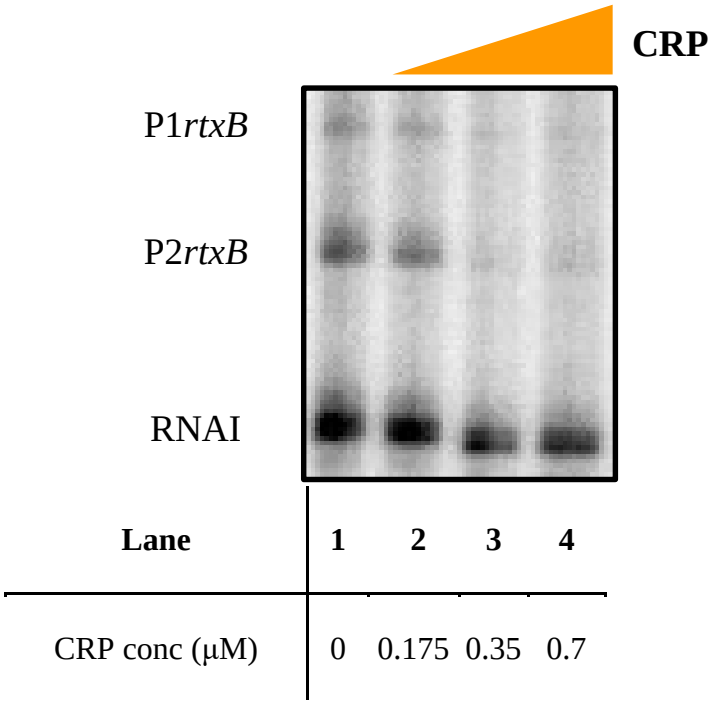

Figure 4.7. Transcripts derived from *rtxBDE* regulatory region are repressed by VcCRP

The gel shows transcripts generated by *V. cholerae* RNA polymerase σ^{70} holoenzyme and VcCRP with cAMP using the *rtxBDE* intergenic region, cloned in plasmid pSR, as a DNA template. The RNAI serves as an internal control. Increasing concentrations of VcCRP are depicted by the orange wedge and corresponding VcCRP concentrations are listed below each lane. Assays were done using overnight cultures grown in LB media.

4.5 Activity of the *rtxBDE* promoters observed in the absence of VcCRP binding requires P1*rtxB* and P2*rtxB*

Having established a role for VcCRP in repression of *rtxBDE* transcription a further experiment was designed to check that these effects required P1*rtxB* and P2*rtxB*. Hence, 3 new promoter DNA fragments were generated with point mutations in either P1*rtxB*, P2*rtxB* or both (mutations are as shown in Figure 4.1B). These mutations were made in the context of the truncated *rtxB.1* fragment that lacks the VcCRP binding site and hence has higher activity than the full length regulatory region (see first three bars in Figure 4.8A). the constructs are illustrated schematically in Figure 4.8B.The *rtxB.1* derivatives have been given the prefix P1, P2 or P1,P2 to indicate which promoter has been mutated. The various fragments were cloned upstream of *lacZ* in plasmid pRW50T and the resulting plasmids were used to transform *V. cholerae* strain N16961 by conjugation. Promoter activity was determined using lysates of the transformants. β-galactosidase activity assays confirmed that increased gene expression due to deletion of the VcCRP sites was due to P1*rtxB* and P2*rtxB* (Figure 4.8B).

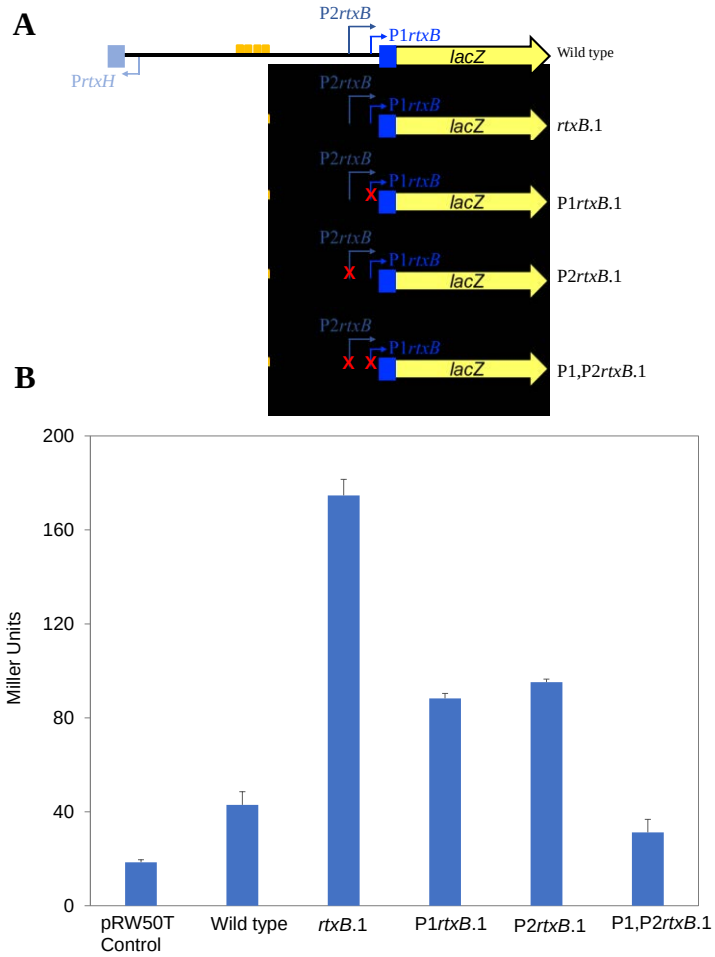

Figure 4.8. The *rtxBDE* gene expression is from both promoters

Panel A shows a schematic of each of the constructs whereby the VcCRP sites (orange) are either disrupted (shown with red X) or made consensus (green tick). Yellow arrow represents the *lacZ* gene. Panel B shows results of a β-galactosidase assays done using lysates of N16961 cells transformed with derivatives of the *lacZ* reporter plasmid, pRW50T, where *lacZ* expression is controlled by P*rtxB* and its derivatives. Empty pRW50T was used as a control. Assays were done using mid-log phase cultures grown in LB media. Activity is measured in Miller Units. The error bars represent standard deviation for three biological replicates.

4.6 Effect of nutrient availability on *rtxBDE* promoter activity

To further understand the role of VcCRP, P1*rtxB* and P2*rtxB*, we mutated the various DNA elements in the context of the full length regulatory DNA region. The mutations were as described in Figure 4.1B and the constructs are illustrated schematically in Figure 4.9A. The ability of CRP to bind DNA *in vivo* is regulated by the ligand cAMP whose level is determined by nutrient availability (Chattopadhyay and Parrack, 2006). Hence, CRP binds target sites when cells are grown in M9 minimal medium but binding is reduced in LB broth and abolished upon addition of glucose (Haycocks *et al.*, 2015). As such, repression of *rtxBDE* should be relieved in rich media. Hence, strains carrying the regulatory region derivatives were grown in M9 minimal media, LB broth or LB broth supplemented with 0.4% glucose. As expected, compared to cells grown in M9 minimal media, β-galactosidase activity due to the wild type regulatory region increased in LB broth and rose further upon addition of glucose (compare second bar for each culture condition in Figure 4.9). Consistent with our predictions, the effect of mutating the CRP sites was reduced in rich media. Furthermore, mutation of the promoter -10 elements greatly reduced *lacZ* expression in all conditions.

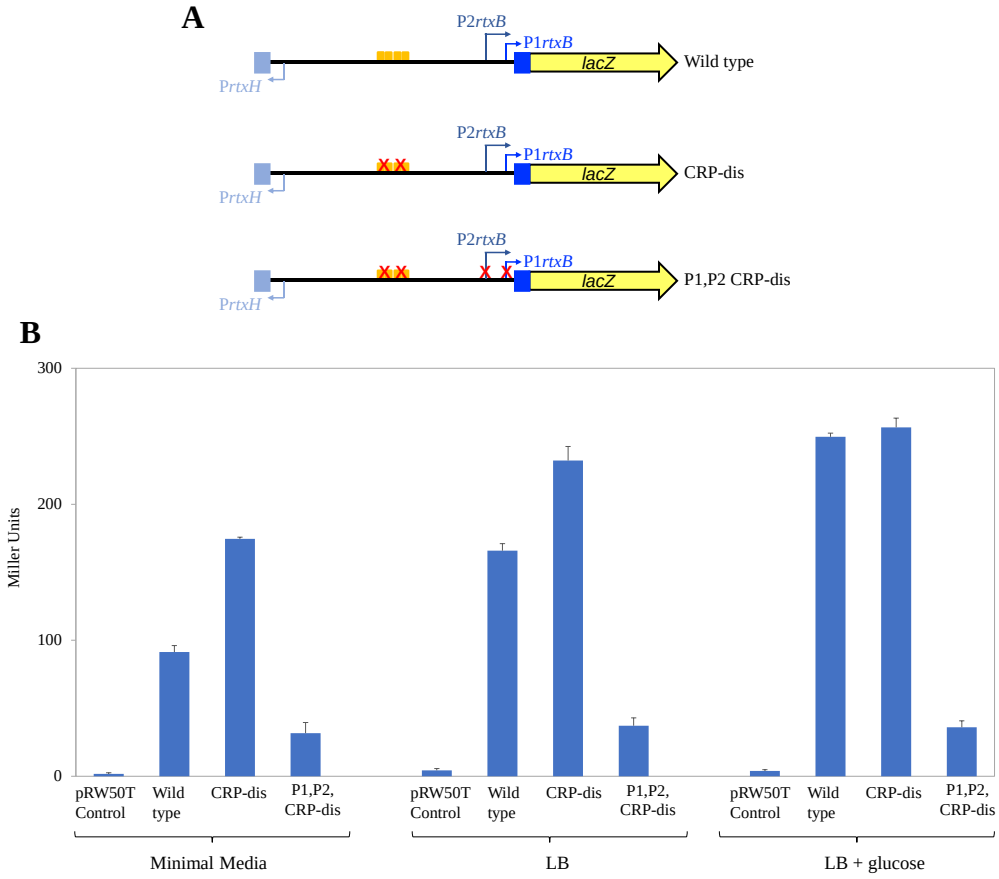

Figure 4.9. VcCRP represses *rtxBDE* expression in response to nutrient availability

Panel A shows a schematic of each of the derivatives, the wild type P*rtxB* promoter, P*rtxB* CRP-dis whereby the VcCRP site (orange) is disrupted (shown with red X) and P12*rtxB* CRP-dis whereby both the promoters (blue arrows) and VcCRP site (orange) are disrupted (disruption is depicted by red X). Yellow arrow represents the *lacZ* gene. Panel B shows results of a β-galactosidase assays done using lysates of N16961 cells transformed with derivatives of the *lacZ* reporter plasmid, pRW50T, carrying different P*rtxB* derivatives. Cells were grown in M9 minimal media, LB or LB supplemented with 0.4 % (v/v) glucose. Empty pRW50T was used as a control. Assays were done using mid-

log phase cultures. Activity is measured in Miller Units. The error bars represent standard deviation for three biological replicates.

4.7 The expression of the *rtxBDE* operon is derepressed in *V. cholerae* lacking the *crp* gene

We next sought to generate a Δ*crp* mutant *V. cholerae* strain using the MuGENT technique (Dalia *et al.*, 2014b). However, N16961, has a non-functional *hapR* gene, which enables *V. cholerae* to be naturally transformed, and cannot be used in MuGENT experiments (Heidelberg *et al.*, 2000; Joelsson *et al.*, 2006). Hence, further work was done using *V. cholerae* El Tor E7946. The Δ*crp* derivative was generated and had the expected phenotype on MacConkey maltose agar (Figure 4.10). The primers used to construct the deletion are listed in table 2.3 (Chapter 2). The pRW50T plasmids containing the full length wild type *rtxBDE* regulatory region, and its derivatives, was transferred into both wild type E7946 and the Δ*crp* mutant strains by conjugation. Promoter activities were inferred by measuring β-galactosidase activity in lysates of the transformants. Data for the assays are shown in Figure 4.11. As expected, β-galactosidase activity due to the wild type DNA fragment increased 6-fold in the *crp* mutant compared to the wildtype strain. A much smaller 2-fold increase in activity was observed for the DNA derivative with the VcCRP sites disrupted. This is likely due to residual VcCRP binding. As in previous experiments, mutation of the promoter -10 elements abolished *lacZ* expression as seen for the P1,P2,CRP-dis DNA fragment.

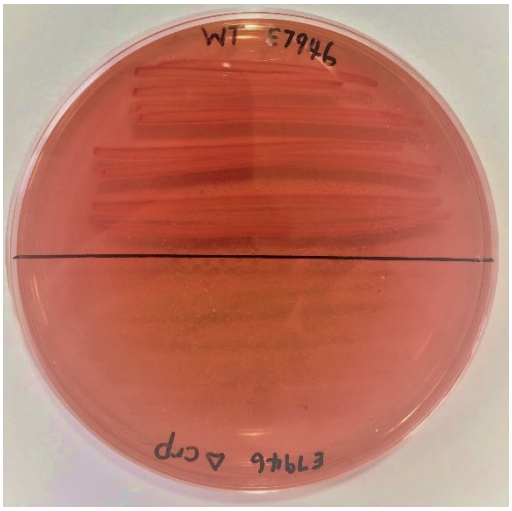

Figure 4.10. Image of wildtype *V. cholerae* growing alongside Δ*crp* on solid MacConkey maltose agar

The image shows the phenotypic difference between the Δ*crp* and E7946 strain when grown on MacConkey maltose agar. VcCRP is required for the expression of the *mal* gene in *V. cholerae*. Loss of the *crp* gene prevents the expression of maltase and the metabolism of maltose. As a result, maltose is not fermented and there is no pH change in the agar giving rise to pale colonies compared to the wild type.

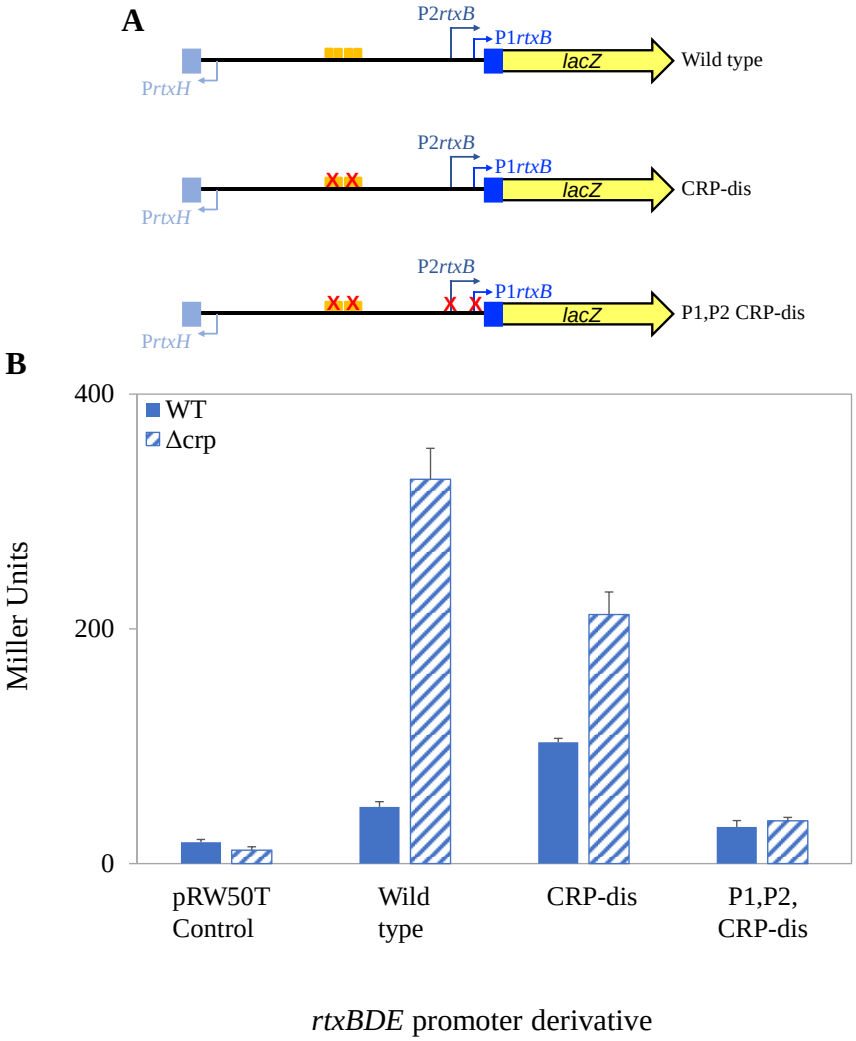

Figure 4.11. Expression of the *rtxBDE* operon is derepressed in the *crp* mutant

Panel A shows a schematic of each of the derivatives, the wild type P*rtxB* promoter, P*rtxB* CRP-dis whereby the CRP site (orange) is disrupted (shown with red X) and P12*rtxB* CRP-dis whereby both the promoters (blue arrows) and CRP site (orange) are disrupted (disruption is depicted by red X). Yellow arrow represents the *lacZ* gene. Panel B shows a β-galactosidase assays done using lysates of E7946 and Δ*crp* cells transformed with derivatives of the *lacZ* reporter plasmid, pRW50T, carrying different P*rtxB* derivatives.

Cells were grown in M9 minimal media to mid-log phase. Empty pRW50T was used as a control. Activity is measured in Miller Units. The error bars represent standard deviation for three biological replicates.

4.8 Conclusions

The aim of the work described in this chapter was to investigate the role of VcCRP at the regulatory region shared by the *rtxBDE* and *rtxHCA* operons. These sets of genes, encoding the RTX toxin and export machinery respectively, play an important role in *V. cholerae* pathogenicity (Olivier *et al.*, 2007; Satchell, 2015). Using a combination of biochemical and genetic assays we were able to identify two binding sites for VcCRP within the regulatory DNA (Figure 4.2). We showed that CRP had no effect on *rtxHCA* transcription and that these genes appear to be constitutively expressed (Figure 4.5). Conversely, we conclude that *rtxBDE* is repressed by VcCRP and, that this repression is relieved in rich growth media (Figure 4.9). These findings are consistent with previous work by Boardman *et al.* (2007) who noted repression of *rtxBDE* in nutrient poor environments but were unaware of the role played by VcCRP. Similar observations were reported in RNA-seq experiments comparing the *V. cholerae* transcriptome in nutrient poor and rich media (Mandlik *et al.*, 2011). We argue that VcCRP mediates these effects directly, by binding sites upstream of the *rtxBDE* promoters, rather than indirectly by interfering with the activity of an undefined activator of *rtxBDE*. Consistent with this, VcCRP was able to repress both P1*rtxB* and P2*rtxB in vitro* in the absence of other protein factors (Figure 4.11).

Role of CRP during colonisation of an aquatic host

Chapter 5

5.1 Introduction

The notion that fish may be reservoirs of *V. cholerae,* and play role in dissemination, has been suggested by many groups (Senderovich *et al.*, 2010; Halpern and Izhaki, 2017). For example, colonisation of certain fish species may have sustained epidemicity in India and serve as disease reservoirs in certain parts of Africa (Pandit C. G., 1951; Hounmanou *et al.*, 2016). Indeed, a recent study found up to 87% of fish species were colonised by *V. cholerae* in certain localities (Senderovich *et al.*, 2010). Since fish and humans have similar gut mucosa, it has been postulated that certain fish species are suitable models to study *V. cholerae* intestinal colonisation and infection (Gomez *et al.*, 2013; Rowe *et al.*, 2014).

As demonstrated by Runft *et al.* (2014), the zebrafish larvae model is particularly useful. Hence, bacteria are added to saltwater solutions in which larvae are free swimming and colonisation follows without intervention. Given that changes in nutrient availability are associated with host colonisation we examined the effects of colonisation on gene regulation by VcCRP. Hence, this chapter describes the role that VcCRP plays during colonisation of an aquatic host. I have focused on the *rtxBDE* regulatory region described in previous chapter.

5.2 CRP plays a vital role during colonisation of an aquatic host

To crudely understand the importance of VcCRP during host colonisation, we generated a derivative of *V. cholerae* E7946 that expresses green fluorescent protein (GFP) encoded by plasmid pMW-GFP. This facilitates visualisation of the bacterium during colonisation. To study colonisation we used four-day old zebrafish larvae. Figure 5.1A shows a single larva with labelled anatomical features. Larvae were infected with 10^6 *V. cholerae* cells per ml and the infection was tracked by monitoring fluorescence. Infections due to the wild type strain are disseminated throughout the intestinal tract as shown in panel B of Figure 5.1. Conversely, infections caused by cells lacking CRP or TCP are limited to the anterior intestinal tract and fail to colonize the mid-intestine and posterior intestine as observed in panels B and C. Quantification of fluorescence from the microscopy images revealed a 3-fold reduction in fluorescence, across the entire intestinal tract, for the Δ*crp* and Δ*tcpA* strains compared to the wildtype (Figure 5.2).

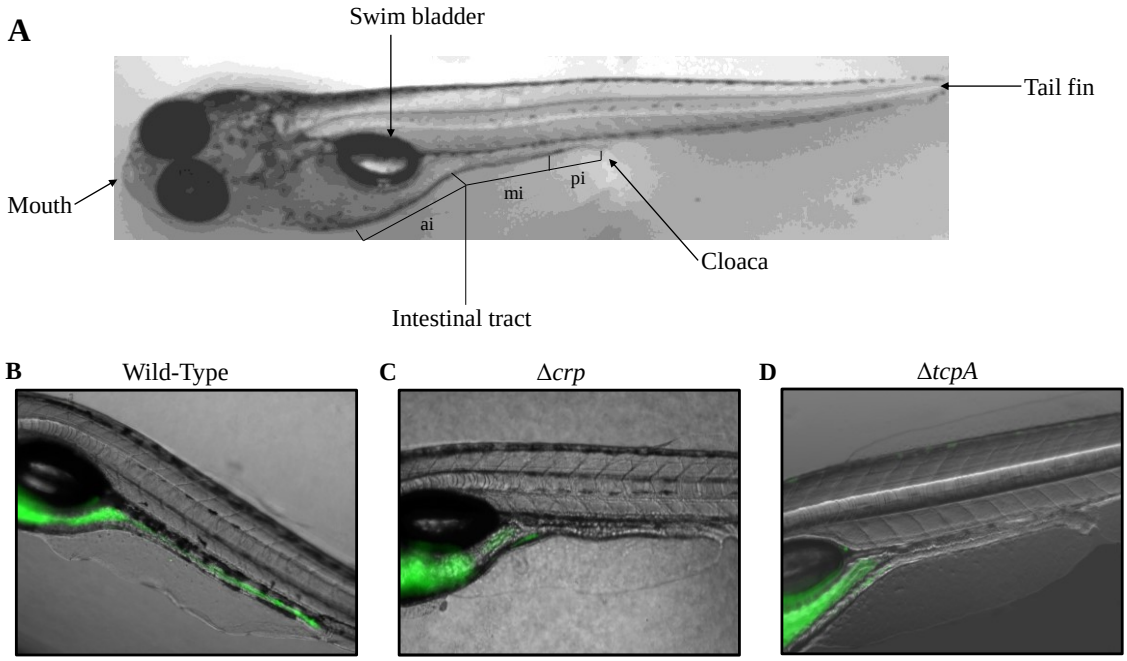

Figure 5.1. Zebrafish larvae infected with *V. cholerae* E7946 and derivatives

The figure shows the anatomy (panel A) and representative fluorescent microscopy images of a 4-day old zebrafish larvae (panel B-D). Panels B, C and D show microscopy images of zebrafish larvae colonised with the indicated *V. cholerae* strain. All bacterial strains were transformed with plasmid pMW-GFP to express green fluorescent protein allowing their detection. Larvae were immobilised by mounting onto 0.4% low melting point agarose dissolved in 1X E3 media and 160 µg/ml tricaine. Epifluorescence shown (green) is representative of merged bright-field and gfp images to show the colonisation of the intestinal tract with *V. cholerae* cells. (ai: anterior intestine; mi: mid intestine; pi: posterior intestine).

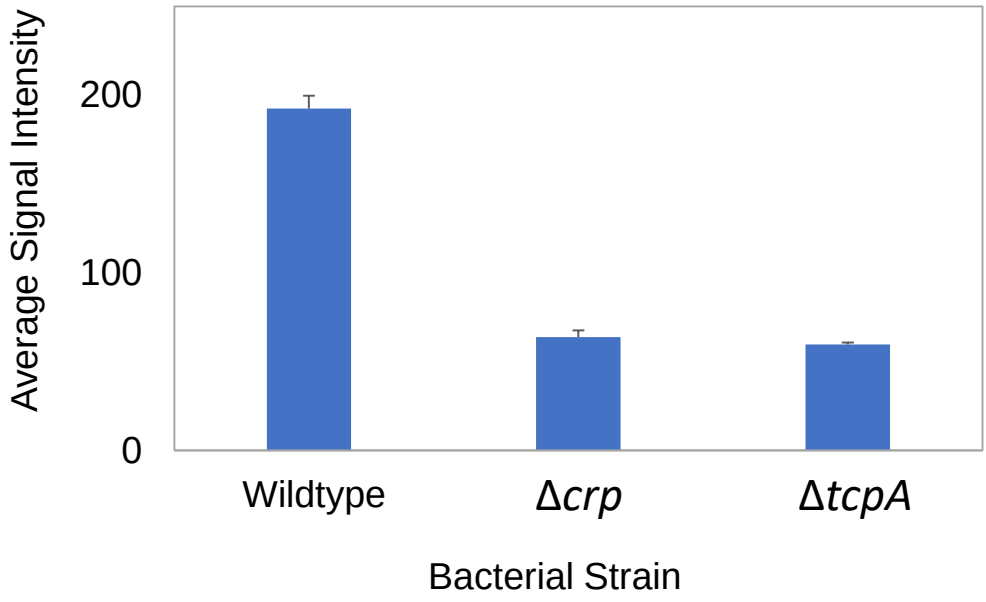

Figure 5.2. Average signal intensities of larvae infected with *V. cholerae* E7946 and derivatives

The graph shows the average GFP signal intensities from microscopic images of *V. cholerae* E7946 and derivatives. Each bar represents the mean intensities from 20 individual images condensed in a microscope. Signal intensities were determined using the ImageJ image processing package (NIH) software. Error bars represent the standard deviation of the mean.

To quantify virulence of the various strains, we monitored survival of the larvae during incubation with the bacteria (Figure 5.3). Zebrafish larvae were infected with undiluted culture (wildtype: 9.1 x 10^9 cells; derivatives: 5.4 x 10^9 cells), or dilutions containing 10^9, 10^8, 10^7 or 10^6 *V. cholerae* cells. Briefly, overnight cultures of each strain were used to inoculate a culture and, once in mid-log phase, cells were recovered by centrifugation, washed in sterile 1x E3 media, and resuspended in E3 media. Ten larvae per well were incubated with each of the derivatives at varying dilutions and monitored hourly for 12 hours post infection. Larvae were assessed for vital signs such as movement and appearance and each experiment was conducted with three independent replicates. All larvae infected with wild type *V. cholerae* were dead by the end of the time course for the undiluted, 10^9 and 10^8 conditions (black line). Conversely, infections caused by strains lacking CRP or TCP were not usually fatal. We conclude that, both CRP and TCP are important for colonisation of fish (Skorupski and Taylor, 1997a).

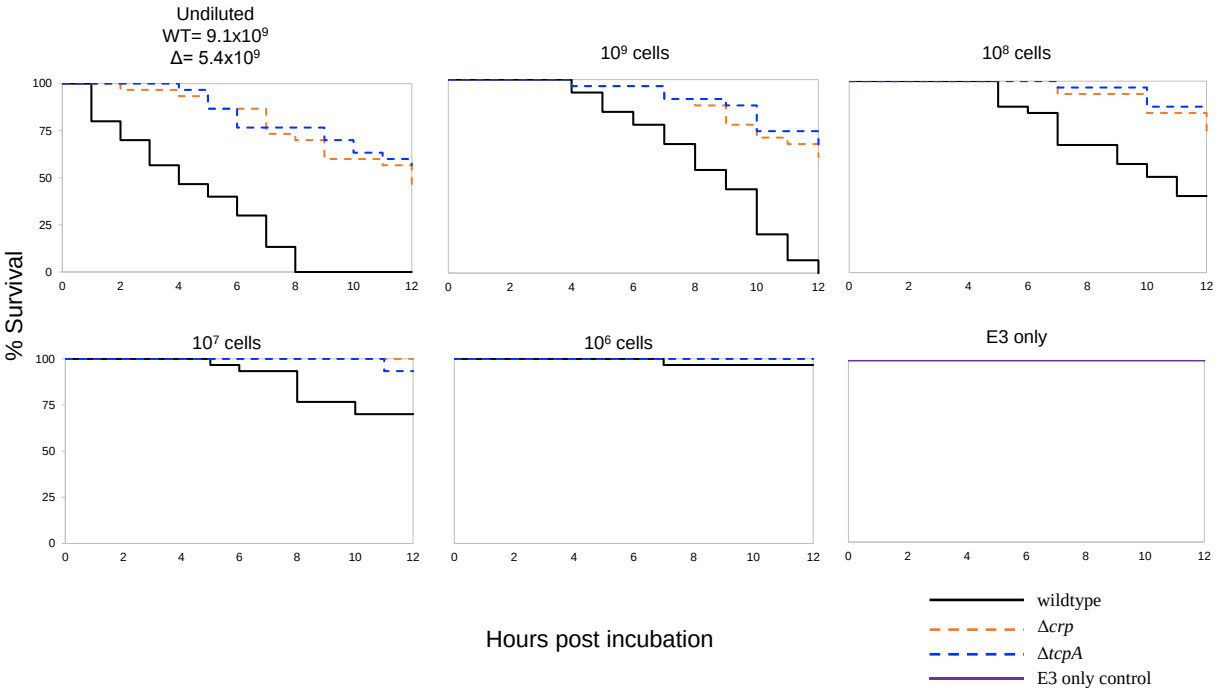

Figure 5.3. Survival of zebrafish larvae following infection with *V. cholerae* strains E7946, Δ*crp* or Δ*tcpA*

Each graph shows Kaplan-Meier estimators of survival for zebrafish larvae infected with wildtype (solid black line), Δ*crp* (broken orange line) or Δ*tcpA* (broken blue line) *V. cholerae* E7946 strains. The different panels illustrate experiments with the correspondingly labelled *V. cholerae* concentration. A cell free negative control of E3 media only is shown in the last panel (solid purple line). Larvae were assessed for vital signs (presence of movement and appearance) every 1 hour and percent survival plotted using Kaplan-Meier analysis (n=10 larvae per condition, over three independent experiments). Statistical significance was assessed using a Mantel-Cox test.

5.3 CRP mediates the induction of the *rtxBDE* operon during host colonisation

In chapter 3 I showed that that transcription from the *rtxBDE* promoters was triggered during colonisation of the intestinal tract. I hypothesised that this induction might result from reduced VcCRP-dependent repression. To test this, zebrafish larvae were inoculated with either wild type or Δ*crp* derivatives of *V. cholerae* carrying the wild type *rtxBDE*::*lacZ* fusion in plasmid pRW50T. After colonisation, larvae were separated from planktonic bacteria present in the media and washed in E3 media to remove any residual bacteria. The larvae were then sacrificed to release the intestinal bacteria. Levels of β-galactosidase expression were determined from lysates of the planktonic and larvae populations. The data obtained are shown in Figure 5.4. in wild type cells, low *rtxBDE* expression was measured for planktonic *V. cholerae* and *rtxBDE* expression increased substantially during colonisation of the larval intestinal tract (Figure 5.4A, open bar). As expected, this increase in expression required both P1*rtxB* and P2*rtxB* promoters (Figure 5.4A). However, in Δ*crp* cells, expression of *rtxBDE* was uncoupled from host colonisation as high activity was measured in both planktonic and intestinal populations (Figure 5.4B). The differences observed are not due to the different colonisation properties of the Δ*crp* strain as deregulation of *rtxBDE* occurs in planktonic populations and not within the larvae. Again, the measured activity required the P1*rtxB* and P2*rtxB* promoters (Figure 5.4B).

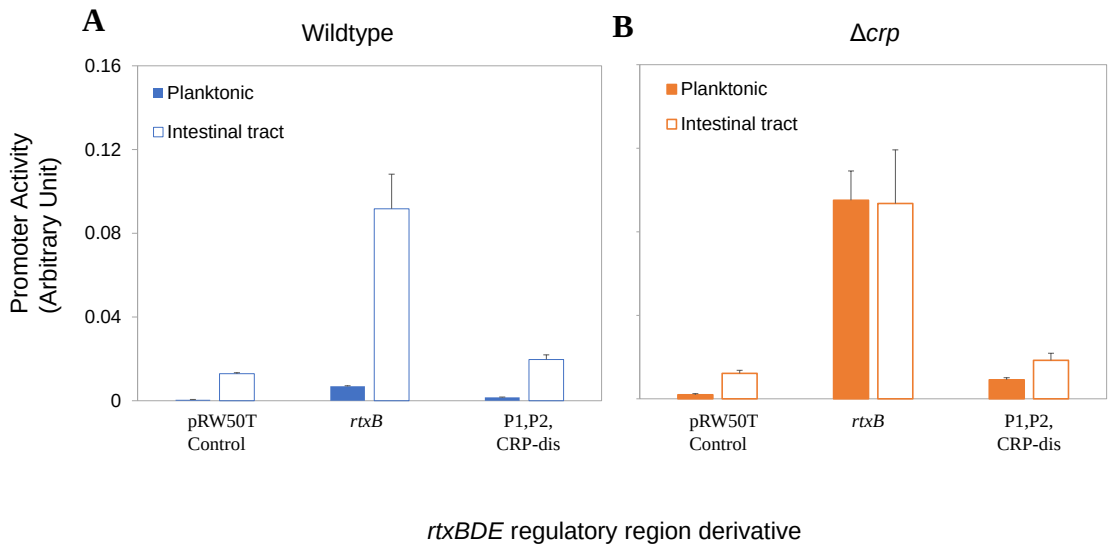

Figure 5.4. Expression of *rtxBDE* is induced by larvae colonisation

The graphs show the result of a β-galactosidase assay done using lysates of bacterial cells growing planktonically (filled bars) in E3 media or obtained from the zebrafish intestinal tract (open bars). Strains used for the infection are indicated above each panel. Panel A (blue) shows wildtype and panel B (orange) Δ*crp* strains. Each of the strains were transformed with pRW50T encoding the different derivatives of *rtxBDE*::*lacZ* fusions. Empty pRW50T was used as a control. Assays were done using mid-log phase cultures. Promoter activity is measured as arbitrary units. The error bars represent standard deviation for three biological replicates.

5.4 CRP modulates the expression of many *V. cholerae* genes during host colonisation

Logically, other VcCRP targeted promoters should also lose the ability to differentiate between aquatic environments and the host intestinal tract in the absence of VcCRP. To test this, four promoters were selected using our ChIP-seq data. The four promoters are organised as two pairs of divergently transcribed genes with a CRP site in the associated intergenic region like the *rtx* locus. The genes were *tolC* (encoding an outer membrane channel important for bile tolerance and export of the *rtxA* toxin), *acfA* (encoding accessory colonisation factor A), *acfD* (encoding accessory colonisation factor D) and *nudF* (encoding a pyrophosphatase) (Minato *et al.*, 2011; Parsot and Mekalanos, 1992; Bessman *et al.*, 1996).

To confirm binding, purified VcCRP was used in DNAse I footprinting assays with DNA fragments derived from the *tolC-nudF* and *acfA-acfD* intergenic regions. The sequence of each intergenic region is shown below each gel in Figures 5.5B and 5.6B. Maxim/Gilbert GA sequencing ladders were used to calibrate the footprinting gels (Figure 5.5A and 5.6A) and numbering corresponds to the transcription start site (+1) relative to the promoter indicated as obtained from Papenfort *et al*., (Papenfort *et al.*, 2015). For both footprints lane 1 shows the pattern of DNAse I cleavage in the absence of VcCRP. Upon addition of CRP (lanes 2-8) a change in the cleavage pattern was observed. The results generated from the footprints are consistent with CRP binding to the putative sites for both intergenic regions.

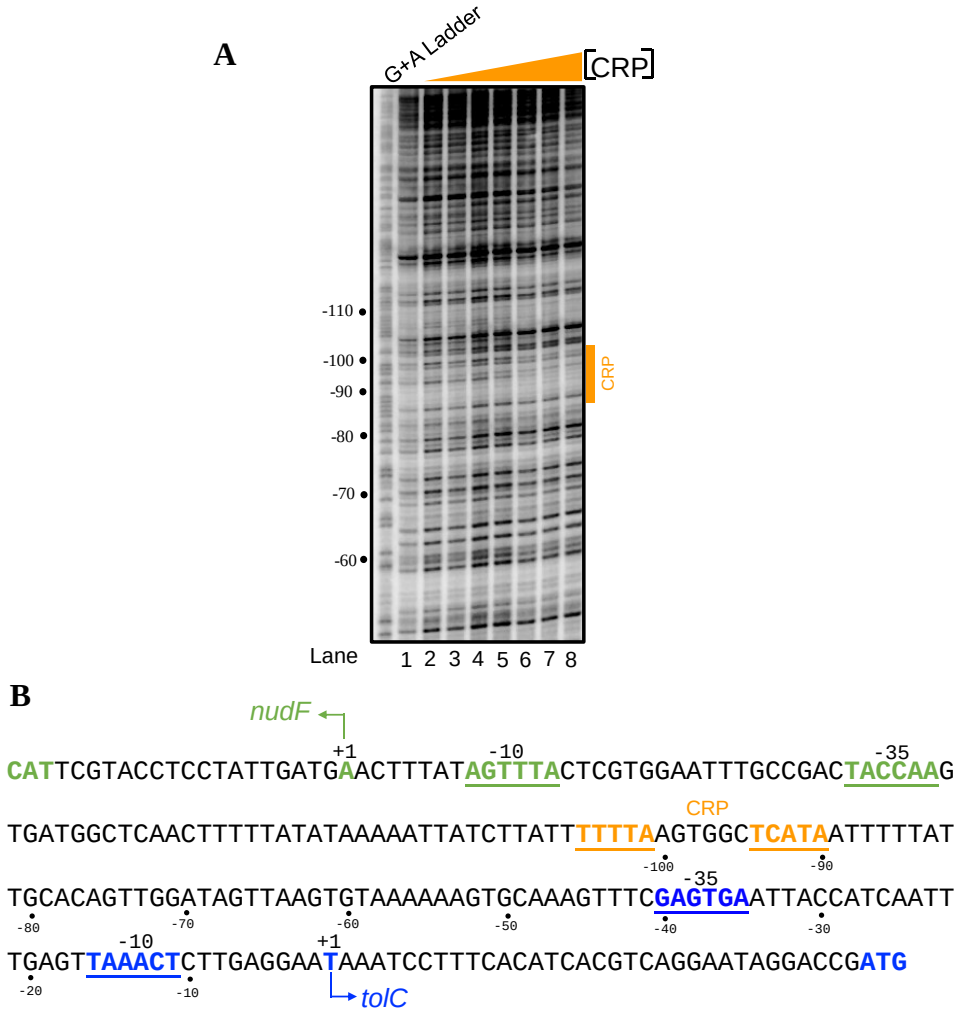

Figure 5.5. DNAse I footprint of VcCRP binding to *tolC-nudF* intergenic region

Panel A shows the results of a DNAse I footprinting experiment using the *tolC-nudF* intergenic region and purified *V. cholerae* CRP and cAMP. The experiment was calibrated with a Maxam-Gilbert GA sequencing ladder and panel B shows positions of the *tolC* (blue) and *nudF* (green) transcription start sites (+1) as labelled. The triangle indicates addition of CRP and lanes 1-8 correspond to concentrations of 0, 0.175, 0.35, 0.7, 1.4, 2.1 and 2.8 µM respectively. Orange box shows the position of the predicted VcCRP binding site, also labelled as orange underlined text in panel B.

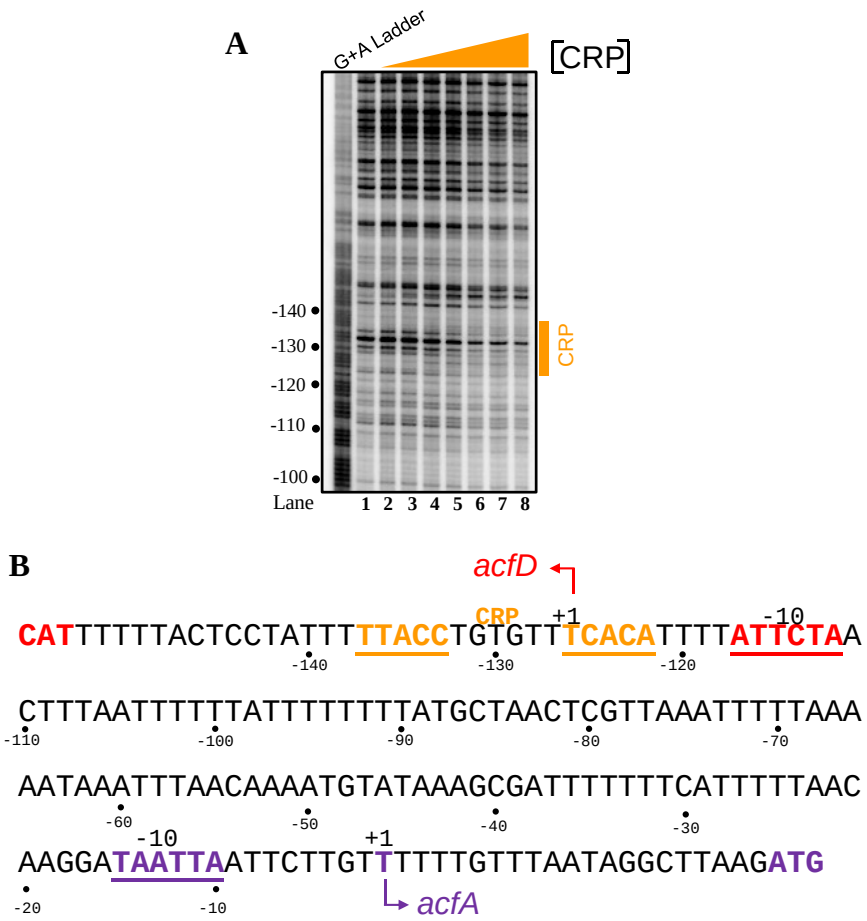

Figure 5.6. DNAse I footprint of VcCRP binding to *acfA-acfD* intergenic region

Panel A shows the results of a DNAse I footprinting experiment using the *acfA-acfD* intergenic region and purified VcCRP and cAMP. The experiment was calibrated with a Maxam-Gilbert GA sequencing ladder and positions of the *acfD* (red) and *acfA* (purple) transcription start sites (+1) are labelled (panel B). The triangle indicates addition of VcCRP and lanes 1-8 correspond to concentrations of 0, 0.175, 0.35, 0.7, 1.4, 2.1 and 2.8 µM respectively. Orange box shows the position of the predicted VcCRP binding site, also labelled as orange underlined text in panel B.

To understand the regulatory effect of VcCRP during host colonisation the promoter regions were cloned upstream of *lacZ* in plasmid pRW50T. The plasmids were then used to transform *V. cholerae* E7946 and the Δ*crp* derivative. Zebrafish larvae were inoculated with either wild type or Δ*crp* derivatives of *V. cholerae* carrying the *tolC*, *nudF*, *acfA* or *acfD*::*lacZ* fusions in plasmid pRW50T. After infection, larvae were separated from planktonic bacteria and β-galactosidase activity was determined from the lysates of the planktonic and larvae populations (Figure 5.7).

The data shows that in the wildtype strains, all the genes expressed were downregulated in intestinal compared to planktonic populations (Figure 5.7). However, when the experiment was repeated using Δ*crp* cells, expression of all genes was rendered insensitive to host colonisation (compare open and closed bars).

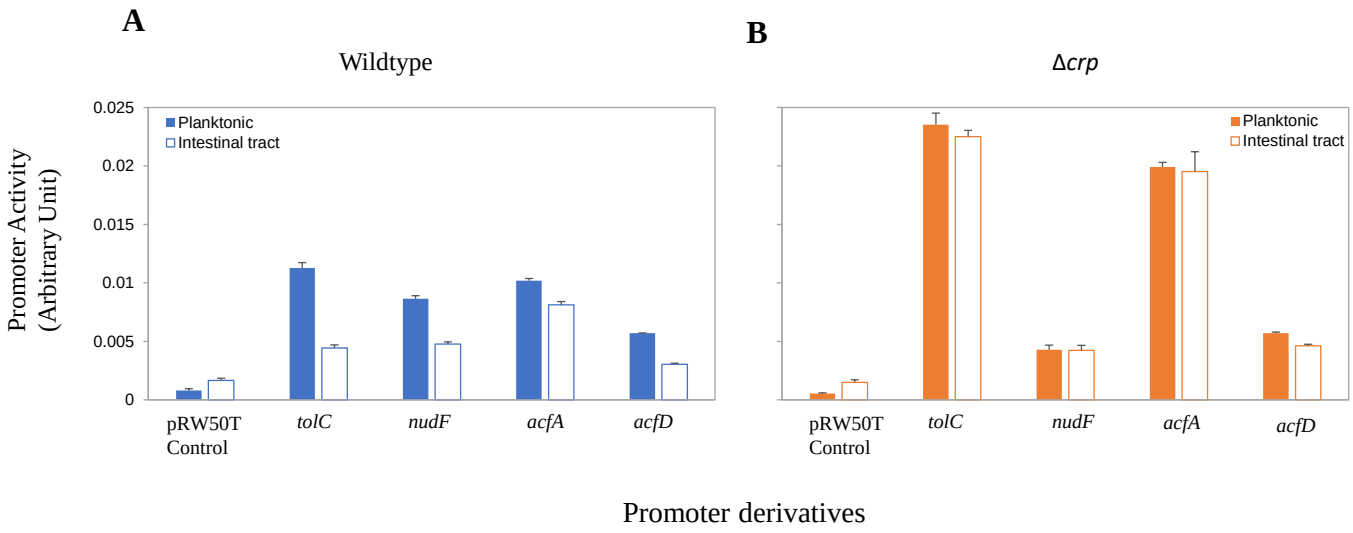

Figure 5.7. Expression of other promoters downregulated by CRP in host colonisation with wild type strain

The graphs show the result of β-galactosidase assays done using lysates of bacterial cells growing planktonically (filled bars) in E3 media or obtained from the zebrafish intestinal tract (open bars). Strains used for the infection are indicated above each panel, with wildtype shown in panel A (blue) and Δ*crp* in panel B (orange). Each of the strains were transformed with pRW50T encoding the different derivatives of *tolC*; *nudF*, *acfA* or *acfD*::*lacZ* fusions. Empty pRW50T was used as a control. Assays were done using mid-log phase cultures. Promoter activity is measured as arbitrary units. The error bars represent standard deviation for three biological replicates.

5.5 Conclusions

This chapter examines the role of VcCRP during colonisation of the zebrafish host. I focused on the *rtxBDE* regulatory region and showed that host specific induction of transcription is regulated by VcCRP in a zebrafish model (Figure 5.4). The data is consistent with repression of *rtxBDE* by VcCRP that is relieved within the intestinal tract and other nutrient rich environments as also seen in chapter 4. Previous transcriptome analysis led to speculation that VcCRP may modulate the expression of *V. cholerae* virulence factors in response to host colonisation (Mandlik *et al.*, 2011; Papenfort *et al.*, 2015). Here,using the zebrafish larvae colonisation model, I was able to establish that, for all genes examined, differential expression in planktonic and intestinal populations required CRP (Figure 5.7).

Previous host colonisation studies such as that done by Mandlik and colleagues support our model (Mandlik *et al.*, 2011). Their work monitored global transcription in *V. cholerae* using RNA-seq and their data demonstrate induction of *rtxBDE* within the intestinal tracts of both mice and rabbits (Mandlik *et al.*, 2011). As we see in Figure 5.7, other promoters also required CRP to respond to the intestinal environment. Hence, VcCRP is integral to the regulatory network that controls *V. cholerae* lifestyle switching.

Final Conclusions and Discussion

Chapter 6

Regulation of gene expression allows bacteria to adapt to changes in nutrient availability, temperature, and pH. Gene expression can be regulated at any step from transcription to translation. However, the most common and cost effect is the control of transcription initiation.

The focus of this work has been regulation of transcription initiation in *V. cholerae* in response to host colonisation. I have focused on the transcription factor VcCRP and demonstrate a role in the control of lifestyle switching by *V. cholerae*. The ability of *V. cholerae* to persist in environmental reservoirs, colonise the intestinal tract, and cause disease, requires careful co-ordination of gene expression. The mechanism through which *V. cholerae* achieves the ability to switch lifestyle remains unclear. Identifying the role of VcCRP in lifestyle switching will enable a better understanding of *V. cholerae* and how it has evolved to efficiently occupy different niches.

Using ChIP-seq, biochemical assays and zebrafish studies, I was able to focus on the *rtxBDE* and *rtxHCA* regulatory region and provide a better understanding on the regulatory effect of VcCRP. I optimised the protocols required to characterise specific *V. cholerae* genes *in vitro, in vivo* and in the context of a host. Having paid particularly close attention to genes encoding the RTX toxin and export machinery, I was able to show that the *rtxBDE* genes are transcribed from two promoters; P1*rtxB* and P2*rtxB*. The *rtxHCA* and *rtxBDE* genes encode the RTX toxin and toxin export machinery respectively (Satchell, 2015). The RTX toxin is known to contribute to pathogenesis by causing the depolymerisation and crosslinking of actin (Sheahan *et al.*, 2004). This work also identified and characterised two VcCRP sites within the *rtxBDE* intergenic region and

showed that these sites repress gene transcription in nutrient poor environments. Furthermore, I detected repression of *rtxBDE* in M9 minimal media compared to LB broth. Previous work by Mandlik *et al.* (2011), monitoring global transcription in *V. cholerae* using RNA-seq, demonstrate induction of *rtxBDE* within the intestinal tracts of both mice and rabbits. The same study also detected repression of *rtxBDE* in M9 minimal media compared to LB broth (Mandlik *et al.*, 2011). Similarly, Boardman *et al.* (2007) also noted repression of *rtxBDE* in nutrient poor environments. The data presented here, in chapters 4 and 5, is also consistent with repression of *rtxBDE* by VcCRP that is relieved within the intestinal tract and other nutrient rich environments. Given the location of the VcCRP sites in respect to promoters, I argue that VcCRP mediates these effects directly by binding sites upstream of the *rtxBDE* promoters, similarly shown in previous studies where tandem binding by *E. coli* CRP lead to repression (Lee and Busby, 2012). This de-repression of *rtxBDE* by VcCRP in nutrient rich environments suggests that the toxin is only exported when the bacteria encounters host cells. This target or contact specific export of RTX toxin was observed in *V. vulnificus*, whereby the toxin kills the cell only after contact of the bacteria with host cells (Kim *et al.*, 2008).

Our work showed that VcCRP had no effect on the expression of the *rtxHCA* genes and we put forward a model that the toxin is constitutively expressed and only exported upon entry into nutrient rich environments such as a host. A hypothesis supported by our data. Boardman *et al.* (2007) also suggested constitutive expression of the toxin but showed that neither the toxin nor mRNA transcript was accumulated in the cytoplasm of the bacteria. Recent work by Papenfort *et al.* (2015) show that the *rtxHCA* region is regulated post transcriptionally by the regulatory RNA, VqmR. VqmR directly represses the

translation of *rtx* toxin transcripts, by binding to the mRNA transcripts in a quorum sensing dependent manner (Papenfort *et al.*, 2015).

Previous transcriptome analysis by Liang *et al.* (2007) suggested that CRP may modulate the expression of other *V. cholerae* virulence factors in response to host colonisation. Here we have tested this prediction using the zebrafish larvae colonisation model, used by Runft *et al.* (2014), and show that apart from the *rtxBDE* and *rtxHCA* regulatory region, other genes, such as *tolC* and *acfA/D*, involved in *V. cholerae* pathogenicity were also targets for VcCRP. For all genes examined differential expression in planktonic and intestinal populations required CRP. Taken together, previous host colonisation studies support our model that VcCRP is integral to the regulatory network that controls *V. cholerae* lifestyle switching.

Finally, it is of note that VcCRP regulates genes expression in response to the availability of glucose; this sugar is a major component of oral rehydration solutions at the forefront of cholera treatment. Hence, it may be possible to optimise such solutions to alter the regulatory effect of VcCRP during infection.

References

ALI, M., NELSON, A. R., LOPEZ, A. L. & SACK, D. A. 2015. Updated Global Burden of Cholera in Endemic Countries. *PLoS Neglected Tropical Diseases,* 9**,** e0003832.

ALMAGRO-MORENO, S., PRUSS, K. & TAYLOR, R. K. 2015. Intestinal Colonization Dynamics of Vibrio cholerae. *PLoS Pathog,* 11**,** e1004787.

AMIT, R., OPPENHEIM, A. B. & STAVANS, J. 2003. Increased Bending Rigidity of Single DNA Molecules by H-NS, a Temperature and Osmolarity Sensor. *Biophysical Journal,* 84**,** 2467-2473.

ATLUNG, T. & INGMER, H. 1997. H-NS: a modulator of environmentally regulated gene expression. *Molecular Microbiology,* 24**,** 7-17.

AUSTIN, B. 2010. Vibrios as causal agents of zoonoses. *Veterinary Microbiology,* 140**,** 310-317.

AYALA, J. C., SILVA, A. J. & BENITEZ, J. A. 2017. H-NS: an overarching regulator of the Vibrio cholerae life cycle. *Res Microbiol,* 168**,** 16-25.

AZIZ, K. M. S., MOHSIN, A. K. M., HARE, W. K. & PHILLIPS, R. A. 1968. Using the Rat as a Cholera [ldquo]Model[rdquo]. *Nature,* 220**,** 814-815.

BAE, B., FEKLISTOV, A., LASS-NAPIORKOWSKA, A., LANDICK, R. & DARST, S. A. 2015. Structure of a bacterial RNA polymerase holoenzyme open promoter complex. *eLife,* 4**,** e08504.

BANERJEE, S., CHALISSERY, J., BANDEY, I. & SEN, R. 2006. Rho-dependent Transcription Termination: More Questions than Answers. *Journal of microbiology (Seoul, Korea),* 44**,** 11-22.

BELLAIR, M. & WITHEY, J. H. 2008. Flexibility of Vibrio cholerae ToxT in Transcription Activation of Genes Having Altered Promoter Spacing. *Journal of Bacteriology,* 190**,** 7925-7931.

BESSMAN, M. J., FRICK, D. N. & O'HANDLEY, S. F. 1996. The MutT Proteins or "Nudix" Hydrolases, a Family of Versatile, Widely Distributed, "Housecleaning" Enzymes. *Journal of Biological Chemistry,* 271**,** 25059-25062.

BEYHAN, S., TISCHLER, A. D., CAMILLI, A. & YILDIZ, F. H. 2006. Differences in Gene Expression between the Classical and El Tor Biotypes of Vibrio cholerae O1. *Infection and Immunity,* 74**,** 3633-3642.

BLATTNER, F. R., PLUNKETT, G., BLOCH, C. A., PERNA, N. T., BURLAND, V., RILEY, M., COLLADO-VIDES, J., GLASNER, J. D., RODE, C. K., MAYHEW, G. F., GREGOR, J., DAVIS, N. W., KIRKPATRICK, H. A., GOEDEN, M. A., ROSE, D. J., MAU, B. & SHAO, Y. 1997. The Complete Genome Sequence of Escherichia coli K-12. *Science,* 277**,** 1453-1462.

BLOKESCH, M. & SCHOOLNIK, G. K. 2008. The Extracellular Nuclease Dns and Its Role in Natural Transformation of Vibrio cholerae. *Journal of Bacteriology,* 190**,** 7232-7240.

BLOW, N. S., SALOMON, R. N., GARRITY, K., REVEILLAUD, I., KOPIN, A., JACKSON, F. R. & WATNICK, P. I. 2005. Vibrio cholerae infection of Drosophila melanogaster mimics the human disease cholera. *PLoS Pathog,* 1**,** e8.

BOARDMAN, B. K. & FULLNER SATCHELL, K. J. 2004. Vibrio cholerae Strains with Mutations in an Atypical Type I Secretion System Accumulate RTX Toxin Intracellularly. *Journal of Bacteriology,* 186**,** 8137-8143.

BOARDMAN, B. K., MEEHAN, B. M. & FULLNER SATCHELL, K. J. 2007. Growth Phase Regulation of Vibrio cholerae RTX Toxin Export. *Journal of Bacteriology,* 189**,** 1827-1835.

BOTSFORD, J. L. & HARMAN, J. G. 1992. Cyclic AMP in prokaryotes. *Microbiol Rev,* 56**,** 100-22.

BROWNING, D. F. & BUSBY, S. J. W. 2004. The regulation of bacterial transcription initiation. *Nat Rev Micro,* 2**,** 57-65.

BROWNING, D. F. & BUSBY, S. J. W. 2016. Local and global regulation of transcription initiation in bacteria. *Nat Rev Micro,* 14**,** 638-650.

BURR, T., MITCHELL, J., KOLB, A., MINCHIN, S. & BUSBY, S. 2000. DNA sequence elements located immediately upstream of the –10 hexamer in Escherichia coli promoters: a systematic study. *Nucleic Acids Research,* 28**,** 1864-1870.

BUSBY, S. & EBRIGHT, R. H. 1997. Transcription activation at class II CAP-dependent promoters. *Mol Microbiol,* 23**,** 853-9.

BUSBY, S. & EBRIGHT, R. H. 1999. Transcription activation by catabolite activator protein (CAP). *Journal of Molecular Biology,* 293**,** 199-213.

BUSBY, S., KOTLARZ, D. & BUC, H. 1983. Deletion mutagenesis of the Escherichia coli galactose operon promoter region. *Journal of Molecular Biology,* 167**,** 259-274.

CAREY, M. F., PETERSON, C. L. & SMALE, S. T. 2012. Experimental Strategies for the Identification of DNA-Binding Proteins. *Cold Spring Harbor Protocols,* 2012**,** pdb.top067470.

CARPENTER, C. C., SACK, R. B., FEELEY, J. C. & STEENBERG, R. W. 1968. Site and characteristics of electrolyte loss and effect of intraluminal glucose in experimental canine cholera. *J Clin Invest,* 47**,** 1210-20.

CASADABAN, M. J. & COHEN, S. N. 1980. Analysis of gene control signals by DNA fusion and cloning in Escherichia coli. *Journal of Molecular Biology,* 138**,** 179-207.

CHANG, Y.-W., KJÆR, A., ORTEGA, D. R., KOVACIKOVA, G., SUTHERLAND, J. A., RETTBERG, L. A., TAYLOR, R. K. & JENSEN, G. J. 2017. Architecture of the Vibrio cholerae toxin-coregulated pilus machine revealed by electron cryotomography. 2**,** 16269.

CHATTOPADHYAY, R. & PARRACK, P. 2006. Cyclic AMP-dependent functional forms of cyclic AMP receptor protein from Vibrio cholerae. *Archives of Biochemistry and Biophysics,* 447**,** 80-86.

CHAUDHURI, K. & CHATTERJEE, S. N. 2009. *Cholera Toxins*, Springer.

CHILDERS, B. M. & KLOSE, K. E. 2007. Regulation of virulence in Vibrio cholerae: the ToxR regulon. *Future Microbiology,* 2**,** 335-344.

CHOY, H. E. & ADHYA, S. 1992. Control of gal transcription through DNA looping: inhibition of the initial transcribing complex. *Proceedings of the National Academy of Sciences of the United States of America,* 89**,** 11264-11268.

CLEMENS, J. D., NAIR, G. B., AHMED, T., QADRI, F. & HOLMGREN, J. 2017. Cholera. *The Lancet,* 390**,** 1539-1549.

COLWELL, R. R. & HUQ, A. 1994. Environmental Reservoir of Vibrio cholerae The Causative Agent of Choleraa. *Annals of the New York Academy of Sciences,* 740**,** 44-54.

COLWELL, R. R., HUQ, A., ISLAM, M. S., AZIZ, K. M. A., YUNUS, M., KHAN, N. H., MAHMUD, A., SACK, R. B., NAIR, G. B., CHAKRABORTY, J., SACK, D. A. & RUSSEK-COHEN, E. 2003. Reduction of cholera in Bangladeshi villages by simple filtration. *Proceedings of the National Academy of Sciences of the United States of America,* 100**,** 1051-1055.

DALIA, A. B., LAZINSKI, D. W. & CAMILLI, A. 2014a. Identification of a Membrane-Bound Transcriptional Regulator That Links Chitin and Natural Competence in Vibrio cholerae. *mBio,* 5.

DALIA, A. B., MCDONOUGH, E. & CAMILLI, A. 2014b. Multiplex genome editing by natural transformation. *Proceedings of the National Academy of Sciences of the United States of America,* 111**,** 8937-8942.

DALIA, A. B., SEED, K. D., CALDERWOOD, S. B. & CAMILLI, A. 2015. A globally distributed mobile genetic element inhibits natural transformation of Vibrio cholerae. *Proceedings of the National Academy of Sciences of the United States of America,* 112**,** 10485-10490.

DE CROMBRUGGHE, B., BUSBY, S. & BUC, H. 1984. Cyclic AMP receptor protein: role in transcription activation. *Science,* 224**,** 831-838.

DE, S. N. & CHATTERJE, D. N. 1953. An experimental study of the mechanism of action of Vibriod cholerae on the intestinal mucous membrane. *J Pathol Bacteriol,* 66**,** 559-62.

DIRITA, V. J., PARSOT, C., JANDER, G. & MEKALANOS, J. J. 1991. Regulatory cascade controls virulence in Vibrio cholerae. *Proceedings of the National Academy of Sciences of the United States of America,* 88**,** 5403-5407.

DORMAN, CHARLES J. 2013. Co-operative roles for DNA supercoiling and nucleoid-associated proteins in the regulation of bacterial transcription. *Biochemical Society Transactions,* 41**,** 542.

DUAN, F. & MARCH, J. C. 2010. Engineered bacterial communication prevents Vibrio cholerae virulence in an infant mouse model. *Proceedings of the National Academy of Sciences,* 107**,** 11260-11264.

DZIEJMAN, M., BALON, E., BOYD, D., FRASER, C. M., HEIDELBERG, J. F. & MEKALANOS, J. J. 2002. Comparative genomic analysis of Vibrio cholerae: Genes that correlate with cholera endemic and pandemic disease. *Proceedings of the National Academy of Sciences,* 99**,** 1556-1561.

EBRIGHT, R. H. 1993. Transcription activation at Class I CAP-dependent promoters. *Molecular Microbiology,* 8**,** 797-802.

EL-ROBH, M. S. & BUSBY, S. J. W. 2002. The Escherichia coli cAMP receptor protein bound at a single target can activate transcription initiation at divergent promoters: a systematic study that exploits new promoter probe plasmids. *Biochemical Journal,* 368**,** 835-843.

ENGESZER, R. E., PATTERSON, L. B., RAO, A. A. & PARICHY, D. M. 2007. Zebrafish in the wild: a review of natural history and new notes from the field. *Zebrafish,* 4**,** 21-40.

ESTREM, S. T., ROSS, W., GAAL, T., CHEN, Z. W. S., NIU, W., EBRIGHT, R. H. & GOURSE, R. L. 1999. Bacterial promoter architecture: subsite structure of UP

elements and interactions with the carboxy-terminal domain of the RNA polymerase α subunit. *Genes & Development,* 13**,** 2134-2147.

FANG, F. C. & RIMSKY, S. 2008. New Insights into Transcriptional Regulation by H-NS. *Current opinion in microbiology,* 11**,** 113-120.

FARUQUE, S. M., ALBERT, M. J. & MEKALANOS, J. J. 1998. Epidemiology, Genetics, and Ecology of Toxigenic Vibrio cholerae. *Microbiology and Molecular Biology Reviews,* 62**,** 1301-1314.

FEKLISTOV, A. 2013. RNA polymerase: in search of promoters. *Annals of the New York Academy of Sciences,* 1293**,** 25-32.

FEKLISTOV, A. & DARST, S. A. 2011. Structural basis for promoter –10 element recognition by the bacterial RNA polymerase σ subunit. *Cell,* 147**,** 1257-1269.

FEKLÍSTOV, A., SHARON, B. D., DARST, S. A. & GROSS, C. A. 2014. Bacterial Sigma Factors: A Historical, Structural, and Genomic Perspective. *Annual Review of Microbiology,* 68**,** 357-376.

FIELD, M. 1979. Mechanisms of action of cholera and Escherichia coli enterotoxins. *The American Journal of Clinical Nutrition,* 32**,** 189-96.

FIGURSKI, D. H. & HELINSKI, D. R. 1979. Replication of an origin-containing derivative of plasmid RK2 dependent on a plasmid function provided in trans. *Proceedings of the National Academy of Sciences,* 76**,** 1648-1652.

FONG, J. C. N. & YILDIZ, F. H. 2008. Interplay between Cyclic AMP-Cyclic AMP Receptor Protein and Cyclic di-GMP Signaling in Vibrio cholerae Biofilm Formation. *Journal of Bacteriology,* 190**,** 6646-6659.

GOLDMAN, S. R., EBRIGHT, R. H. & NICKELS, B. E. 2009. Direct detection of abortive RNA transcripts in vivo. *Science,* 324**,** 927-8.

GOMEZ, D., SUNYER, J. O. & SALINAS, I. 2013. The mucosal immune system of fish: the evolution of tolerating commensals while fighting pathogens. *Fish & shellfish immunology,* 35**,** 1729-1739.

GRAINGER, D. C. 2016. Structure and function of bacterial H-NS protein. *Biochemical Society Transactions,* 44**,** 1561.

GRAINGER, D. C. & BUSBY, S. J. 2008. Methods for studying global patterns of DNA binding by bacterial transcription factors and RNA polymerase. *Biochem Soc Trans,* 36**,** 754-7.

GRANT, S. G., JESSEE, J., BLOOM, F. R. & HANAHAN, D. 1990. Differential plasmid rescue from transgenic mouse DNAs into Escherichia coli methylation-restriction

mutants. *Proceedings of the National Academy of Sciences of the United States of America,* 87**,** 4645-4649.

GRIMES, D. J., JOHNSON, C. N., DILLON, K. S., FLOWERS, A. R., NORIEA, N. F. & BERUTTI, T. 2009. What Genomic Sequence Information Has Revealed About Vibrio Ecology in the Ocean—A Review. *Microbial Ecology,* 58**,** 447-460.

GRYLAK-MIELNICKA, A., BIDNENKO, V., BARDOWSKI, J. & BIDNENKO, E. 2016. Transcription termination factor Rho: a hub linking diverse physiological processes in bacteria. *Microbiology,* 162**,** 433-447.

HALPERN, M. & IZHAKI, I. 2017. Fish as Hosts of Vibrio cholerae. *Frontiers in Microbiology,* 8**,** 282.

HAYCOCKS, J. R. J., SHARMA, P., STRINGER, A. M., WADE, J. T. & GRAINGER, D. C. 2015. The Molecular Basis for Control of ETEC Enterotoxin Expression in Response to Environment and Host. *PLOS Pathogens,* 11**,** e1004605.

HEIDELBERG, J. F., EISEN, J. A., NELSON, W. C., CLAYTON, R. A., GWINN, M. L., DODSON, R. J., HAFT, D. H., HICKEY, E. K., PETERSON, J. D., UMAYAM, L., GILL, S. R., NELSON, K. E., READ, T. D., TETTELIN, H., RICHARDSON, D., ERMOLAEVA, M. D., VAMATHEVAN, J., BASS, S., QIN, H., DRAGOI, I., SELLERS, P., MCDONALD, L., UTTERBACK, T., FLEISHMANN, R. D., NIERMAN, W. C., WHITE, O., SALZBERG, S. L., SMITH, H. O., COLWELL, R. R., MEKALANOS, J. J., VENTER, J. C. & FRASER, C. M. 2000. DNA sequence of both chromosomes of the cholera pathogen Vibrio cholerae. *Nature,* 406**,** 477-483.

HERRINGTON, D. A., HALL, R. H., LOSONSKY, G., MEKALANOS, J. J., TAYLOR, R. K. & LEVINE, M. M. 1988. Toxin, toxin-coregulated pili, and the toxR regulon are essential for Vibrio cholerae pathogenesis in humans. *J Exp Med,* 168**,** 1487-92.

HIBBING, M. E., FUQUA, C., PARSEK, M. R. & PETERSON, S. B. 2010. Bacterial competition: surviving and thriving in the microbial jungle. *Nature reviews. Microbiology,* 8**,** 15-25.

HOBLEY, L., HARKINS, C., MACPHEE, C. E. & STANLEY-WALL, N. R. 2015. Giving structure to the biofilm matrix: an overview of individual strategies and emerging common themes. *FEMS Microbiology Reviews*.

HOUNMANOU, Y. M. G., MDEGELA, R. H., DOUGNON, T. V., MHONGOLE, O. J., MAYILA, E. S., MALAKALINGA, J., MAKINGI, G. & DALSGAARD, A. 2016. Toxigenic Vibrio cholerae O1 in vegetables and fish raised in wastewater irrigated fields and stabilization ponds during a non-cholera outbreak period in Morogoro, Tanzania: an environmental health study. *BMC Research Notes,* 9**,** 466.

HULBERT, R. R. & TAYLOR, R. K. 2002. Mechanism of ToxT-Dependent Transcriptional Activation at the Vibrio cholerae tcpA Promoter. *Journal of Bacteriology,* 184**,** 5533-5544.

J.F, S. K. 2011. Structure and Function of MARTX Toxins and Other Large Repetitive RTX Proteins. *Annual Review of Microbiology,* 65**,** 71-90.

JOELSSON, A., LIU, Z. & ZHU, J. 2006. Genetic and Phenotypic Diversity of Quorum-Sensing Systems in Clinical and Environmental Isolates of Vibrio cholerae. *Infection and Immunity,* 74**,** 1141-1147.

KAPANIDIS, A. N., MARGEAT, E., HO, S. O., KORTKHONJIA, E., WEISS, S. & EBRIGHT, R. H. 2006. INITIAL TRANSCRIPTION BY RNA POLYMERASE PROCEEDS THROUGH A DNA-SCRUNCHING MECHANISM: Single-molecule fluorescence-resonance-energy-transfer experiments establish that initial transcription proceeds through a "scrunching" mechanism, in which RNA polymerase remains fixed on promoter DNA and pulls downstream DNA into itself and past its active center. *Science (New York, N.Y.),* 314**,** 1144-1147.

KAPER, J. B., MORRIS, J. G. & LEVINE, M. M. 1995. Cholera. *Clinical Microbiology Reviews,* 8**,** 48-86.

KAZI, M. I., CONRADO, A. R., MEY, A. R., PAYNE, S. M. & DAVIES, B. W. 2016. ToxR Antagonizes H-NS Regulation of Horizontally Acquired Genes to Drive Host Colonization. *PLoS Pathog,* 12**,** e1005570.

KIM, E. J., LEE, D., MOON, S. H., LEE, C. H., KIM, S. J., LEE, J. H., KIM, J. O., SONG, M., DAS, B., CLEMENS, J. D., PAPE, J. W., NAIR, G. B. & KIM, D. W. 2014. Molecular Insights Into the Evolutionary Pathway of Vibrio cholerae O1 Atypical El Tor Variants. *PLoS Pathogens,* 10**,** e1004384.

KIM, Y. R., LEE, S. E., KOOK, H., YEOM, J. A., NA, H. S., KIM, S. Y., CHUNG, S. S., CHOY, H. E. & RHEE, J. H. 2008. Vibrio vulnificus RTX toxin kills host cells only after contact of the bacteria with host cells. *Cell Microbiol,* 10**,** 848-62.

KIRN, T. J., JUDE, B. A. & TAYLOR, R. K. 2005. A colonization factor links Vibrio cholerae environmental survival and human infection. *Nature,* 438**,** 863-866.

KIRN, T. J., LAFFERTY, M. J., SANDOE, C. M. P. & TAYLOR, R. K. 2000. Delineation of pilin domains required for bacterial association into microcolonies and intestinal colonization by Vibrio cholerae. *Molecular Microbiology,* 35**,** 896-910.

KLOSE, K. E. 2000. The suckling mouse model of cholera. *Trends Microbiol,* 8**,** 189-91.

KOLB, A., BUSBY, S., H. BUC, GARGES, S. & ADHYA, S. 1993. Transcriptional Regulation by cAMP and Its Receptor Protein. *Annual Review of Biochemistry,* 62**,** 749-797.

KOLB, A., KOTLARZ, D., KUSANO, S. & ISHIHAMA, A. 1995. Selectivity of the Escherichia coli RNA polymerase E sigma 38 for overlapping promoters and ability to support CRP activation. *Nucleic Acids Research,* 23**,** 819-826.

KUDRYASHOVA, E., HEISLER, D., ZYWIEC, A. & KUDRYASHOV, D. S. 2014. Thermodynamic properties of the effector domains of MARTX toxins suggest their unfolding for translocation across the host membrane. *Mol Microbiol,* 92**,** 1056-71.

LAWSON, C. L., SWIGON, D., MURAKAMI, K. S., DARST, S. A., BERMAN, H. M. & EBRIGHT, R. H. 2004. Catabolite activator protein: DNA binding and transcription activation. *Current Opinion in Structural Biology,* 14**,** 10-20.

LEE, D. J. & BUSBY, S. J. W. 2012. Repression by Cyclic AMP Receptor Protein at a Distance. *mBio,* 3**,** e00289-12.

LEE, D. J., MINCHIN, S. D. & BUSBY, S. J. W. 2012. Activating Transcription in Bacteria. *Annual Review of Microbiology,* 66**,** 125-152.

LI, J., WEHMEYER, G., LOVELL, S., BATTAILE, K. P. & EGAN, S. M. 2016. 1.65 Å resolution structure of the AraC-family transcriptional activator ToxT from Vibrio cholerae. *Acta Crystallographica. Section F, Structural Biology Communications,* 72**,** 726-731.

LIANG, W., PASCUAL-MONTANO, A., SILVA, A. J. & BENITEZ, J. A. 2007. The cyclic AMP receptor protein modulates quorum sensing, motility and multiple genes that affect intestinal colonization in Vibrio cholerae. *Microbiology,* 153**,** 2964-2975.

LIN, W., FULLNER, K. J., CLAYTON, R., SEXTON, J. A., ROGERS, M. B., CALIA, K. E., CALDERWOOD, S. B., FRASER, C. & MEKALANOS, J. J. 1999. Identification of a Vibrio cholerae RTX Toxin Gene Cluster That Is Tightly Linked to the Cholera Toxin Prophage. *Proceedings of the National Academy of Sciences of the United States of America,* 96**,** 1071-1076.

LIU, B., HONG, C., HUANG, R. K., YU, Z. & STEITZ, T. A. 2017. Structural basis of bacterial transcription activation. *Science,* 358**,** 947.

LODGE, J., FEAR, J., BUSBY, S., GUNASEKARAN, P. & KAMINI, N. R. 1992. Broad host range plasmids carrying the Escherichia coli lactose and galactose operons. *FEMS Microbiology Letters,* 95**,** 271-276.

LOWDEN, M. J., SKORUPSKI, K., PELLEGRINI, M., CHIORAZZO, M. G., TAYLOR, R. K. & KULL, F. J. 2010. Structure of Vibrio cholerae ToxT reveals a mechanism for fatty acid regulation of virulence genes. *Proc Natl Acad Sci U S A,* 107**,** 2860-5.

LUCHT, J. M., DERSCH, P., KEMPF, B. & BREMER, E. 1994. Interactions of the nucleoid-associated DNA-binding protein H-NS with the regulatory region of the osmotically controlled proU operon of Escherichia coli. *Journal of Biological Chemistry,* 269**,** 6578.

MA, A. T., MCAULEY, S., PUKATZKI, S. & MEKALANOS, J. J. 2009. Translocation of a Vibrio cholerae Type VI Secretion Effector Requires Bacterial Endocytosis by Host Cells. *Cell host & microbe,* 5**,** 234-243.

MANDAL, S., MANDAL, M. D. & PAL, N. K. 2011. Cholera: a great global concern. *Asian Pacific journal of tropical medicine,* 4**,** 573-580.

MANDLIK, A., LIVNY, J., ROBINS, W. P., RITCHIE, J. M., MEKALANOS, J. J. & WALDOR, M. K. 2011. RNA-seq-based monitoring of infection-linked changes in Vibrio cholerae gene expression. *Cell host & microbe,* 10**,** 165-174.

MARCHETTI, M., MALINOWSKA, A., HELLER, I. & WUITE, G. J. L. 2017. How to switch the motor on: RNA polymerase initiation steps at the single-molecule level. *Protein Science,* 26**,** 1303-1313.

MARKOV, E. Y., KULIKALOVA, E. S., URBANOVICH, L. Y., VISHNYAKOV, V. S. & BALAKHONOV, S. V. 2015. Chitin and Products of Its Hydrolysis in Vibrio cholerae Ecology. *Biochemistry (Mosc),* 80**,** 1109-16.

MARTíNEZ-ANTONIO, A. & COLLADO-VIDES, J. 2003. Identifying global regulators in transcriptional regulatory networks in bacteria. *Current Opinion in Microbiology,* 6**,** 482-489.

MATHUR, J. & WALDOR, M. K. 2004. The Vibrio cholerae ToxR-regulated porin OmpU confers resistance to antimicrobial peptides. *Infect Immun,* 72**,** 3577-83.

MATSON, J. S., WITHEY, J. H. & DIRITA, V. J. 2007. Regulatory Networks Controlling Vibrio cholerae Virulence Gene Expression. *Infection and Immunity,* 75**,** 5542-5549.

MAYNARD, C. L., ELSON, C. O., HATTON, R. D. & WEAVER, C. T. 2012. Reciprocal Interactions of the Intestinal Microbiota and Immune System. *Nature,* 489**,** 231-241.

MCDONOUGH, K. A. & RODRIGUEZ, A. 2012. The myriad roles of cyclic AMP in microbial pathogens: from signal to sword. *Nat Rev Micro,* 10**,** 27-38.

MEIBOM, K. L., BLOKESCH, M., DOLGANOV, N. A., WU, C.-Y. & SCHOOLNIK, G. K. 2005. Chitin Induces Natural Competence in Vibrio cholerae. *Science,* 310**,** 1824-1827.

MEIBOM, K. L., LI, X. B., NIELSEN, A. T., WU, C.-Y., ROSEMAN, S. & SCHOOLNIK, G. K. 2004. The Vibrio cholerae chitin utilization program. *Proceedings of the National Academy of Sciences of the United States of America,* 101**,** 2524-2529.

MERRELL, D. S., BAILEY, C., KAPER, J. B. & CAMILLI, A. 2001. The ToxR-mediated organic acid tolerance response of Vibrio cholerae requires OmpU. *J Bacteriol,* 183**,** 2746-54.

MILLER, V. L. & MEKALANOS, J. J. 1988. A novel suicide vector and its use in construction of insertion mutations: osmoregulation of outer membrane proteins and virulence determinants in Vibrio cholerae requires toxR. *Journal of Bacteriology,* 170**,** 2575-2583.

MINATO, Y., SIEFKEN, R. L. & HÄSE, C. C. 2011. TolC Affects Virulence Gene Expression in Vibrio cholerae. *Journal of Bacteriology,* 193**,** 5850-5852.

MORRIS, J. G. 2011. Cholera—Modern Pandemic Disease of Ancient Lineage. *Emerging Infectious Disease journal,* 17**,** 2099.

MÜLLER-HILL, B. 1998. Some repressors of bacterial transcription. *Current Opinion in Microbiology,* 1**,** 145-151.

MURAKAMI, K. S. 2013. The X-ray Crystal Structure of Escherichia Coli RNA Polymerase Sigma70 Holoenzyme. *Journal of Biological Chemistry*.

MURAKAMI, K. S. & DARST, S. A. 2003. Bacterial RNA polymerases: the wholo story. *Current Opinion in Structural Biology,* 13**,** 31-39.

NAIR, G. B., QADRI, F., HOLMGREN, J., SVENNERHOLM, A.-M., SAFA, A., BHUIYAN, N. A., AHMAD, Q. S., FARUQUE, S. M., FARUQUE, A. S. G., TAKEDA, Y. & SACK, D. A. 2006. Cholera Due to Altered El Tor Strains of Vibrio cholerae O1 in Bangladesh. *Journal of Clinical Microbiology,* 44**,** 4211-4213.

NIELSEN, A. T., DOLGANOV, N. A., RASMUSSEN, T., OTTO, G., MILLER, M. C., FELT, S. A., TORREILLES, S. & SCHOOLNIK, G. K. 2010. A Bistable Switch and Anatomical Site Control Vibrio cholerae Virulence Gene Expression in the Intestine. *PLoS Pathog,* 6**,** e1001102.

NYE, M. B., PFAU, J. D., SKORUPSKI, K. & TAYLOR, R. K. 2000. Vibrio cholerae H-NS Silences Virulence Gene Expression at Multiple Steps in the ToxR Regulatory Cascade. *Journal of Bacteriology,* 182**,** 4295-4303.

OLIVIER, V., HAINES, G. K., TAN, Y. & SATCHELL, K. J. F. 2007. Hemolysin and the Multifunctional Autoprocessing RTX Toxin Are Virulence Factors during Intestinal Infection of Mice with Vibrio cholerae El Tor O1 Strains. *Infection and Immunity,* 75**,** 5035-5042.

ONO, S., GOLDBERG, MARTIN D., OLSSON, T., ESPOSITO, D., HINTON, JAY C. D. & LADBURY, JOHN E. 2005. H-NS is a part of a thermally controlled mechanism for bacterial gene regulation. *Biochemical Journal,* 391**,** 203.

PANDIT C. G., H. S. L. 1951. The probable role of the hilsa fish, Hilsa ilisa (Ham) in maintaining cholera endemicity in India. *Indian Journal of Medical Sciences,* 5**,** 343–356.

PAPENFORT, K., FÖRSTNER, K. U., CONG, J.-P., SHARMA, C. M. & BASSLER, B. L. 2015. Differential RNA-seq of Vibrio cholerae identifies the VqmR small RNA as a regulator of biofilm formation. *Proceedings of the National Academy of Sciences,* 112**,** E766-E775.

PARK, P. J. 2009. ChIP-Seq: advantages and challenges of a maturing technology. *Nature reviews. Genetics,* 10**,** 669-680.

PARSOT, C. & MEKALANOS, J. J. 1992. Structural analysis of the acfA and acfD genes of Vibrio cholerae: effects of DNA topology and transcriptional activators on expression. *Journal of Bacteriology,* 174**,** 5211-5218.

PEREZ-SOTO, N., MOULE, L., CRISAN, D. N., INSUA, I., TAYLOR-SMITH, L. M., VOELZ, K., FERNANDEZ-TRILLO, F. & KRACHLER, A. M. 2017. Engineering microbial physiology with synthetic polymers: cationic polymers induce biofilm formation in Vibrio cholerae and downregulate the expression of virulence genes. *Chemical Science,* 8**,** 5291-5298.

PETERS, J. M., VANGELOFF, A. D. & LANDICK, R. 2011. Bacterial Transcription Terminators: The RNA 3′-End Chronicles. *Journal of Molecular Biology,* 412**,** 793-813.

PETERSON, K. M. 2002. Expression of Vibrio cholerae virulence genes in response to environmental signals. *Current issues in intestinal microbiology,* 3**,** 29-38.

PULLITZER, R. 1959. Cholera. *WHO iris*.

QUEEN, J. & SATCHELL, K. J. F. 2013. Promotion of Colonization and Virulence by Cholera Toxin Is Dependent on Neutrophils. *Infection and Immunity,* 81**,** 3338-3345.

RAY-SONI, A., BELLECOURT, M. J. & LANDICK, R. 2016. Mechanisms of Bacterial Transcription Termination: All Good Things Must End. *Annual Review of Biochemistry,* 85**,** 319-347.

REIDL, J. & KLOSE, K. E. 2002. Vibrio cholerae and cholera: out of the water and into the host. *FEMS Microbiology Reviews,* 26**,** 125-139.

RHODIUS, V. A. & BUSBY, S. J. W. 2000. Interactions between activating region 3 of the Escherichia coli cyclic AMP receptor protein and region 4 of the RNA polymerase σ70 subunit: application of suppression genetics11Edited by R. Ebright. *Journal of Molecular Biology,* 299**,** 311-324.

RICHARDSON, S. H. 1994. Animal Models in Cholera Research. *Vibrio cholerae and Cholera.* American Society of Microbiology.

RITCHIE, J. M., RUI, H., BRONSON, R. T. & WALDOR, M. K. 2010. Back to the Future: Studying Cholera Pathogenesis Using Infant Rabbits. *mBio,* 1.

RITCHIE, J. M., RUI, H., ZHOU, X., IIDA, T., KODOMA, T., ITO, S., DAVIS, B. M., BRONSON, R. T. & WALDOR, M. K. 2012. Inflammation and Disintegration of Intestinal Villi in an Experimental Model for Vibrio parahaemolyticus-Induced Diarrhea. *PLOS Pathogens,* 8**,** e1002593.

ROJO, F. 1999. Repression of Transcription Initiation in Bacteria. *Journal of Bacteriology,* 181**,** 2987-2991.

ROSS, W., GOSINK, K. K., SALOMON, J., IGARASHI, K., ZOU, C., ISHIHAMA, A., SEVERINOV, K. & GOURSE, R. L. 1993. A third recognition element in bacterial promoters: DNA binding by the alpha subunit of RNA polymerase. *Science,* 262**,** 1407.

ROWE, H. M., WITHEY, J. H. & NEELY, M. N. 2014. Zebrafish as a model for zoonotic aquatic pathogens. *Developmental & Comparative Immunology,* 46**,** 96-107.

RUFF, E. F., RECORD, M. T., JR. & ARTSIMOVITCH, I. 2015. Initial events in bacterial transcription initiation. *Biomolecules,* 5**,** 1035-62.

RUNFT, D. L., MITCHELL, K. C., ABUAITA, B. H., ALLEN, J. P., BAJER, S., GINSBURG, K., NEELY, M. N. & WITHEY, J. H. 2014. Zebrafish as a Natural Host Model for Vibrio cholerae Colonization and Transmission. *Applied and Environmental Microbiology,* 80**,** 1710-1717.

SAFA, A., NAIR, G. B. & KONG, R. Y. C. 2010. Evolution of new variants of Vibrio cholerae O1. *Trends in Microbiology,* 18**,** 46-54.

SASLOWSKY, D. E., CHO, J. A., CHINNAPEN, H., MASSOL, R. H., CHINNAPEN, D. J. F., WAGNER, J. S., DE LUCA, H. E., KAM, W., PAW, B. H. & LENCER, W. I. 2010. Intoxication of zebrafish and mammalian cells by cholera toxin depends on the flotillin/reggie proteins but not Derlin-1 or -2. *The Journal of Clinical Investigation,* 120**,** 4399-4409.

SATCHELL, K. J. F. 2015. Multifunctional-autoprocessing repeats-in-toxin (MARTX) Toxins of Vibrios. *Microbiology Spectrum,* 3.

SAVERY, N., RHODIUS, V. & BUSBY, S. 1996. Protein-protein interactions during transcription activation: the case of the Escherichia coli cyclic AMP receptor protein. *Philos Trans R Soc Lond B Biol Sci,* 351**,** 543-50.

SAVERY, N. J., LLOYD, G. S., BUSBY, S. J. W., THOMAS, M. S., EBRIGHT, R. H. & GOURSE, R. L. 2002. Determinants of the C-Terminal Domain of the Escherichia coli RNA Polymerase α Subunit Important for Transcription at Class I Cyclic AMP Receptor Protein-Dependent Promoters. *Journal of Bacteriology,* 184**,** 2273-2280.

SAVERY, N. J., LLOYD, G. S., KAINZ, M., GAAL, T., ROSS, W., EBRIGHT, R. H., GOURSE, R. L. & BUSBY, S. J. 1998. Transcription activation at Class II CRP-dependent promoters: identification of determinants in the C-terminal domain of the RNA polymerase alpha subunit. *The EMBO Journal,* 17**,** 3439-3447.

SENDEROVICH, Y., IZHAKI, I. & HALPERN, M. 2010. Fish as reservoirs and vectors of Vibrio cholerae. *PLoS One,* 5**,** e8607.

SHEAHAN, K. L., CORDERO, C. L. & SATCHELL, K. J. 2004. Identification of a domain within the multifunctional Vibrio cholerae RTX toxin that covalently cross-links actin. *Proc Natl Acad Sci U S A,* 101**,** 9798-803.

SHIMADA, T., FUJITA, N., YAMAMOTO, K. & ISHIHAMA, A. 2011. Novel roles of cAMP receptor protein (CRP) in regulation of transport and metabolism of carbon sources. *PLoS One,* 6**,** e20081.

SHIMADA, T., YAMAZAKI, Y., TANAKA, K. & ISHIHAMA, A. 2014. The whole set of constitutive promoters recognized by RNA polymerase RpoD holoenzyme of Escherichia coli. *PLoS One,* 9**,** e90447.

SILVA, A. J. & BENITEZ, J. A. 2016. *Vibrio cholerae* Biofilms and Cholera Pathogenesis. *PLoS Negl Trop Dis,* 10**,** e0004330.

SKORUPSKI, K. & TAYLOR, R. K. 1997a. Cyclic AMP and its receptor protein negatively regulate the coordinate expression of cholera toxin and toxin-coregulated pilus in Vibrio cholerae. *Proceedings of the National Academy of Sciences,* 94**,** 265-270.

SKORUPSKI, K. & TAYLOR, R. K. 1997b. Sequence and functional analysis of the gene encoding Vibrio cholerae cAMP receptor protein. *Gene,* 198**,** 297-303.

TAMAYO, R., PATIMALLA, B. & CAMILLI, A. 2010. Growth in a Biofilm Induces a Hyperinfectious Phenotype in Vibrio cholerae. *Infection and Immunity,* 78**,** 3560-3569.

TAYLOR, R. G., WALKER, D. C. & MCINNES, R. R. 1993. E. coli host strains significantly affect the quality of small scale plasmid DNA preparations used for sequencing. *Nucleic Acids Research,* 21**,** 1677-1678.

TAYLOR, R. K., MILLER, V. L., FURLONG, D. B. & MEKALANOS, J. J. 1987. Use of phoA gene fusions to identify a pilus colonization factor coordinately regulated with cholera toxin. *Proc Natl Acad Sci U S A,* 84**,** 2833-7.

TEBBUTT, J., RHODIUS, V. A., WEBSTER, C. L. & BUSBY, S. J. W. 2002. Architectural requirements for optimal activation by tandem CRP molecules at a class I CRP-dependent promoter. *FEMS Microbiology Letters,* 210**,** 55-60.

TESCHLER, J. K., ZAMORANO-SANCHEZ, D., UTADA, A. S., WARNER, C. J. A., WONG, G. C. L., LININGTON, R. G. & YILDIZ, F. H. 2015. Living in the matrix: assembly and control of Vibrio cholerae biofilms. *Nat Rev Micro,* 13**,** 255-268.

THIAGARAJAH, J. R. & VERKMAN, A. S. 2005. New drug targets for cholera therapy. *Trends in Pharmacological Sciences,* 26**,** 172-175.

TSUJIKAWA, L., TSODIKOV, O. V. & DEHASETH, P. L. 2002. Interaction of RNA polymerase with forked DNA: Evidence for two kinetically significant intermediates on the pathway to the final complex. *Proceedings of the National Academy of Sciences,* 99**,** 3493-3498.

TYPAS, A. & HENGGE, R. 2006. Role of the spacer between the -35 and -10 regions in sigmas promoter selectivity in Escherichia coli. *Molecular microbiology,* 59**,** 1037-1051.

VALENTIN-HANSEN, P., SØGAARD-ANDERSEN, L. & PEDERSEN, H. 1996. A flexible partnership: the CytR anti-activator and the cAMP–CRP activator protein, comrades in transcription control. *Molecular Microbiology,* 20**,** 461-466.

VAN DER VALK, R. A., VREEDE, J., QIN, L., MOOLENAAR, G. F., HOFMANN, A., GOOSEN, N. & DAME, R. T. 2017. Mechanism of environmentally driven conformational changes that modulate H-NS DNA bridging activity. *eLife,* 6**,** e27369.

WALDOR, M. K. & MEKALANOS, J. J. 1996. Lysogenic conversion by a filamentous phage encoding cholera toxin. *Science,* 272**,** 1910-1914.

WANG, H., AYALA, J. C., BENITEZ, J. A. & SILVA, A. J. 2015. RNA-Seq Analysis Identifies New Genes Regulated by the Histone-Like Nucleoid Structuring Protein (H-NS) Affecting Vibrio cholerae Virulence, Stress Response and Chemotaxis. *PLoS ONE,* 10**,** e0118295.

WANG, H., CHEN, S., ZHANG, J., ROTHENBACHER, F. P., JIANG, T., KAN, B., ZHONG, Z. & ZHU, J. 2013. Catalases Promote Resistance of Oxidative Stress in Vibrio cholerae. *PLOS ONE,* 7**,** e53383.

WANG, H. H. & CHURCH, G. M. 2011. Chapter eighteen - Multiplexed Genome Engineering and Genotyping Methods: Applications for Synthetic Biology and Metabolic Engineering. *In:* CHRISTOPHER, V. (ed.) *Methods in Enzymology*. Academic Press.

WATSON, J. D. 2014. *Molecular Biology of the Gene*, Pearson.

WEBER, G. G., KLOSE, K. E. & KLOSE 2011. The complexity of ToxT-dependent transcription in Vibrio cholerae. *The Indian Journal of Medical Research,* 133**,** 201-206.

WHO. 2017. *Global Health Observatory (GHO) data: Cholera* [Online]. Available: http://www.who.int/gho/epidemic_diseases/cholera/en/ [Accessed 10/10/2017 2017].

WILLIAMS, R. M., RHODIUS, V. A., BELL, A. I., KOLB, A. & BUSBY, S. J. 1996. Orientation of functional activating regions in the Escherichia coli CRP protein during transcription activation at class II promoters. *Nucleic Acids Research,* 24**,** 1112-1118.

WITHEY, J. H. & DIRITA, V. J. 2006. The toxbox: specific DNA sequence requirements for activation of Vibrio cholerae virulence genes by ToxT. *Molecular Microbiology,* 59**,** 1779-1789.

WU, R., ZHAO, M., LI, J., GAO, H., KAN, B. & LIANG, W. 2015. Direct regulation of the natural competence regulator gene tfoX by cyclic AMP (cAMP) and cAMP receptor protein (CRP) in Vibrios. *Scientific Reports,* 5**,** 14921.

YANG, X. & LEWIS, P. J. 2010. The interaction between bacterial transcription factors and RNA polymerase during the transition from initiation to elongation. *Transcription,* 1**,** 66-69.

YU, R. R. & DIRITA, V. J. 2002. Regulation of gene expression in Vibrio cholerae by ToxT involves both antirepression and RNA polymerase stimulation. *Molecular Microbiology,* 43**,** 119-134.

ZAHID, M. S. H., AWASTHI, S. P., ASAKURA, M., CHATTERJEE, S., HINENOYA, A., FARUQUE, S. M. & YAMASAKI, S. 2015. Suppression of Virulence of Toxigenic Vibrio cholerae by Anethole through the Cyclic AMP (cAMP)-cAMP Receptor Protein Signaling System. *PLoS ONE,* 10**,** e0137529.

ZHANG, Y., FENG, Y., CHATTERJEE, S., TUSKE, S., HO, M. X., ARNOLD, E. & EBRIGHT, R. H. 2012. STRUCTURAL BASIS OF TRANSCRIPTION INITIATION. *Science (New York, N.Y.),* 338**,** 1076-1080.

ZHOU, Y., KOLB, A., BUSBY, S. J. W. & WANG, Y.-P. 2014. Spacing requirements for Class I transcription activation in bacteria are set by promoter elements. *Nucleic Acids Research,* 42**,** 9209-9216.

ZHOU, Y., ZHANG, X. & EBRIGHT, R. H. 1993. Identification of the activating region of catabolite gene activator protein (CAP): isolation and characterization of mutants of CAP specifically defective in transcription activation. *Proceedings of the National Academy of Sciences of the United States of America,* 90**,** 6081-6085.

ZHU, J. & MEKALANOS, J. J. 2003. Quorum Sensing-Dependent Biofilms Enhance Colonization in Vibrio cholerae. *Developmental Cell,* 5**,** 647-656.

ZUO, Y. & STEITZ, THOMAS A. 2015. Crystal Structures of the E. coli Transcription Initiation Complexes with a Complete Bubble. *Molecular Cell,* 58**,** 534-540.